Universidad Politécnica de Cartagena

ESCUELA INTERNACIONAL DE DOCTORADO

PROGRAMA DE DOCTORADO EN TECNOLOGÍAS INDUSTRIALES

TESIS DOCTORAL

APLICACIÓN DE MODELOS MATEMÁTICOS PARA LA OPTIMIZACIÓN Y MEJORA DE PROCESOS LOGÍSTICOS RELACIONADOS: REDUCCIÓN DE LA HUELLA DE CARBONO Y CONDUCCIÓN EFICIENTE

Presentada por D. Adrián Valverde Mateo para optar al grado de Doctor
por la Universidad Politécnica de Cartagena

Dirigida por:
Dr. D. Juan Luis García Guirao

Cartagena, 2023

DOCTORAL PROGRAMME IN INDUSTRIAL TECHNOLOGIES

PhD THESIS

APPLICATION OF MATHEMATICAL MODELS FOR THE OPTIMIZATION AND IMPROVEMENT OF RELATED LOGISTIC PROCESSES: REDUCTION OF CARBON FOOTPRINT AND EFFICIENT DRIVING

Presented by Mr. Adrián Valverde Mateo
to the Technical University of Cartagena in fulfilment of
the thesis requirement for the award of PhD

Supervisor:
Dr. Mr. Juan Luis García Guirao

Cartagena, 2023

This PhD thesis is presented according to the Compendium of Publications mode, regulated under art. 20 of the Regulation of Official Doctoral Studies of the Technical University of Cartagena of March 24, 2021. The articles have been published with the express approval of the Supervisor of this PhD thesis and carried out further to the enrollment of doctoral studies. The references of these papers are listed below:

Publications

Article 1.-: M. Arshad, T. Kifayat, J.L.G. Guirao, J.M. Sánchez, A. Valverde, 2022. *Using Maxwell Distribution to Handle Selector's Indecisiveness in Choice Data: A new Latent Bayesian Choice Model.* **Applied Sciences**, **12(13)**, 6337, DOI: https://doi.org/10.3390/app12136337

- 2022 Impact Factor 2.7,
- Q2 Engineering, Multididisciplinary

Article 2.-: M. Arshad, S.A. Cheema, J.L.G. Guirao, J.M. Sánchez, A. Valverde, 2023. *Assisting the decision making - A generalization of choice models to handle the binary choices.* **AIMS Mathematics**, **8(2)**, 3083–3100,
DOI: http://www.aimspress.com/article/doi/10.3934/math.2023159

- 2022 Impact Factor 2.2,
- Q1 Mathematics, Applied

Article 3.-: Z. Sabir, T. Saeed, J.L.G. Guirao, J.M. Sánchez, A. Valverde, 2023. *A Swarming Meyer Wavelet Computing Approach to Solve the Transport System of Goods.* **Axioms**, **12(5)**, 456, DOI: https://doi.org/10.3390/axioms12050456

- 2022 Impact Factor 2,
- Q2 Mathematics, Applied

Article 4.-: J.M. Sánchez, A. Valverde, J.L.G. Guirao, H. Chen, 2023. *Mathematical Modeling for the development of traffic based on the theory of system dynamics.* **AIMS Mathematics**, **8(11)**, 27626–27642, DOI: 10.3934/math.20231413

- 2022 Impact Factor 2.2,
- Q1 Mathematics, Applied

Acknowlegments/Agradecimientos

A mis padres, Antonio Valverde y Reme Mateo, porque les debo la vida y por su apoyo incondicional en todas mis decisiones. Todo el esfuerzo y sacrificio de sus vidas, ha pasado porque mi hermana Sandra y yo tuviéramos la mejor educación y oportunidades a nuestro alcance, siempre en su detrimento. Porque a pesar de tanto, nos queremos y querremos siempre. Porque son los mejores padres del mundo y soy tan afortunado de tenerlos.

A mi hermana Sandra Valverde, porque siempre ha sido y será, mi mejor y más cercana referencia de la que poder fijarme y aprender.

A mi jefe y compañero de viaje Juan Conesa y a mi tan querida Primafrio, por haberme dado mi primera oportunidad cuando más lo necesitaba y haberme enseñado lo que es la vida. Por permitirme creer posible mi sueño desde niño y hacerlo realidad.

A mi director de tesis y amigo Juan Luis García, porque es el mejor profesor y científico que conozco y nunca nada ni nadie podrá cambiar esto. Por haber sido fuente de inspiración constante desde que nos conocimos tanto en el sector académico como en lo profesional.

A mi mejor amigo Juan Manuel Sánchez Parra, por todas las batallas que hemos compartido juntos desde que nos conocimos y que nos han hecho más fuertes. Por haberme animado a hacer el Doctorado y presentarme a mi amigo y director, Juan Luis.

A mi responsable de estancia internacional Michael Woywode, por haberme abierto las puertas de Mannheim Universität en mi estancia internacional en Alemania (Stuttgart-Mannheim) y por su apoyo y confianza en los resultados de mi investigación.

A la pasión y sueño de mi vida, FERRARI, porque de niño me enamoré de su belleza y su cultura, que ha supuesto siempre en mi admiración, respeto, motivación y cariño, así como a mi ídolo, Michael Schumacher, no por lo que ganó sino por la forma en que lo hizo siendo todo una inspiración y referencia.

Al amor de mi vida, Lidia Quereda, por haber sido desde que nos conocimos con 7 años, una motivación constante cada día y haber llenado mi vida de pasión y amor, porque sin ti, no hubiera podido superar todas mis metas y ser quien soy hoy.

Siempre estaré agradecido con todos vosotros. Porque vosotros, sois los verdaderos artífices de mis logros y sueños cumplidos. Porque este doctorado para mí significa todo el agradecimiento y cariño que os tengo. Por todos los momentos que hemos compartido. Porque todos nos lo merecemos.

Resumen

La actual tesis doctoral presentada por D. Adrián Valverde Mateo, Responsable de Investigación en **Grupo Logístico Primarfio** en España defendida bajo menciones de doctorado industrial e internacional tiene varios objetivos. Grupo Primafrio es una empresa líder en el movimiento de mercancías refrigeradas. Esta empresa es un referente en Europa en el sector del transporte por carretera y la logística. Evidentemente, la optimización de sus procesos en términos de ahorro económico, reducción de huella de carbono y conducción eficiente pueden ser los principales retos en la actualidad. Por tanto, la presente tesis doctoral ha tenido dos conjuntos de objetivos diferentes alineados con los intereses antes descritos de la empresa.

El primer gran objetivo tiene que ver con la implementación de procesos de optimización en la toma de decisiones necesarias en la actividad logística. En este sentido, había un problema abierto con respecto a la indecisión en los datos de elección que tratamos usando la distribución de Maxwell para manejar la indecisión del selector en los datos de elección; de hecho, proponemos un nuevo modelo de elección bayesiano latente. Por otro lado, en el mismo marco de problemas, abordamos la asistencia en la toma de decisiones en el caso binario, en este sentido proponemos una generalización de modelos de elección para el escenario binario. Estas dos contribuciones constituyen el contenido de los Artículos 1 y 2.

El segundo bloque de problemas aborda la cuestión abierta de medir cómo una conducción eficiente reduce la huella de carbono en términos de ahorro de combustible. Por tanto, planteamos un modelo reactivo donde podemos analizar el impacto del conductor en el proceso. Podemos resolver este modelo creando un enjambre de ondas Meyer. Las conclusiones fueron que para el mismo nivel de tráfico una mejor eficiencia en la conducción reduce los costes. Cuando el nivel de tráfico es alto, este ahorro es aún más importante, por lo que no tiene sentido reducir

costes e invertir en la formación de conductores para una conducción eficiente. Estos resultados constituyen el contenido del Artículo 3.

Finalmente, en el Artículo 4, hemos desarrollado un modelo global de tráfico donde combinamos por primera vez el efecto del tren en el proceso logístico de movimiento de mercancías. Como colaboramos en este objetivo con Profesor Huatao Chen de la División de Dinámica y Control, Facultad de Matemáticas y Estadística, Universidad Tecnológica de Shandong, Zibo 255000, China, Jefe del Laboratorio de Control de Tráfico, hemos utilizado los datos de la provincia de Shandong en China, que tiene una infraestructura ferroviaria profunda. Este modelo es exportable a otra parte del mundo con una complejidad operativa similar. En este sentido, se demuestra que la operación vial así como el tránsito ferroviario promueven el desarrollo del tránsito, mientras que los accidentes de tránsito inhiben el desarrollo del tránsito. Además, se obtiene el error máximo entre los datos de salida y las datos estadísticos proporcionados por la autoridad, a partir del cual se dan algunas previsiones para el desarrollo del tráfico en el futuro, se dan algunas sugerencias y esquemas de optimización para el desarrollo del tráfico. Finalmente, también se deriva un modelo de red neuronal del desarrollo del tráfico en esta provincia.

Summary

The current PhD thesis presented by Mr. Adrián Valverde Mateo, Chief of Research duties at **Primarfio Logistics Group** in Spain defended under the label of industrial and international doctorate has several aims. Grupo Primafrio is a leader company in the movement of refrigerated goods. This company is a reference in Europe in road transport and logistics sector. Obviously, the optimization of their processes in terms of economic saving, reduction of carbon footprint and efficient driving can be the main challenges in recent days. Therefore the current PhD thesis has had two different sets of objectives.

The first big objective deals with the optimization approach at the decision making needed at the logistics process. In this sense, there was an open problem regarding the indecisiveness in choice data that we treat by using Maxwell distribution to handle selector's indecisiveness in choice data, in fact we propose a new latent Bayesian choice model. On the other hand, in the same frame of problems, we deal with the assistance at the decision making at the binary case, in this sense we propose a generalization of choice models for the binary scenario. These two contributions constitute the content of Papers 1 and 2.

Second block of problems deals with the open question of measuring how efficient driving reduce the footprint carbon in terms of saving fuel. Therefore, we state a reactive model where we can analyze the impact of driver at the process. We are able to solve this model by creating a swarming Meyer wavelet. The conclusions were that for the same level of traffic a better efficiency at driving reduce costs. When traffic level is high this save is even more important, therefore make not sense to reduce cost invest in the driving formation on efficient driving. This item is presented at Paper 3.

Finally, in Paper 4, we have developed a global model of traffic where we combine for first time the effect of train in the logistic process of moving goods. As

colaborate at this aim with Professor Huatao Chen from Division of Dynamics and Control, School of Mathematics and Statistics, Shandong University of Technology, Zibo 255000, China, Head of the Laboratory of Traffic Control we have used the data of Shandong Province in China which has a deep railway infrastructure. This model is exportable to other part of the work with a similar operational complexity. In this sense, it is shown that highway operation as well as rail transit promotes the development of traffic, while traffic accidents inhibit traffic development. Moreover, the maximum error between the output data and the statistics bureau, based on which some forecasts for the development of traffic in the future are given, is obtained, some suggestions and optimization schemes for traffic development are given. Finally, a neural network model of the development of Shandong traffic is also derived.

Zusammenfassung

Die aktuelle Doktorarbeit, die von Herrn Adrián Valverde Mateo, Forschungsleiter der Primarfio Logistics Group in Spanien, vorgelegt und unter dem Label eines industriellen und internationalen Doktortitels verteidigt wird, verfolgt mehrere Ziele. Grupo Primafrio ist ein führendes Unternehmen im Transport von Kühlgütern. Dieses Unternehmen ist eine Referenz in Europa im Straßentransport- und Logistiksektor. Offensichtlich kann die Optimierung ihrer Prozesse im Hinblick auf wirtschaftliche Einsparungen, die Reduzierung des CO2-Fußabdrucks und effizientes Fahren die größten Herausforderungen der letzten Tage sein. Daher hatte die vorliegende Doktorarbeit zwei unterschiedliche Zielsetzungen. Das erste große Ziel befasst sich mit dem Optimierungsansatz bei der Entscheidungsfindung, die im Logistikprozess erforderlich ist. In diesem Sinne gab es ein offenes Problem hinsichtlich der Unentschlossenheit in Auswahldaten, das wir behandeln, indem wir die Maxwell-Verteilung verwenden, um die Unentschlossenheit des Selektors in Auswahldaten zu handhaben. Tatsächlich schlagen wir ein neues latentes Bayes'sches Auswahlmodell vor. Andererseits befassen wir uns im gleichen Problemrahmen mit der Unterstützung bei der Entscheidungsfindung im binären Fall. In diesem Sinne schlagen wir eine Verallgemeinerung von Auswahlmodellen für das binäre Szenario vor. Diese beiden Beiträge bilden den Inhalt der Aufsätze 1 und 2. Der zweite Problemblock befasst sich mit der offenen Frage, wie effizientes Fahren den CO2-Fußabdruck im Hinblick auf die Kraftstoffeinsparung verringert. Daher erstellen wir ein reaktives Modell, mit dem wir die Auswirkungen des Treibers auf den Prozess analysieren können. Wir können dieses Modell lösen, indem wir ein schwärmendes Meyer-Wavelet erzeugen. Die Schlussfolgerungen waren, dass bei gleichem Verkehrsaufkommen eine bessere Effizienz beim Fahren die Kosten senkt. Bei hohem Verkehrsaufkommen ist diese Einsparung umso wichtiger, daher macht es keinen Sinn, in die Fahrausbildung für effizientes Fahren zu investieren, um die Kosten zu senken. Dieser Artikel wird in Paper 3 vorgestellt. Schließlich haben wir in Aufsatz 4 ein globales Verkehrsmodell

entwickelt, in dem wir zum ersten Mal die Auswirkung des Zuges auf den logistischen Prozess des Gütertransports kombinieren. In Zusammenarbeit mit Professor Huatao Chen von der Abteilung für Dynamik und Steuerung, Fakultät für Mathematik und Statistik, Shandong University of Technology, Zibo 255000, China, Leiter des Labors für Verkehrskontrolle, haben wir die Daten der Provinz Shandong in China verwendet verfügt über eine umfassende Eisenbahninfrastruktur. Dieses Modell ist auf andere Teile der Arbeit mit ähnlicher betrieblicher Komplexität exportierbar. In diesem Sinne zeigt sich, dass sowohl der Autobahnbetrieb als auch der Schienenverkehr die Verkehrsentwicklung fördern, während Verkehrsunfälle die Verkehrsentwicklung hemmen. Darüber hinaus wird der maximale Fehler zwischen den Ausgabedaten und dem Statistikamt ermittelt, auf dessen Grundlage einige Prognosen für die Entwicklung des Verkehrs in der Zukunft gegeben werden, und es werden einige Vorschläge und Optimierungspläne für die Verkehrsentwicklung gegeben. Schließlich wird auch ein neuronales Netzwerkmodell der Entwicklung des Shandong-Verkehrs abgeleitet.

Contents

Chapter 1

Objectives

Mr. Adrián Valverde Mateo working under supervision of **Professor Juan Luis García Guirao** (UPCT), Full Professor of Applied Mathematics and Head of the Dynamical Systems applied to Engineering Research Group of Region of Murcia has worked in the field of application of mathematical methods for optimizing and improving logistics processes in the frame of the transportation of goods by road in a truck. Currently Mr. Valverde works as a chief of research duties at **Primarfio Logistics Group** in Spain. Primafrio is a company devoted to the movements of good refrigerated by road in trucks and in such frame the PhD Thesis projects aims to implement improvements in this sector. This PhD will be defended under the industrial doctorate mention apart from the International one, the research stay has been done at **Mannheim Universität (Germany)** under the supervision of **Professor Micheal Woywode** expert in logistic optimization.

The work had two main aims. On the one we worked in problems related with the optimizing cargo/storage process of goods in the trucks. It is obvious that these type of problems are close related with decision making. So, our two first works deals with this problem. As first aim, treated at the first paper, we develop new pathways to facilitate the resolving of the long debated issue of handling ties or the degree of indecisiveness precipitated in comparative information. The decision chaos is accommodated by the elegant application of the choice axiom ensuring intact utility when imperfect choices are observed. The objectives are facilitated by inducing an additional parameter in the probabilistic set up of Maxwell to retain the extent of indecisiveness prevalent in the choice data. The operational soundness of the proposed model is elucidated through the rigorous employment of Gibbs sampling—a popular approach of the Markov chain Monte Carlo methods. The outcomes of this research clearly substantiate the applicability of the proposed scheme in retaining the advantages of discrete comparative data when the freedom of no indecisiveness is permitted. The legitimacy of the devised mechanism is enumerated on multi-fronts such as the estimation of preference probabilities and assessment of worth parameters, and through the quantification of the significance of choice hierarchy. The outcomes of the research highlight the effects of sample size and the extent of indecisiveness exhibited in the choice data. The estimation efficiency is estimated to be improved with the increase in sample size. For the largest considered sample of size 100, we estimated an average confidence width of 0.0097, which is notably more compact than the contemporary samples of size 25 and 50.

As a second problem, solved at paper two, we endeavor to provide a generalized framework to assist the launch of paired comparison models while dealing with discrete binary choices. The purpose is served by exploiting the fundaments of the exponential family of distributions. The proposed generalization is proved to cater to seven paired comparison models as members of this newly developed mechanism. The legitimacy of the devised scheme is demonstrated through rigorous simulation-based investigation as well as keenly persuaded empirical evaluations. A detailed analysis, covering a wide range of parametric settings, through the launch of Gibbs Sampler—a notable extension of Markov Chain Monte Carlo methods, is conducted under the Bayesian paradigm. The outcomes of this research substantiate the legitimacy of the devised general structure by not only successfully retaining the preference ordering but also by staying consistent with the established theoretical framework of comparative models.

The second big block of objectives of the PhD was the statement of traffic models in order to measure the impact of efficient driving and the impact of the combination at the logistic operation of the train. Note that Primafrio Group, via **Primavia** is combining this type of logistic operation where the goods are moving in combination truck/train.

In the paper number three, we stated a reactive traffic model inspired at the blood movement inside the human body where we consider the effect of driver formation as a parameter to measure efficient driving. You can imagine that in a company like Primafrio this is a key problem because they have more that 2500 trucks moving every day. The motive of this work is to provide the numerical performances of the reactive transport model that carries trucks with goods on roads by exploiting the stochastic procedures based on the Meyer wavelet (MW) neural network. An objective function is constructed by using the differen- tial model and its boundary conditions. The optimization of the objective function is performed through the hybridization of the global and local search procedures, i.e., swarming and interior point algorithms. Three different cases of the model have been obtained, and the exactness of the stochastic procedure is observed by using the comparison of the obtained and Adams solutions. The negligible absolute error enhances the exactness of the proposed MW neural networks along with the hybridization of the global and local search schemes. Moreover, statistical interpretations based on different operators, histograms, and boxplots are provided to validate the constancy of the designed stochastic structure.

The conclusions were that for the same level of traffic a better efficiency at driving reduce costs. When traffic level is high this save is even more important, therefore make not sense to reduce cost invest in the driving formation on efficient driving.

Finally, in paper number four, we have developed a global model of traffic where we combine for first time the effect of train in the logistic process of moving goods. As colaborate at this aim with Professor Huatao Chen from Division of Dynamics and Control, School of Mathematics and Statistics, Shandong University of Technology, Zibo 255000, China, Head of the Laboratory of Traffic Control we have used the data of Shandong Province in China which has a deep railway infrastructure. This model is exportable to other part of the work with a similar operational complexity. In this sense, it is shown that highway operation as well as rail transit promotes the development of traffic, while traffic accidents inhibit traffic development. Moreover, the maximum error between the output data and the statistics bureau, based on which some forecasts for the development of traffic in the future are given, is obtained, some suggestions and optimization schemes for traffic development are given. Finally, a neural network model of the development of Shandong traffic is also derived.

Chapter 2

Introduction and State of the Art

At logistics companies, the optimization of their processes in terms of economic saving, reduction of carbon footprint and efficient driving can be the main challenges in recent days. This is the case of the Spanish company **Grupo Primafrio**. It is a family business based in Murcia holding 60 years of experience in the road transport and logistics sector. Framed within the Murcia business sector and with a turnover of 572.7 million euros in 2022, it has currently become an international logistics operator, a leader in Europe for the transport of goods at controlled temperatures based on technology and energy. It has eight logistic headquarters spread across the Iberian Peninsula, and its high capillarity allows it to connect reference producers with the markets of the European continent, 27 countries in total, offering high quality logistics solutions, always adapted to the needs of its clients.

Primafrio Group today has a great infrastructure and logistics capacity, a fleet made up of 3,000 trucks with which it transports more than 5.2 million tons of goods per year, and a human team made up of 5,000 professionals, who provide it with the flexibility and operational capacity necessary to meet the challenges and demands of the demanding supply chain. Primafrio Group is specialized in export and groupage services of fruit and vegetable products from the production areas, in Spain and Portugal, to the main points of influence in Europe. In addition, it offers transport solutions for pharmaceutical products through Primapharma, dangerous goods (ADR) through LogistCargo and high-value products, such as technological, telecommunications, industrial or cosmetic products.

The current PhD thesis presented by the chief of research duties at **Primarfio Logistics Group** in Spain deals with the answers of two blocks of problems related with the thematic previously described. On the one hand the optimization approach at the decision making needed at the logistics process. In this sense, there was an open problem regarding the indecisivess in choice data. The competent decision making requires variety of cognitive skills assisting the notion of search for value information to enhance the working potentials, especially when dealing with complex multifaceted environment (see [1]). This process demands comparing and mastering available choices while simultaneously dealing with practical limitations ((see [2])). Therefore, the enchanted status of analyzing and modeling choice behaviors in multidisciplinary research literature is of no surprise. The well-directed historic tour of Young ([3]), traced the roots of the comparative notions in seventeenth century in France, where Condorcet [4] advocated the use of comparative models (in very abstract form) as a method to ensure higher levels of fairness in electoral process. However, it was seminal contributions of Thurstone [5] and Bradley and Terry [6] which laid the foundational blocks communicable through mathematical rigors to encapsulate individual differences and associated choice behaviors. The aforementioned efforts instigated the idea of paired comparison (PC) experiments and related models into the lime light. Since then, PC methodologies have attracted the attention of many researchers from diverse fields of enquiry ranging from health surveillance to sport analysis. For example, in past Mazzuchi et al. [7] explored the applicability of PC models to evaluate the performance of industrial accessories. Further, Cattelan et al. [8] and Schauberger and Tutz [9] elucidated the use of PC approach to analyze sporting events and predict their outcomes. In recent past, Sung and Wu [10] argued the PC schemes as an alternative to the Likert scale for the ranking of psychological markers and indicators' evaluation. Moreover, Chorus [11] and Leibe et al. [12] competently elaborated the interlinkages coupling the choice modelling strategies and numerous variants of rational choice theory governing the preference attitudes in political science, sociology and criminology. For comprehensive accounts documenting the utility of PC methodologies in investigative pursuit, one may also consult Elsenbroich and Payette [13], Pink et al. [14] and Leibe and Meyerhoff [15].

In general, comparative experiments peruse the complexity of rational decision making by comprehending vital ingredients such as, attribute-level combinations, repeated choices and utility-based trade-off, by offering mutually exclusive choice alternatives to the selectors or judges. The inherent randomness of individual choices is explained by assuming probabilistic model, whereas, the associated utility is delineated through the stimuli governing the overall choice dynamics. In simplest form the judges, say n, are inquired about their preferences while pair wise comparing say m, items, objects or individuals, through a simple question, that is, "Do you prefer item i over item j?". One may notice immediate relevance of the inquiry in all sorts of human behavioral assessment mechanisms. Thus, in a complete two factorial setup.

The numerous delicacies have been introduced through rich stream of ongoing efforts in above given simple structure enabling choice models to deal with complexities of real phenomena. For more recent, interesting and knowledgeable account of more notable contributions, one may consult Borriello and Rose [16], Frith [17], Feinberg et al. [18] and Leeper et al. [19]. Our main aim at paper one focuses on the entertainment of selectors' indecisiveness in choice reporting, at methodological and modeling levels. The issue of handling ties in preference data has long been debated and remains a primary component of the available literature focusing the analysis of discrete choices. The opinion chaos has rightly been summarized by Dras [20] who noted "the key point is that modeling of ties explicitly can be important, although there is no consensus on how this should be done; no approach apart from ignoring ties appears to be in widespread use". The aim of paper two is to focus on binary choices.

Efficient driving is a driving style that reduces fuel bills, cuts carbon emissions and lowers accident rates. It is about becoming a better driver, rather than sacrificing the performance or enjoyment of driving. For electric vehicles (EVs), efficient driving also brings greater vehicle range.

Save on fuel, reduce carbon emissions and improve air quality by following our driving tips and thinking about your vehicle choice. Driving efficiently also has safety benefits due to its strong focus on better anticipation.

In paper number 3 we deal with this problem by stating a reactive model of traffic where the rol of the driver is included, we inspired our selves in a model proceeding from the biology.

The study of steady-state one-dimensional reactive transport nonlinear model

(RTNM) is multiscale model in nature. This model is generally implemented to solve the systems based on the solute transport fluid of microvessels and soft tissues, see [21]. The dynamical RTNM is helpful to examine the physical and biological processes to produce actions in many Earth-related investigations [22]. The study of RTNM provides a platform to incorporate and test a new theoretic knowledge about biological, transport procedures and geochemical, as well as, quantitative conduct of mass transmission in the Earth organizations [23]. In the life of humans, the heat/mass transfer RTNM phenomenon plays a dynamic role to investigate the change effects on transport and pollutants, temperature in air and water, which happen due to diffusion and convection features [24, 25]. The one-dimensional steady state form of the RTNM is written as [26]:

$$\begin{aligned} Df''(\Psi) - Vf'(\Psi) - r(f) = 0, \\ 0 \le \Psi \le L, \\ f(L) = f_s, f'(\Psi_0) = 0. \end{aligned} \tag{2.1}$$

where V, $r(f)$ and D represent the advective velocity, the reaction process and diffusivity parameters, respectively. Note that (2.1) by using the expression of non–dimensional quantities, $f(x) = \dfrac{f(\Psi)}{f_s}$, $x = \dfrac{\Psi}{L}$ and Peclet number $P = \dfrac{LV}{D}$ becomes as:

$$\begin{aligned} f''(x) - Qf'(x) - r(x) = 0, \\ 0 \le x \le 1. \end{aligned} \tag{2.2}$$

Since we want to model the transport of goods by truck in a road, in model (2.2) we must chose $L = 1$ and $Q = 0$, i.e., we remove the advective transport which is applied for porous catalyst pellets in reaction and diffusion because in our problem does not play any role. On the other hand, if we inspire ourselves in the reaction Michaelis–Menten term $r(x)$, then model (2.2) becomes as:

$$\begin{aligned} f''(x) - \frac{af(x)}{b + f(x)} = 0, \\ 0 \le x \le 1, \\ f(1) = 1, f'(0) = 0. \end{aligned} \tag{2.3}$$

where $f(x)$ means the costs that the company owner of the trucks has to move the goods from the starting point to point x, a is a parameter which measures the traffic flow situation and b is a parameter which measures the so called *efficient drive*. Solving this model we will have information on how the traffic level and the driving skills affect to the costs for the logistic company owner of the trucks.

Finally, since in 2018, Primavia was born, the union for intermodal logistics solutions between two leading companies in their sector, Primafrio and VIIA, which guarantees fast, ecological and responsible transportation. Its activity responds to the commitment to the environment, and contributes to improving the efficiency of the service by meeting the needs and demands of the current market. This joint-venture focuses its activity on international multimodal transport, a combination of road transport and rail transport specially designed for the temperature-controlled transport of fruits and vegetables between Spain and Europe, allowing for the reduction of up to 1 ton of CO2 per 1,000 kilometers traveled, which allows to not only adapt logistically but also to the needs of the emissions reduction plan of our clients and interest groups. We planned to develop a traffic model which computes de effect of the dual rail transportation and it is what we do in paper number 4 attending this demand.

Chapter 3

Original Scientific Papers

In this section we present a summary and the full context of the published papers which composes the Compendium of Publications of the current PhD Thesis.

3.1 PAPER 1

Article 1.-: M. Arshad, T. Kifayat, J.L.G. Guirao, J.M. Sánchez, A. Valverde, 2022. *Using Maxwell Distribution to Handle Selector's Indecisiveness in Choice Data: A new Latent Bayesian Choice Model.* **Applied Sciences**, **12(13)**, 6337, DOI: https://doi.org/10.3390/app12136337

EXTENDED ABSTRACT

Methodology: This research is primarily focused on pioneering innovative approaches aimed at addressing the long-standing issue of handling ties or the level of indecisiveness encountered in comparative data analysis. The central strategy in managing decision uncertainty involves meticulously applying the choice hypothesis to ensure that the overall utility remains intact even when faced with imperfect choices. To achieve our objectives, we introduce an additional parameter into the probabilistic framework developed by Maxwell, allowing us to better capture and retain the inherent indecisiveness observed in choice data. To validate the effectiveness of our model, we employ a rigorous method known as Gibbs sampling, a well-established technique within the realm of Markov chain Monte Carlo methods. **Results**: The outcomes of this research unequivocally affirm the viability and advantages of the proposed methodology when dealing with discrete comparative data, particularly when we allow for the possibility of no indecisiveness. The efficacy of our devised approach is validated across various dimensions, encompassing the estimation of preference probabilities and the evaluation of worth parameters. Additionally, it extends to the quantification of the significance of choice hierarchies, shedding light on the intricate dynamics that underlie decision-making processes. **Conclusions**: The findings of our research bring to the forefront the pivotal role played by sample size and the extent of indecisiveness present in choice data. Notably, we observe that increasing the sample size enhances estimation efficiency. For instance, when considering the largest sample size of 100, we found an average confidence interval width of 0.0097, significantly narrower than what is typically observed in contemporary samples of sizes 25 and 50. This underscores the benefits of working with larger datasets and suggests that, in the context of our proposed approach, a larger sample size leads to more precise and reliable results.

applied sciences

Article

Using Maxwell Distribution to Handle Selector's Indecisiveness in Choice Data: A New Latent Bayesian Choice Model

Muhammad Arshad [1], Tanveer Kifayat [2], Juan L. G. Guirao [3,4,*], Juan M. Sánchez [3] and Adrián Valverde [3]

1 Department of Applied Sciences, School of Science, National Textile University, Faisalabad 37610, Pakistan; muhammadarshad@ntu.edu.pk
2 Department of Computer Science, SZABIST Islamabad, Islamabad 44000, Pakistan; tanveerkifayat.qau@gmail.com
3 Department of Applied Mathematics and Statistics, Hospital de Marina, Technical University of Cartagena, 30203 Cartagena, Spain; juanmasanchezparra@gmail.com (J.M.S.); adrian_valverde12@hotmail.com (A.V.)
4 Nonlinear Analysis and Applied Mathematics (NAAM)-Research Group, Department of Mathematics, Faculty of Science, King Abdulaziz University, P.O. Box 80203, Jeddah 21589, Saudi Arabia
* Correspondence: juan.garcia@upct.es

Abstract: This research primarily aims at the development of new pathways to facilitate the resolving of the long debated issue of handling ties or the degree of indecisiveness precipitated in comparative information. The decision chaos is accommodated by the elegant application of the choice axiom ensuring intact utility when imperfect choices are observed. The objectives are facilitated by inducing an additional parameter in the probabilistic set up of Maxwell to retain the extent of indecisiveness prevalent in the choice data. The operational soundness of the proposed model is elucidated through the rigorous employment of Gibbs sampling—a popular approach of the Markov chain Monte Carlo methods. The outcomes of this research clearly substantiate the applicability of the proposed scheme in retaining the advantages of discrete comparative data when the freedom of no indecisiveness is permitted. The legitimacy of the devised mechanism is enumerated on multi-fronts such as the estimation of preference probabilities and assessment of worth parameters, and through the quantification of the significance of choice hierarchy. The outcomes of the research highlight the effects of sample size and the extent of indecisiveness exhibited in the choice data. The estimation efficiency is estimated to be improved with the increase in sample size. For the largest considered sample of size 100, we estimated an average confidence width of 0.0097, which is notably more compact than the contemporary samples of size 25 and 50.

Keywords: Bayesian approach; choices; comparative models; Maxwell distribution; preference ordering

check for updates

Citation: Arshad, M.; Kifayat, T.; Guirao, J.L.G.; Sánchez, J.M.; Valverde, A. Using Maxwell Distribution to Handle Selector's Indecisiveness in Choice Data: A New Latent Bayesian Choice Model. *Appl. Sci.* **2022**, *12*, 6337. https://doi.org/10.3390/app12136337

Academic Editors: Zhenglei He, Yi Man and Kim Phuc Tran

Received: 24 May 2022
Accepted: 17 June 2022
Published: 22 June 2022

1. Introduction

Competent decision making requires a variety of cognitive skills assisting the notion of the search for value information to enhance the working potentials, especially when dealing with a complex multifaceted environment [1]. This process demands comparing and mastering the available choices while simultaneously dealing with the practical limitations [2]. Therefore, the enchanted status of analyzing and modeling choice behaviors in the multidisciplinary research literature is of no surprise. The well-directed historic tour of [3] traced the roots of the comparative notions in seventeenth century France, where [4] advocated the use of comparative models (in a very abstract form) as a method to ensure higher levels of fairness in the electoral process. However, it was the seminal contributions of [5,6] that laid the foundational blocks communicable through mathematical rigors to encapsulate individual differences and associated choice behaviors. The aforementioned efforts instigated the idea of paired comparison (PC) experiments and brought related models into the lime light. Since then, PC methodologies have attracted the attention of many researchers from diverse fields of enquiry ranging from health surveillance to sport analysis. For example, in the past, [7] explored the applicability of PC models to evaluate the performance of industrial accessories. Furthermore, [8,9] elucidated the use of the PC approach to analyze sporting events and predict their outcomes. In the recent past, [10] argued the PC schemes were an alternative to the Likert scale for the ranking of psychological markers and indicators' evaluation. Moreover, [11,12] competently elaborated on the interlinkages coupling the choice modelling strategies and the numerous variants of rational choice theory governing the preference attitudes in political science, sociology and criminology. For comprehensive accounts documenting the utility of PC methodologies in investigative pursuit, one may also consult [13–15].

In general, comparative experiments peruse the complexity of rational decision making by providing comprehension of the vital ingredients, such as attribute-level combinations, repeated choices and utility-based trade-off, by offering mutually exclusive choice alternatives to the selectors or judges. The inherent randomness of individual choices is explained by assuming the probabilistic model, whereas the associated utility is delineated through the stimuli governing the overall choice dynamics. In its simplest form the judges, say n, are asked about their preferences while pairwise comparing, say m, items, objects or individuals through a simple question, that is, "*Do you prefer item i over item j?*". One may notice the immediate relevance of the inquiry in all sorts of human behavioral assessment mechanisms. Thus, in a complete two factorial setup, each judge provides $\binom{m}{2}$ responses in regard to the above inquiry. Table 1 presents the binary string of comparative choice hierarchy recorded by a single selector or judge while conducting a paired comparison experiment.

Table 1. Hypothetical choice matrix involving single selector and m objects, Y = yes and N = No.

Objects	1	2	3	4	5	-	m
1	-	Y	Y	Y	N	-	Y
2	-	-	N	N	N	-	N
3		-	-	N	Y	-	Y
4			-	-	Y	-	Y
5				-	-	-	N
-					-	-	-
m							-

It is trivial to extend the above reported structure to the incorporation of comparative information accumulated over n selectors.

The numerous delicacies have been introduced through a rich stream of ongoing efforts in the above given simple structure, enabling choice models to deal with the complexities of real phenomena. For more recent, interesting and knowledgeable accounts of the more notable contributions, one may consult [16–19]. This article fundamentally focuses on the entertainment of selectors' indecisiveness in choice reporting, at methodological and modeling levels. The issue of handling ties in preference data has long been debated and remains a primary component of the available literature focusing on the analysis of discrete choices. The opinion chaos has rightly been summarized by [20] who noted "the key point is that modelling of ties explicitly can be important, although there is no consensus on how this should be done; no approach apart from ignoring ties appears to be in widespread use".

This article is mainly divided into five partitions. Section 2 is dedicated to documenting the mathematical foundations of the proposed procedure, whereas Section 3 provides a rigorous account of the simulation-based evaluations of the proposal while mimicking numerous experimental states. Section 4 delineates the applicability of the suggested approach while analyzing drinking water brands' choice data. Lastly, the main findings are discussed along with some future possible research avenues in Section 5.

2. Methods and Materials

2.1. Preliminaries

Let us consider that full factorial pairwise comparison set up is launched to generate comparative information among m objects by n judges, where pair of stimuli elicits a continuous discriminal process. The latent preference hierarchy between $i\prime th$ object and object j is then thought to follow one dimensional Maxwell distribution over the consistent support in the population, such as

$$f(x_i) = \sqrt{\frac{2}{\pi}} x_i^2 \frac{e^{\frac{-x_i^2}{2\theta_i^2}}}{\theta_i^3}, x_i > 0,\ \theta_i > 0,$$

and

$$f(x_j) = \sqrt{\frac{2}{\pi}} x_j^2 \frac{e^{\frac{-x_j^2}{2\theta_j^2}}}{\theta_j^3}, x_j > 0,\ \theta_j > 0. \quad (1)$$

Here, θ_i and θ_j are scale parameters of the hallmark structure connecting the probability density of the particle's kinetic energies to the temperature of the system while taking into account the configurational fluctuations of the system [21]. It is noteworthy that the traditional competency of Maxwell formation in encapsulating the atomic velocity distribution with the assumption of lacking potentials provides natural foundations to model preference stimuli while considering utility as a latent phenomenon. In the case of binary string of choice alternatives, the interest lies in the deduction of preference probabilities as a function of worth parameters dictating the comparative utility precipitation of competing objects. Mathematically, probability of preferring object i over object j that is, $(i \to j)$, remains quantifiable, such as $p_{i.ij} = P(X_i > X_j)$. Similarly, $p_{j.ij} = P(X_j > X_i)$ represents the preference probability of $(j \to i)$, as a function of estimated worth parameters [22]. Recently, [23] provided the simplified form of preference probabilities such as

$$p_{i.ij} = 1 + \frac{2}{\pi}\left[\frac{\theta_i\theta_j({\theta^2}_i - {\theta^2}_j)}{({\theta^2}_i + {\theta^2}_j)^2} - arctan \quad \frac{\theta_i}{\theta_j}\Big)\right]$$

and

$$p_{j.ij} = 1 + \frac{2}{\pi}\left[\frac{\theta_i\theta_j({\theta^2}_j - {\theta^2}_i)}{({\theta^2}_i + {\theta^2}_j)^2} + arctan\left(\frac{\theta_j}{\theta_i}\right)\right] \quad (2)$$

2.2. Proposed Model

In preference data, when ties are permitted, selectors are indeed offered three potential responses while confronting the task of choosing $(i \to j)$, those are "yes", "no" or "no preference". Thereby, it is to be noted that in the case of a balanced factorial comparative experiment, the selector responses distinguishing each pair follow trinomial distribution. For notational purposes, the preference probability of $(i \to j)$ is denoted as $p_{i.ij}$, where $p_{j.ij}$ represents preference for $(j \to i)$. The probability highlighting the extent of indistinctiveness or indecisiveness while comparing both competing objects is reported as $p_{o.ij}$, that is $(i = j)$ when no preference is given between the paired items under comparison. The accommodation of ties is proceeded in accordance with [24] proposition ensuring intact utility of [25] *choice axiom* allowing the occurrence of imperfect choices as follows

$$p_{o.ij} = \tau\sqrt{(p_{i.ij})(p_{j.ij})} \quad (3)$$

where $\tau > 0$ is the constant of proportionality representing the tie parameter and independent of the (i, j) pair, whereas preference probabilities, $p_{i.ij}$ and $p_{j.ij}$, are as given in Equation (2). Moreover, $p_{i.ij}$ and $p_{j.ij} \neq 0, 1$ and $p_{o.ij} + p_{i.ij} + p_{j.ij} = 1$. It is noteworthy that the proportionality functional in Equation (3) ensures that the probability of no preference is dependent upon the extent of distinguishability of pairs. Furthermore, the use of geometric formulation permits representation of the compared item on a linear scale when logarithmic function is applied.

Thus, by using tie adjusted formation supported by the liberty of imperfect choices and preference probability sum, it remains verifiable that the preference probability of $(i \to j)$ remains simplified as

$$p_{i.ij} = \frac{\pi\left(\theta_i^2+\theta_j^2\right)^2 + 2\left\{\left(\theta_i^3\theta_{j-}\theta_i\theta_j^3\right) - \left(\theta_i^2+\theta_j^2\right)^2 tan^{-1}\left(\frac{\theta_j}{\theta_i}\right)\right\}}{\pi\left(\theta_i^2+\theta_j^2\right)^2 + \tau\sqrt{\left[\pi\left(\theta_i^2+\theta_j^2\right)^2 + 2\left\{\left(\theta_i^3\theta_{j-}\theta_i\theta_j^3\right) - \left(\theta_i^2+\theta_j^2\right)^2 tan^{-1}\left(\frac{\theta_j}{\theta_i}\right)\right\}\right]\left[2\left\{\left(\theta_i\theta_j^3-\theta_i^3\theta_j\right) + \left(\theta_i^2+\theta_j^2\right)^2 tan^{-1}\left(\frac{\theta_j}{\theta_i}\right)\right\}\right]}} \tag{4}$$

Similarly, governed by the one dimensional Maxwell distribution, the preference probability of $(j \to i)$ is calculated as

$$p_{j.ij} = \frac{2\left\{\left(\theta_i\theta_j^3-\theta_i^3\theta_j\right) + \left(\theta_i^2+\theta_j^2\right)^2 tan^{-1}\left(\frac{\theta_j}{\theta_i}\right)\right\}}{\pi\left(\theta_i^2+\theta_j^2\right)^2 + \tau\sqrt{\left[\pi\left(\theta_i^2+\theta_j^2\right)^2 + 2\left\{\left(\theta_i^3\theta_{j-}\theta_i\theta_j^3\right) - \left(\theta_i^2+\theta_j^2\right)^2 tan^{-1}\left(\frac{\theta_j}{\theta_i}\right)\right\}\right]\left[2\left\{\left(\theta_i\theta_j^3-\theta_i^3\theta_j\right) + \left(\theta_i^2+\theta_j^2\right)^2 tan^{-1}\left(\frac{\theta_j}{\theta_i}\right)\right\}\right]}} \tag{5}$$

Furthermore, the extent of indistinguishability is estimable such as

$$p_{0.ij} = \frac{\tau\sqrt{\left[\pi\left(\theta_i^2+\theta_j^2\right)^2 + 2\left\{\left(\theta_i^3\theta_{j-}\theta_i\theta_j^3\right) - \left(\theta_i^2+\theta_j^2\right)^2 tan^{-1}\left(\frac{\theta_j}{\theta_i}\right)\right\}\right]\left[2\left\{\left(\theta_i\theta_j^3-\theta_i^3\theta_j\right) + \left(\theta_i^2+\theta_j^2\right)^2 tan^{-1}\left(\frac{\theta_j}{\theta_i}\right)\right\}\right]}}{\pi\left(\theta_i^2+\theta_j^2\right)^2 + \tau\sqrt{\left[\pi\left(\theta_i^2+\theta_j^2\right)^2 + 2\left\{\left(\theta_i^3\theta_{j-}\theta_i\theta_j^3\right) - \left(\theta_i^2+\theta_j^2\right)^2 tan^{-1}\left(\frac{\theta_j}{\theta_i}\right)\right\}\right]\left[2\left\{\left(\theta_i\theta_j^3-\theta_i^3\theta_j\right) + \left(\theta_i^2+\theta_j^2\right)^2 tan^{0-1}\left(\frac{\theta_j}{\theta_i}\right)\right\}\right]}} \tag{6}$$

In the case of m competing objects and n selectors, let $\boldsymbol{w} = \left(w_{0,ij}, w_{i,ij}, w_{j,ij}\right)$ represent the vector comprehending the observed preferences when object i is competing with object j. Additionally, n_{ij} denotes the total number of possible comparisons in r replications by n selectors, where $i \neq j; i \geq 1, j \leq m$. Then the likelihood function of realized choice data generated through the complete factorial set up consists of w trials with the permission of ties, is written as

$$l(\boldsymbol{w},\, \boldsymbol{\theta}, \boldsymbol{\tau}) = \prod\nolimits_{i<j=1}^{m} \frac{n_{ij}!}{w_{0.ij}!w_{i.ij}!(\,n_{ij}-w_{i.ij}-w_{0.ij})!} p_{0.ij}^{w_{0.ij}} p_{i.ij}^{w_{i.ij}}\; p_{j.ij}^{n_{ij}-w_{i.ij}-w_{0.ij}}, 0 < \theta_i < 1 \; and \; 0 < \tau < 1. \tag{7}$$

Here, the issue of identifiability is resolved by ensuring $\sum_{i=1}^{m} \theta_i = 1$, and θ_i is associated worth parameter attached with $i'th$ object dictating the degree of preference of the object, where $i = 1,\ 2,\ \ldots,\ m$.

2.3. Incorporating Prior Information

In this era of next generation computing hardware, the utility of prior information for the execution of more sound and knowledgeable policy interventions has gain unprecedented momentum in scientific rigors. It is noteworthy that under the considered formation, two priors are required, one to explain stochastic behavior of worth parameters and second for the capsulation of tie parameter. For demonstration, we consider informative prior in the form of Dirichlet prior for the elaboration of worth parameters as follows

$$p_D(\boldsymbol{\theta}) = \prod\nolimits_{i=1}^{m} \frac{\Gamma(d_1+d_2+\ldots+d_m)}{\Gamma d_1 \ldots \Gamma d_m} \theta_i^{d_i-1}, 0 < \theta_i < 1 \tag{8}$$

Similarly, Gamma prior is considered for the conceptualization of tie parameter as under

$$p_G(\tau) = \frac{{a_2}^{a_1}}{\Gamma a_1} \tau^{a_1-1} e^{-a_2\tau}, 0 < \tau < 1 \tag{9}$$

Here, d_i, a_1 and a_2 are the hyperparameters of the prior structure. The motivation behind the use of Dirichlet prior remains intact under the notion of parsimony, as it employs fewer number of hyperparameters and thereby is thought to be providing more concise estimates. Furthermore, the Gamma prior remains attractive for tie parameter as both distributional spaces are bounded over $(0,\ 1)$ range, and thus offers natural support to the estimation efforts.

2.4. Posterior Distribution and Estimation of the Worth Parameters

By using the prior distributions given in Equations (8) and (9) along with likelihood function of Equation (7), the joint posterior distribution is deducted as below

$$p(\theta_1, \theta_2, \ldots, \theta_m|\boldsymbol{w}) = \frac{1}{k}\prod_{i<j=1}^{m} \theta_i^{d_i-1}\tau^{a_1-1}e^{-a_2\tau}p_{0.ij}^{w_{0.ij}}p_{i.ij}^{w_{i.ij}}p_{j.ij}^{n_{ij}-w_{i.ij}-w_{0.ij}}, \tag{10}$$

where $k = \int_0^1 \int_0^{1-\theta_1} \ldots \int_{\theta_m=0}^{1-\sum_{i=1}^{m-1}\theta_i} \prod_{i<j=1}^{m} \theta_i^{d_i-1}\tau^{a_1-1}e^{-a_2\tau}p_{0.ij}^{w_{0.ij}}p_{i.ij}^{w_{i.ij}}p_{j.ij}^{n_{ij}-w_{i.ij}-w_{0.ij}}$ $d\theta_{m-1}\ldots d\theta_2 d\theta_1$ and represents the normalizing constant. The deduction of marginal posterior distributions requires the resolve of complex integrations involved in the expression of joint posterior distribution. The objective is attained by the launch of Gibbs sampling—popular approach of Markov chain Monte Carlo methods [26]. In general, Gibbs sampling proceeds by assuming $P(\underline{\theta};\underline{x})$ be the joint posterior density, where $\underline{\theta} = (\theta_1, \theta_2, \ldots, \theta_m)$. The conditional densities of worth parameters are then given by $P(\theta_1 \mathrm{I} \theta_2, \theta_3 \ldots, \theta_m), P(\theta_2 \mathrm{I} \theta_1, \theta_3 \ldots, \theta_m) \ldots$ $P(\theta_m \mathrm{I} \theta_1, \theta_2 \ldots, \theta_{m-1})$. The Gibbs sampler now initiates by assuming initial values upon worth parameters such as $\left(\theta_2{}^{(0)}, \theta_3{}^{(0)}, \ldots, \theta_m{}^{(0)}\right)$ and conceptualizes the conditional distribution of θ_1 such that $P\left(\theta_1{}^{(1)} \mathrm{I} \theta_2{}^{(0)}, \theta_3{}^{(0)}, \ldots, \theta_m{}^{(0)}\right)$. The iterative procedure continues until the convergence occurs. For demonstration purposes, the expression for the marginal posterior distribution of worth parameter associated with $m\prime th$ object, that is θ_m, is solved as follows

$$p(\theta_m|\boldsymbol{w}) = \tfrac{1}{k}\int_{\theta_1=0}^{1-\theta_m} \ldots \int_{\theta_m=0}^{1-\sum_{i=1}^{m-2}\theta_i-\theta_m} \prod_{i<j=1}^{m} \theta_i^{d_i-1}\tau^{a_1-1}e^{-a_2\tau}p_{0.ij}^{w_{0.ij}}p_{i.ij}^{w_{i.ij}}p_{j.ij}^{n_{ij}-w_{i.ij}-w_{0.ij}} d\theta_{m-1}\ldots d\theta_1, \quad 0<\theta_m<1 \tag{11}$$

The $(1-\alpha)100\%$ credible intervals attached with θ_m, say C_r, are obtained numerically by solving the given expression

$$\int p(\theta_k : \boldsymbol{x}, w, \tau)d\theta_m = 1-\alpha, \tag{12}$$

which is a subset of $\theta_m\prime s$ parametric space. Figure 1 below presents the flow diagram summarizing the working of the proposed scheme along with algorithmic advancements.

2.5. Bayes Hypothesis Testing

Now, we proceed towards the evaluation of statistical significance of the underlying comparative hierarchy. In Bayesian framework, the task is accomplished by quantifying the posterior probabilities and resultant Bayes factors associated with concerned hypothesis. The complementary hypothesis streaming pair of objects is given as

$$H_{ij} : \theta_i \geq \theta_j \,.H_{ji} : \theta_j < \theta_i.$$

The posterior probabilities deciding upon the existent discrepancies remain calculable as

$$\phi_{ij} = \int_{\zeta=0}^{1}\int_{\eta=\zeta}^{(1+\zeta)/2} P(\zeta, \eta I\omega)d\eta d\zeta, \tag{13}$$

where $\eta = \theta_i$, $\zeta = \theta_i - \theta_j$. It is trivial to show that $\phi_{ji} = 1 - \phi_{ij}$. The Bayes factor now remains estimable with straightforward operation such that $BF = \phi_{ij}/\phi_{ji}$. Generally accepted criterion nominating the degree of significance while employing Bayes factor is given as

$BF \geq 1$, support H_{ij}

$10^{-0.5} \leq \mathrm{BF} \leq 1$, minimal evidence against H_{ij}

$10^{-1} \leq BF \leq 10^{-0.5}$, substantial evidence against H_{ij}

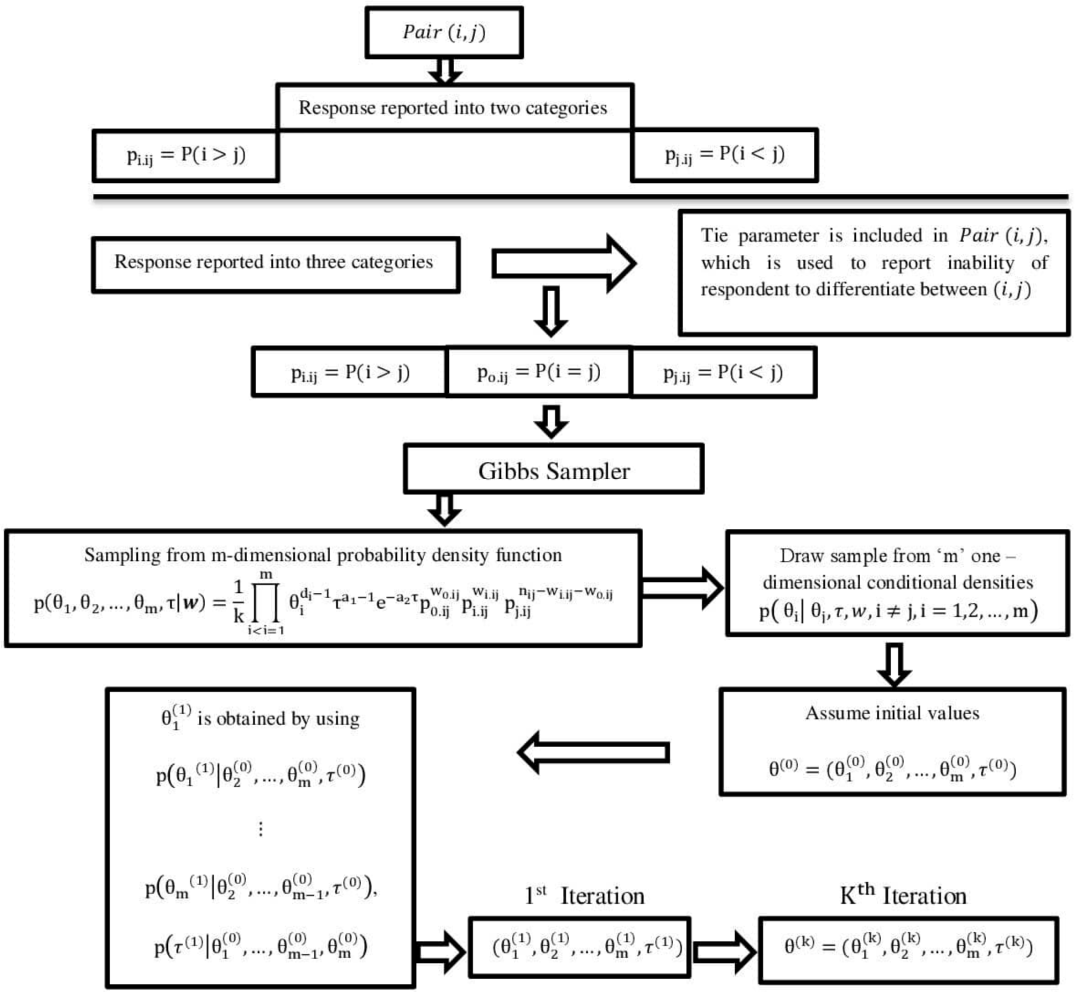

Figure 1. Flow diagram of the proposed scheme.

Figure 1. Flow diagram of the proposed scheme.

2.6. Limitations of the Proposed Scheme

It is important to note the limitations of the proposed mechanism at this stage. Our newly developed model is demonstrated to be workable for the adjustment of the response of "no choice or tie". However, the existence of ties in comparative data is not the only challenge. The choice data may suffer from two other sources of contamination that are: (i) the order of presenting the objects, most commonly known as order effect, and (ii) the tendency to report socially desirable responses while hiding the true status of the matter. It is noteworthy that the origin of these complications is different from the documented response of no choice. The indecisiveness arises from either indistinguishable nature of the competing objects or from the judge(s) lacking the capability to distinguish the objects, whereas desirability bias generates due to the fondness of the respondent(s) towards being socially acceptable or approved. On the other hand, order effect indicates the lack of

2.5. Bayes Hypothesis Testing

Now, we proceed towards the evaluation of statistical significance of the underlying comparative hierarchy. In Bayesian framework the task is accomplished by quantifying the posterior probabilities and resultant Bayes factors associated with certain hypothesis. The complementary hypothesis concerning pair of objects is given as

$$H_{ij}: \theta_i \geq \theta_j \;\; vs. \;\; H_{ij}: \theta_i < \theta_j$$

The posterior probabilities depending upon the existent discrepancies remain calculable as

$$\phi_{ij} = \int^{1} \int^{(1+\zeta)/2} P(\zeta, \eta | \omega)\, d\eta\, d\zeta, \quad (13)$$

consistency of the judge(s). Keeping the inherent differences in mind, it is anticipated that new post hoc strategy capable of entertaining aforementioned complexities, one by one or simultaneously, is desirable in future. It can be reported that the devised scheme is capable of catering ties in its present formation. However, the treatment of aforementioned challenges is an attractive future research scope.

3. Simulation-Based Evaluation

At first, rigorous simulation-based investigation is launched to explore the dynamics of the proposed scheme. The performance of the devised mechanism is studied while considering a wide range of parametric settings, including varying sample sizes and the parameter defining the extent of indecisiveness. We consider three samples as, n = 25, 50 and 100, for two values of tie parameters, that is, $\tau = 0.1$ and 0.2. These states are then studied for three competing objects, that is, $m = 3$, under a preset preference ordering where $\theta_3 > \theta_2 > \theta_1$ and $\theta_1 = 0.24$, $\theta_2 = 0.36$ and $\theta_3 = 0.40$. Table 2 presents the artificially generated data sets resulting from the aforementioned parametric settings.

Table 2. Artificial data under the preset experimental states.

n	$w_{1.12}$	$w_{2.12}$	$w_{0.12}$	$w_{1.13}$	$w_{3.13}$	$w_{0.13}$	$w_{2.23}$	$w_{3.23}$	$w_{0.23}$
				$\tau = 0.10$					
25	8	16	1	6	18	1	5	19	1
50	11	37	2	9	39	2	16	33	1
100	27	72	1	19	73	8	44	51	5
				$\tau = 0.20$					
25	5	18	2	6	17	2	10	12	3
50	15	27	8	12	34	4	19	26	5
100	19	72	9	24	73	3	37	52	11

Tables 3–5 demonstrate the relevant summaries highlighting the various performance aspects of the schemes. Table 3 provides the Bayes estimates of worth parameters along with the associated 95% credible intervals.

Table 3. Estimates of worth parameters and associated 95% credible intervals (in parenthesis) for pre-defined experimental settings.

n	$\hat{\theta}_1$	$\hat{\theta}_2$	$\hat{\theta}_3$	$\hat{\tau}$
		$\tau = 0.10$		
25	0.2549 (0.2448, 0.2651)	0.3014 (0.2905, 0.3122)	0.4437 (0.4301, 0.4571)	0.0865 (0.0728, 0.1002)
50	0.2414 (0.2330, 0.2498)	0.3403 (0.3389, 0.3415)	0.4183 (0.4091, 0.4275)	0.0911 (0.0806, 0.1016)
100	0.2491 (0.2337, 0.2494)	0.3516 (0.3508, 0.3603)	0.3992 (0.3964, 0.4022)	0.0986 (0.0933, 0.1039)
		$\tau = 0.20$		
25	0.2689 (0.2640, 0.2738)	0.3739 (0.3619, 0.3860)	0.3832 (0.3610, 0.3954)	0.1881 (0.1715, 0.2048)
50	0.2428 (0.2327, 0.2528)	0.3510 (0.3489, 0.3647)	0.3958 (0.3896, 0.4275)	0.2128 (0.1956, 0.2199)
100	0.2421 (0.2390, 0.2454)	0.3594 (0.3556, 0.3624)	0.3969 (0.3939, 0.4098)	0.1926 (0.1894, 0.2086)

Table 4. Posterior probabilities and resultant Bayes factors associated with competing hypothesis.

n	Posterior Probabilities			Bayes Factor		
	H_{12}	H_{13}	H_{23}	B_{12}	B_{13}	B_{23}
			$\tau = 0.10$			
25	0.1085	0.0001	0.0026	0.1217	0.0001	0.0026
50	0.0377	0.0002	0.0234	0.0392	0.0002	0.0240
100	0.0126	0.0001	0.0527	0.0128	0.0001	0.0557
			$\tau = 0.20$			
25	0.0006	0.0004	0.3549	0.0006	0.0004	0.5502
50	0.0039	0.0001	0.0414	0.0039	0.0001	0.0432
100	0.0005	0.0001	0.1876	0.0005	0.0001	0.2309

Table 5. Posterior preference probabilities of pairwise competing objects when ties are permitted.

n	$p_{1.12}$	$p_{2.12}$	$p_{0.12}$	$p_{1.13}$	$p_{3.13}$	$p_{0.13}$	$p_{2.23}$	$p_{3.23}$	$p_{0.23}$
					$\tau = 0.10$				
25	0.3789	0.5804	0.0405	0.1871	0.7797	0.0330	0.2607	0.7021	0.0370
50	0.2819	0.6782	0.0398	0.1885	0.7766	0.0348	0.3555	0.6022	0.0421
100	0.2802	0.6768	0.0429	0.2201	0.7399	0.0398	0.4001	0.5534	0.0464
					$\tau = 0.20$				
25	0.2295	0.6953	0.0751	0.2189	0.7069	0.0740	0.4427	0.4712	0.0859
50	0.3229	0.5846	0.0924	0.2523	0.6607	0.0869	0.3708	0.5344	0.0947
100	0.2757	0.6431	0.0811	0.2197	0.7044	0.0757	0.3857	0.5273	0.0868

The summaries presented in the above table competently indicate the legitimacy of the proposed model in retaining the predefined underlying ordering of the competing objects, that is, $\theta_3 \rightarrow \theta_2 \rightarrow \theta_1$, when ties in the discrete choice data are permitted. Additionally, it is noteworthy that the proposition competently captures the degree of indecisiveness precipitated in the comparative information. This fact is realized regardless of the varying sample sizes and different values of the tie parameter. However, a more profound performance of the approach under discussion is witnessed with an increased sample size. For example, the closest and most precise estimation of both delicacies, that is, the worth parameters and tie parameter, are witnessed for the case of $n = 100$, where the proposed scheme closely estimates the values of both the worth parameters and tie parameter. Moreover, the decreased width of the credible interval shows the precision of the procedure with which it remains capable of estimating the preset experimental states. This realization is further highlighted in Figure 2 depicting the prevalent variability in the Bayes estimates through side-by-side box plots. One may notice that minimal variation is attributed with a larger sample size.

The significance of the utility differences of the competing objects are demonstrated by quantifying the posterior probabilities and related Bayes factors for the complementary hypothesis. The results are summarized in Table 4. The establishment of a predefined preference ranking and its associated significance is observable from the calculated posterior probabilities and Bayes factors. Regardless of the varying sample sizes and the extent of indecisiveness, we witnessed maintained ordering such as, $\theta_3 \rightarrow \theta_2 \rightarrow \theta_1$; however, with different extents of associated significance. In general, we estimate that for $\tau = 0.10$, substantial evidence exists indicating that $\theta_2 \rightarrow \theta_1$, and decisive evidence is observed highlighting $\theta_3 \rightarrow \theta_1$, whereas strong evidence establishes the significance of $\theta_3 \rightarrow \theta_2$. This observation is realized for all considered sample sizes. Furthermore, in the case

Bayes estimates through side-by-side box plots. One may notice that minimal variation is attributed with a larger sample size.

of $\tau = 0.20$, strong evidence is attached with $\theta_2 \to \theta_1$ and $\theta_3 \to \theta_1$ along with strong indications of the instance of $\theta_3 \to \theta_2$.

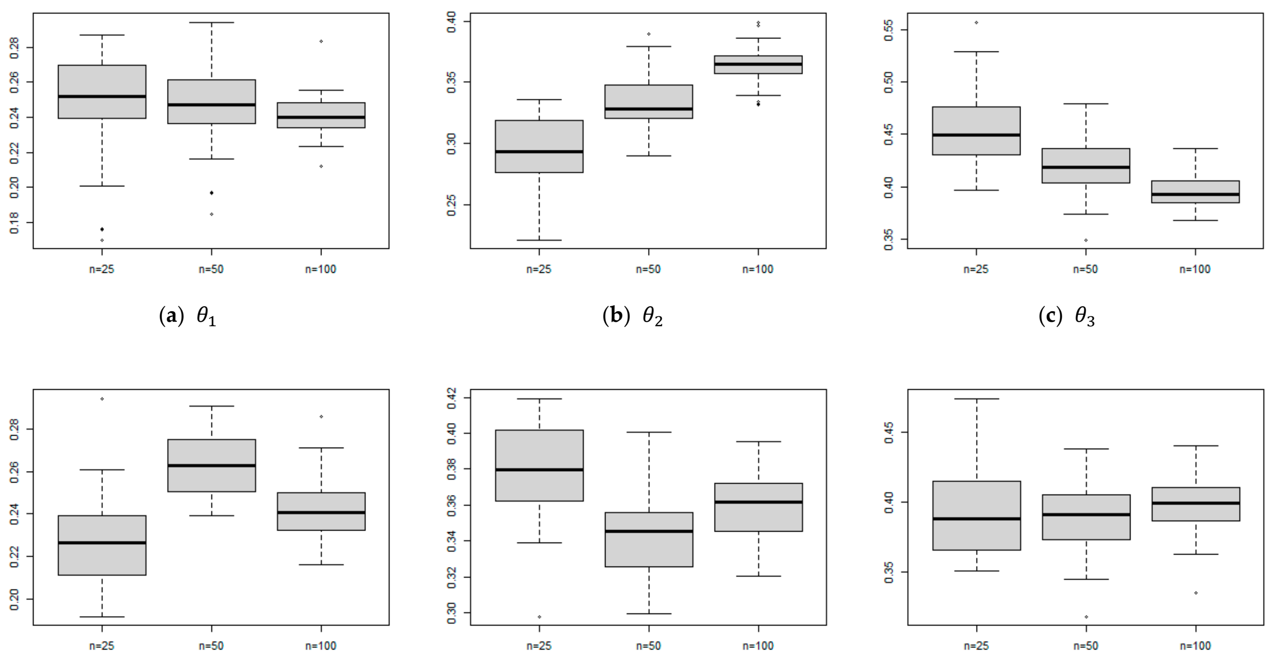

(**a**) θ_1 (**b**) θ_2 (**c**) θ_3

(**d**) θ_1 (**e**) θ_2 (**f**) θ_3

Figure 2. Side-by-side box plots depicting the extent of variability observed in the estimation of worth parameters; top panel projects the variation for $\tau = 0.10$, whereas lower panel shows the behavior for $\tau = 0.20$. The * indicates the presence of outliers.

Figure 2. Side-by-side box plots depicting the extent of variability observed in the estimation of worth parameters; top panel projects the variation for $\tau = 0.10$, whereas lower panel shows the behavior for $\tau = 0.20$. The * indicates the presence of outliers.

The estimated posterior probabilities of the preferences while pairwise comparing all three objects are assembled in Table 5. The outcomes seal the consistent behavior of the proposed mechanism.

4. Application—Preference of Drinking Water Brands

We now proceed by demonstrating the applicability of the devised model by studying the choice data of three drinking water brands commonly available in market. The pairwise comparative data with permitted ties were collected from fifty local residents of Islamabad, Pakistan, by inquiring about their preferred brand among (i)—Aquafina (AQ), (ii)—Nestle (NL) and (iii)—Kinley (KN). One may notice that in this situation $n = 50$ and $m = 3$. Table 6 displays the collected data, whereas Figure 3 depicts the distribution of counts in the relevant predefined classifications.

The significance of the utility differences of the competing objects are demonstrated by quantifying the posterior probabilities and related Bayes factors for the complementary hypothesis. The results are summarized in Table 4. The establishment of a predefined preference ranking and its associated significance is observable from the calculated posterior probabilities and Bayes factors. Regardless of the varying sample sizes and the extent of indecisiveness we witnessed maintained ordering such as $\theta_3 \to \theta_2 \to \theta_1$; however, with different extents of associated significance. In general, we estimate that for $\tau = 0.10$, substantial evidence exists indicating that $\theta_2 \to \theta_1$ and decisive evidence is observed highlighting $\theta_3 \to \theta_1$, whereas strong evidence establishes the significance of $\theta_3 \to \theta_2$. This observation is realized for all considered sample sizes. Furthermore, in the case of $\tau = 0.20$, strong evidence is attached with $\theta_2 \to \theta_1$ and $\theta_3 \to \theta_1$ along with strong indications of the instance of $\theta_3 \to \theta_2$.

The estimated posterior probabilities of the preferences while pairwise comparing all three objects are assembled in Table 5. The outcomes seal the consistent behavior of the proposed mechanism.

Table 6. Preference counts pairwise choices of the drinking water brands.

Pairs (*i,j*)	$w_{i.ij}$	$w_{j.ij}$	$w_{0.ij}$
(AQ, NT)	17	27	6
(AQ, KL)	26	19	5
(NT, KL)	28	18	4

4. Application—Preference of Drinking Water Brands

We now proceed by demonstrating the applicability of the devised model by studying the choice data of three drinking water brands commonly available in market. The pairwise comparative data with permitted ties were collected from fifty local residents of Islamabad, Pakistan, by inquiring about their preferred brand among (i)—Aquafina (AQ), (ii)—Nestle (NL) and (iii)—Kinley (KN). One may notice that in this situation $n = 50$ and

$m = 3$. Table 6 displays the collected data, whereas Figure 3 depicts the distribution of counts in the relevant predefined classifications.

Table 6. Preference counts pairwise choices of the drinking water brands.

Pairs (i, j)	$w_{i.ij}$	$w_{j.ij}$	$w_{0.ij}$
(AQ, NT)	17	27	6
(AQ, KL)	26	19	5
(NT, KL)	28	18	4

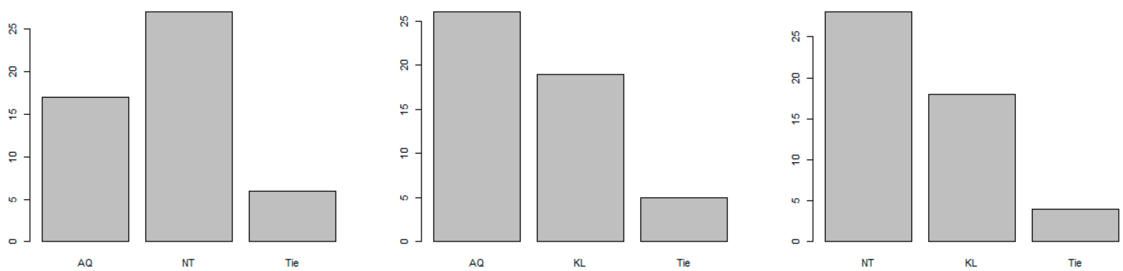

Figure 3. The distribution of discrete preferences along with counts of indecisiveness for drinking water brands' data.

We start the exploration by first eliciting the hyperparameters using confidence levels by the use of the joint posterior distribution of Equation (10) and defining the prior predictive distribution as under

$$p(w_{i.ij}, w_{0.ij}) = \int_0^1 \int_0^\infty \prod_{i<j=1}^{m} Q_{ij}\theta_i^{d_i-1}(1-\theta_i)^{d_j-1}\tau^{a_1-1}e^{-a_2\tau} p_{0.ij}^{w_{0.ij}} p_{i.ij}^{w_{i.ij}} p_{j.ij}^{n_{ij}-w_{i.ij}-w_{0.ij}} d\tau d\theta_i$$

Here, $Q_{ij} = \frac{n_{ij}!}{w_{0.ij}!w_{i.ij}!(n_{ij}-w_{i.ij}-w_{0.ij})!}\frac{\Gamma(d_i+d_j)}{\Gamma d_i \Gamma d_j}\frac{a_2^{a_1}}{\Gamma a_1}$. Ref [27] proposed the elicitation of hyperparameters through the function as follows

$$\Psi(c) = argmin_c \sum_{i=1}^{k} |(CCL)_i - (ECL)_i|,$$

where c is the set of elicited hyperparameters, whereas k represents the number interval required to elicit the hyperparameters. Additionally, $(CCL)_i$ and $(ECL)_i$ are the confidence level and elicited confidence level, respectively, characterized with the specific hyperparameter. By exploiting the joint posterior distribution, the confidence levels are given as

$$\sum_{w_{1.12}=0}^{2}\sum_{w_{0.12}=0}^{1} p(w_{1.12}, w_{0.12}) = 0.05, \sum_{w_{1.12}=3}^{5}\sum_{w_{0.12}=0}^{1} p(w_{1.12}, w_{0.12}) = 0.07,$$

$$\sum_{w_{1.13}=0}^{2}\sum_{w_{0.13}=0}^{1} p(w_{1.13}, w_{0.13}) = 0.05, \sum_{w_{1.13}=3}^{5}\sum_{w_{0.13}=0}^{1} p(w_{1.13}, w_{0.13}) = 0.07,$$

$$\sum_{w_{2.23}=0}^{2}\sum_{w_{0.23}=0}^{1} p(w_{2.23}, w_{0.23}) = 0.05, \sum_{w_{2.23}=3}^{5}\sum_{w_{0.23}=0}^{1} p(w_{2.23}, w_{0.23}) = 0.07.$$

The elicited values of the hyperparameters for both priors, that is, Dirichlet prior for worth parameters and Gamma prior for the tie parameter, are $d_1 = 2.5012$, $d_2 = 2.6595$, $d_3 = 2.7001$, $a_1 = 2.1086$ and $a_1 = 5.4596$. Table 7 presents the Bayes estimates of the worth parameters dictating the choice hierarchy of the comparative data gathered from the drinking water experiment along with the associated evidence of significance. The proposed scheme establishes the choice ranking as such: $\hat{\theta}_{NL} \rightarrow \hat{\theta}_{AQ} \rightarrow \hat{\theta}_{KL}$, indicating that most of the individuals selected in the sample preferred the Nestle brand, followed by Aquafina, whereas Kinley was the least preferred. This hierarchy can also be anticipated from the observed data. Moreover, the preference ordering is observed to be statistically significant with strong evidence associated with the instances of $\hat{\theta}_{NL} \rightarrow \hat{\theta}_{AQ}$ and $\hat{\theta}_{NL} \rightarrow \hat{\theta}_{KL}$, whereas we witnessed substantial evidence attached with $\hat{\theta}_{AQ} \rightarrow \hat{\theta}_{KL}$. These realizations are further supported by the posterior probability estimates of the comparative preferences, given in Table 8.

Table 7. Summaries of the analysis of the drinking water choice data.

Estimates				Bayes Factor	
$\hat{\theta}_i$		$\hat{\tau}_{ij}$		B_{ij}	
$\hat{\theta}_{NL}$	0.37153	$\hat{\tau}_{NL,AQ}$	0.12504	$B_{NL,AQ}$	16.181
$\hat{\theta}_{AQ}$	0.32643	$\hat{\tau}_{NL,KL}$	0.13252	$B_{NL,KL}$	56.306
$\hat{\theta}_{KL}$	0.30204	$\hat{\tau}_{AQ,KL}$	0.12878	$B_{AQ,KL}$	3.062

Table 8. Posterior preference probabilities of comparative choices.

Preference Probabilities					
$p_{NL.NL,AQ}$	0.54696	$p_{NL.NL,KL}$	0.59222	$p_{AQ.AQ,KL}$	0.51621
$p_{AQ.NL,AQ}$	0.39331	$p_{KL.NL,KL}$	0.34921	$p_{KL.AQ,KL}$	0.42357
$p_{0.NL,AQ}$	0.05973	$p_{0.NL,KL}$	0.05856	$p_{0.AQ,KL}$	0.06022

5. Discussion and Conclusions

The realization and confrontation of choices is unavoidable in every aspect of daily life. Thereby, the methods facilitating the fundamentals of choice dynamics have a long and well cherished history in the multidisciplinary research literature. It has been competently argued in the existing literature that the foundations of rational decision making stand on the essential elements of (i) ***utility***: the latent factor derived by the choice axiom [28] and (ii) ***consistency***: the extent of judgment following the axiom using inferential soundness [29]. Therefore, the search for such methods capable of entertaining both fundamentals simultaneously, has attracted noticeable attention in research circles [30]. However, the issue of handling the indecisiveness of selector(s) in reporting choice data remains long standing. There is undoubted consensus over the misleading nature of indecisive responses, but, unfortunately, the available literature lacks in its ability to demonstrate feasible solutions, especially at the methodological level. Motivated by the aforementioned factors, this article proposes a new choice model in conjunction with the Bayesian paradigm when the judge or selectors have the opportunity of reporting a "no preference" response. The proposed scheme is fundamentally advantageous in reducing the forced response bias. It is anticipated that by permitting the occurrence of ties while reporting the preferences, the selector(s) are offered extended flexibility to be able to report their true status. Moreover, by devising a workable approach, the scheme enables the investigator to estimate the influence of ties in the reported data through methodological sound pathways. The applicability of the suggested approach is affirmed on multiple fronts, such as through mathematically derived expressions, and by the launch of rigorous simulations and being demonstrated empirically. The outcomes of the research substantiate the legitimacy of the proposed mechanism, especially on four frontiers. Firstly, it is witnessed that the newly suggested model delicately maintains the inherent ordered structure of the observed choice data. This is observed with respect to all considered sample sizes and the varying extent of choice parameters. Secondly, the proposed scheme enables us to estimate the degree of indecisiveness prevalent in the comparative information. Furthermore, in concordance with asymptotic theory, the estimated subtitles become more obvious with an increased sample size. Lastly, the suggested model assists the rational decision making notions by providing sound inferential aspects facilitated through the Bayesian framework.

At this stage, it is obligatory to report the limitations of the newly developed model that offers attractive research pursuits for the future. Along with ties, the choice data show numerous concerns of practical significance such as the order of presentation of the competing objects (order effect) and socially-motivated preferences (desirability bias). If not treated appropriately, the aforementioned contaminations pose serious threats to the validity of the modeling strategies by producing misleading results. It is noteworthy that this research encapsulates the issue of ties and is not capable of entertaining other documented complexities. In future, it will be interesting to further elaborate the proposed procedure for the accommodation of order effects and desirability bias.

Author Contributions: M.A.: model statement; J.L.G.G.: model validation; T.K.: literature search and review; A.V. and J.M.S.: manuscript writing and editing. All authors have read and agreed to the published version of the manuscript.

Funding: This research was funded by Primafrio-UPCT Cátedra.

Informed Consent Statement: Not applicable.

Conflicts of Interest: The authors declare no conflict of interest.

References

1. Fischhoff, B.; Broomell, S.B. Judgment and decision making. *Annu. Rev. Psychol.* **2020**, *71*, 331–355. [CrossRef]
2. Dhami, M.K.; Mandel, D.R.; Mellers, B.A.; Tetlock, P.E. Improving Intelligence Analysis with Decision Science. *Perspect. Psychol. Sci.* **2015**, *10*, 753–757. [CrossRef]
3. Young, H.P. Condorcet's theory of voting. *Am. Pol. Sci. Rev.* **1988**, *82*, 1231–1244. [CrossRef]
4. Condorcet, M.D. *Essay on the Application of Analysis to the Probability of Majority Decisions*; Imprimerie Royale: Paris, France, 1785.
5. Thurstone, L.L. A law of comparative judgment. *Psychol. Rev.* **1927**, *34*, 273–286. [CrossRef]
6. Bradley, R.A.; Terry, M.E. Rank Analysis of Incomplete Block Designs: I. The Method of Paired Comparisons. *Biometrika* **1952**, *39*, 324. [CrossRef]
7. Mazzuchi, T.A.; Linzey, W.G.; Bruning, A. A paired comparison experiment for gathering expert judgment for an aircraft wiring risk assessment. *Reliab. Eng. Syst. Saf.* **2008**, *93*, 722–731. [CrossRef]
8. Cattelan, M.; Varin, C.; Firth, D. Dynamic Bradley–Terry modelling of sports tournaments. *J. R. Stat. Soc. Ser. C Appl. Stat.* **2013**, *62*, 135–150. [CrossRef]
9. Schauberger, G.; Tutz, G. Subject-specific modelling of paired comparison data: A lasso-type penalty approach. *Statist. Modell.* **2017**, *17*, 223–243. [CrossRef]
10. Sung, Y.-T.; Wu, J.-S. The Visual Analogue Scale for Rating, Ranking and Paired-Comparison (VAS-RRP): A new technique for psychological measurement. *Behav. Res. Methods* **2018**, *50*, 1694–1715. [CrossRef]
11. Chorus, C.G. Capturing alternative decision rules in travel choice models: A critical discussion. In *Handbook of Choice Modelling*; Hess, S., Daly, A., Eds.; Edward Elgar: Northampton, MA, USA, 2014; pp. 290–310.
12. Liebe, U.; Mariel, P.; Beyer, H.; Meyerhoff, J. Uncovering the nexus between attitudes, preferences and behavior in sociological applications of stated choice experiments. *Soc. Methods Res.* **2021**, *50*, 310–347. [CrossRef]
13. Elsenbroich, C.; Payette, N. Choosing to cooperate: Modelling public goods games with team reasoning. *J. Choice Model.* **2020**, *34*, 100203. [CrossRef]
14. Pink, S.; Kretschmer, D.; Leszczensky, L. Choice modelling in social networks using stochastic actor-oriented models. *J. Choice Model.* **2020**, *34*, 100202. [CrossRef]
15. Liebe, U.; Meyerhoff, J. Mapping potentials and challenges of choice modelling for social science research. *J. Choice Model.* **2021**, *38*, 100270. [CrossRef]
16. Borriello, A.; Rose, J.M. Global versus localised attitudinal responses in discrete choice. *Transportation* **2019**, *48*, 131–165. [CrossRef]
17. Frith, M.J. Modelling taste heterogeneity regarding offence location choices. *J. Choice Model.* **2019**, *33*, 100187. [CrossRef]
18. Feinberg, F.; Bruch, E.; Braun, M.; Falk, B.H.; Fefferman, N.; Feit, E.M.; Helveston, J.; Larremore, D.; McShane, B.B.; Patania, A.; et al. Choices in networks: A research framework. *Mark. Lett.* **2020**, *31*, 349–359. [CrossRef]
19. Leeper, T.J.; Hobolt, S.B.; Tilley, J. Measuring subgroup preferences in conjoin experiments. *Polit. Anal.* **2020**, *28*, 207–221. [CrossRef]
20. Dras, M. Evaluating Human Pairwise Preference Judgments. *Comput. Linguist.* **2015**, *41*, 337–345. [CrossRef]
21. Su, X.; Fischer, A.; Cichos, F. Towards Measuring the Maxwell–Boltzmann Distribution of a Single Heated Particle. *Front. Phys.* **2021**, *9*, 342. [CrossRef]
22. Cattelan, M. Models for Paired Comparison Data: A Review with Emphasis on Dependent Data. *Stat. Sci.* **2012**, *27*, 412–433. [CrossRef]
23. Kifayat, T.; Aslam, M.; Cheema, S.A. Maxwell paired comparison model under Bayesian paradigm using Informative priors. *Commun. Stat. Theory Methods* **2022**, *51*, 301–312. [CrossRef]
24. Davidson, R.R. On extending the Bradley-Terry model to accommodate ties in paired comparison experiments. *J. Am. Stat. Assoc.* **1970**, *65*, 317–328. [CrossRef]
25. Luce, R.D. On the possible psychophysical laws. *Psychol. Rev.* **1959**, *66*, 81–95. [CrossRef] [PubMed]
26. Jones, G.L.; Johnson, A.A. Comment: Gibbs Sampling, Exponential Families, and Orthogonal Polynomials. *Stat. Sci.* **2008**, *23*, 183–186. [CrossRef]
27. Aslam, M. An application of prior predictive distribution to elicit the prior density. *J. Stat. Theory Appl.* **2003**, *2*, 70–83.
28. Huber, J.; Payne, J.W.; Puto, C.P. Let's be Honest about the Attraction Effect. *J. Mark. Res.* **2014**, *51*, 520–525. [CrossRef]

29. Walters, D.J.; Fernbach, P.M.; Fox, C.R.; Sloman, S.A. Known Unknowns: A Critical Determinant of Confidence and Calibration. *Manag. Sci.* **2017**, *63*, 4298–4307. [CrossRef]
30. Liu, S.; Spiridonidis, C.V.; Abdulrazzqa, M. Cognitive Computational Model Using Machine Learning Algorithm in Artificial Intelligence Environment. *Appl. Math. Nonlinear Sci.* **2021**, 1–11. [CrossRef]

3.2 PAPER 2

Article 2.-: M. Arshad, S.A. Cheema, J.L.G. Guirao, J.M. Sánchez, A. Valverde, 2023. *Assisting the decision making - A generalization of choice models to handle the binary choices.* **AIMS Mathematics**, **8(2)**, 3083–3100,
DOI: http://www.aimspress.com/article/doi/10.3934/math.2023159

EXTENDED ABSTRACT

Methodology: The fundamental goal of this research is to establish a comprehensive framework that can facilitate the implementation of paired comparison models, particularly in the context of discrete binary choices. To achieve this objective, we delve into the principles of the exponential family of distributions. The proposed generalization of this framework is shown to encompass seven distinct paired comparison models, all of which are integrated into this newly developed mechanism. The credibility and effectiveness of this novel approach are substantiated through an extensive and multifaceted examination, which includes both simulation-based investigations and carefully conducted empirical evaluations. To further explore its utility and performance, we subject the framework to detailed analysis, considering a broad spectrum of parametric settings. This examination is executed under the Bayesian paradigm and employs the Gibbs Sampler, a noteworthy extension of the Markov Chain Monte Carlo methods. **Results**: The research successfully fulfills its primary objective by leveraging the foundational concepts of the exponential family of distributions. This generalization proves to be versatile, accommodating seven different paired comparison models within its framework. The soundness of this proposed scheme is established through a rigorous and multifaceted evaluation process. Simulation-based investigations as well as empirical assessments are conducted with precision, ensuring a comprehensive validation of the framework's utility. Moreover, the Bayesian analysis carried out through the Gibbs-Sampler method covers an extensive range of parametric settings, further confirming the framework's robustness and adaptability.

EXTENDED ABSTRACT

Conclusions: The findings of this research unequivocally support the legitimacy of the newly devised general framework. It not only succeeds in retaining preference orderings effectively but also aligns seamlessly with the established theoretical underpinnings of comparative models. The research serves as a significant step forward in the field of paired comparison models, providing a versatile and robust framework that can be applied to various scenarios involving discrete binary choices. Its empirical and simulation-based validation, along with the Bayesian analysis, underscore its effectiveness and suitability for a wide range of applications within the realm of comparative data analysis.

Mathematics

AIMS Mathematics, 8(2): 3083–3100.
DOI: 10.3934/math.2023159
Received: 04 July 2022
Revised: 17 September 2022
Accepted: 25 September 2022
Published: 15 November 2022

http://www.aimspress.com/journal/Math

Research article

Assisting the decision making-A generalization of choice models to handle the binary choices

Muhammad Arshad[1], Salman A. Cheema[1], Juan L.G. Guirao[2,3,*], Juan M. Sánchez[2] and Adrián Valverde[2]

[1] Department of Applied Sciences, School of Science, National Textile University, Faisalabad, Pakistan, 37610

[2] Department of Applied Mathematics and Statistics, Technical University of Cartagena, Hospital de Marina 30203-Cartagena, Spain

[3] Nonlinear Analysis and Applied Mathematics (NAAM)-Research Group, Department of Mathematics, Faculty of Science, King Abdulaziz University, P.O. Box 80203, Jeddah 21589, Saudi Arabia

* **Correspondence:** Email: juan.garcia@upct.es.

Abstract: This research fundamentally aims at providing a generalized framework to assist the launch of paired comparison models while dealing with discrete binary choices. The purpose is served by exploiting the fundaments of the exponential family of distributions. The proposed generalization is proved to cater to seven paired comparison models as members of this newly developed mechanism. The legitimacy of the devised scheme is demonstrated through rigorous simulation-based investigation as well as keenly persuaded empirical evaluations. A detailed analysis, covering a wide range of parametric settings, through the launch of Gibbs Sampler—a notable extension of Markov Chain Monte Carlo methods, is conducted under the Bayesian paradigm. The outcomes of this research substantiate the legitimacy of the devised general structure by not only successfully retaining the preference ordering but also by staying consistent with the established theoretical framework of comparative models.

Keywords: choice behaviors; comparative models; exponential family of distributions; paired comparison

Mathematics Subject Classification: 03E25

1. Introduction

The utility of paired comparison (PC) models in analyzing choice behaviors is well appreciated in various fields of research. For example, [1,2] demonstrated the applicability of PC schemes in health surveillance. Similarly, [3,4] applied PC methods to study food preferences and quality characteristics. Further, [5,6] persuaded the PC approach in the exploring the socio-political behaviors of the voters. Moreover, [7,8] employed PC models to conduct sports analysis. Recently, [9,10] elucidated the applicability of PC models in public health administration while facilitating the arduous task of project prioritization. For the account of more applications, one may see [11,12] in field of sensory analysis, [13,14] in engineering and reliability and [15,16] for measurement systems.

The PC models usually arise by considering a latent point-scoring process while conducting a pair-wise comparison among streams of objects, strategies or treatments [17]. Avoiding the literary jargon, a selector is requested to answer a simple query in "yes" or "no" fashion "do you prefer item i over item j?" while pairwise comparing a string of competing items. Table 1 below summarizes the hypothetical choice matrix comprehending the binary responses of a single selector resulting from the above inquiry while comparing m rival items. Each cell of the table documents the comparative choice of the decision maker while comparing a pair of objects specified by a certain row and column of the table. The choice strings then follow Binomial distribution where the likelihood of preferences remains estimable as a function of worth parameters defining the relative utility of competing objects.

Table 1. Choice matrix involving single decision maker and m competing items, Y = yes and N = No.

Items	*1*	*2*	*3*	*4*	*5*	-	m
1	-	Y	Y	Y	N	-	Y
2		-	N	N	N	-	N
3			-	N	Y	-	Y
4				-	Y	-	Y
5					-	-	N
-						-	-
m							-

It is trivial to extend the afore-mentioned scenario for k selectors or judges. Despite the simplistic formation, the capability of above documented contingency in facilitating the optimization of complex decision making by inter-relating non-linear functionals is well established [10,18–20].

Inspired by the subtle nature of the pre-describe design, this research aims at the proposition of a generalized framework encapsulating a broad range of choice or comparative models in a single comprehensive expression. The devised generalization is argued to be advantageous especially due to its capability to entertain various probabilistic structures governing the utility functionals as latent phenomena. The objectives are achieved by exploiting the fundaments of the exponential family of distributions. The choice of the exponential family of distribution in this regard is mainly motivated by three facts. Firstly, the family of distributions provides the fundaments of linear models and generalized linear models [21] and therefore is anticipated to offer natural support to the modeling of the binary choice data [22]. Secondly, the ability of the exponential family in encompassing of complex linear and non-linear functions is well cherished [23,24]. Lastly, the involvement of the exponential function in the estimation procedure usually results in more precise estimates [25]. The legitimacy of the proposed scheme is established through meticulously launched methodological and simulation-based operations using the Bayesian paradigm. Moreover, the inferential aspects of the suggested generalization are explored in order to derive a statistically sound and mathematically workable line of actions to attain an optimal decision-making strategy. Furthermore, the applicability of the targeted generalization is advocated by studying the water brand choice data.

This article is mainly divided into five parts. Section 2 delineates the mathematical foundations of the proposed generalization whereas section 3 reports simulation-based outcomes advocating the legitimacy of the devised scheme. Section 4 is dedicated to the empirical evaluation and lastly, section 5 summarizes the main findings in a compact manner.

2. Materials and methods

2.1. Proposed generalization

Let us say that a pairwise comparison is persuaded among m objects by n judges, where the pair of stimuli elicits a continuous discriminal process. The latent preferences of competing object i and object j are then thought to follow exponential family of distributions over the consistent support in the population, such as;

$$\mathrm{f}(\mathrm{x_i};\theta_\mathrm{i}) = \mathrm{a}(\theta_\mathrm{i})\mathrm{b}(\mathrm{x_i})\mathrm{e}^{\mathrm{g}(\mathrm{x_i})\mathrm{h}(\theta_\mathrm{i})},\ \mathrm{c} < \mathrm{x_i} < \mathrm{d},$$

and

$$\mathrm{f}(\mathrm{x_j};\theta_\mathrm{j}) = \mathrm{a}(\theta_\mathrm{j})\mathrm{b}(\mathrm{x_j})\mathrm{e}^{\mathrm{g}(\mathrm{x_j})\mathrm{h}(\theta_\mathrm{j})},\ \mathrm{c} < \mathrm{x_j} < \mathrm{d},$$

where, θ_i and θ_j are worth parameters highlighting the utility associated with respective objects. The interest lies in the deduction of precipitated preferences, such as $p_{ij} = P(X_i > X_j)$ and $p_{ji} = P(X_j > X_i)$, as a function of estimated worth parameters. We proceed by defining a general functional facilitating the estimation of preference probabilities such as;

$$\mathrm{P}(\mathrm{X_i} > \mathrm{X_j}) = \int_\mathrm{c}^\mathrm{d}\int_{\mathrm{x_j}}^\mathrm{d} \mathrm{f}(\mathrm{x_j};\theta_\mathrm{j})\ \mathrm{f}(\mathrm{x_i};\theta_\mathrm{i})\mathrm{dx_i}\mathrm{dx_j}, \tag{1}$$

where, $\int_{x_j}^{d} f(x_i;\theta_i)dx_i = F(d;\theta_i) - F(x_j;\theta_i)$. By using this expression in Eq (1), we obtained:

$$\mathrm{P}(\mathrm{X_i} > \mathrm{X_j}) = \int_\mathrm{c}^\mathrm{d} \mathrm{f}(\mathrm{x_j};\theta_\mathrm{j})\,\mathrm{F}(\mathrm{d};\theta_\mathrm{i})\mathrm{dx_j} - \int_\mathrm{c}^\mathrm{d} \mathrm{f}(\mathrm{x_j};\theta_\mathrm{j})\,\mathrm{F}(\mathrm{x_j};\theta_\mathrm{i})\mathrm{dx_j}. \tag{2}$$

For further simplification, let us denote,

$$\mathrm{A} = \int_\mathrm{c}^\mathrm{d} \mathrm{f}(\mathrm{x_j};\theta_\mathrm{j})\,\mathrm{F}(\mathrm{d};\theta_\mathrm{i})\mathrm{dx_j},$$

and

$$\mathrm{B} = \int_\mathrm{c}^\mathrm{d} \mathrm{f}(\mathrm{x_j};\theta_\mathrm{j})\,\mathrm{F}(\mathrm{x_j};\theta_\mathrm{i})\mathrm{dx_j}.$$

It remain verifiable that on solving, we get

$$\mathrm{A} = \mathrm{F}(\mathrm{d};\theta_\mathrm{i})[\mathrm{F}(\mathrm{d};\theta_\mathrm{j}) - \mathrm{F}(\mathrm{c};\theta_\mathrm{j})].$$

$$\mathrm{B} = \mathrm{F}(\mathrm{d};\theta_\mathrm{i})\,\mathrm{F}(\mathrm{d};\theta_\mathrm{j}) - \mathrm{F}(\mathrm{d};\theta_\mathrm{i})\,\mathrm{F}(\mathrm{c};\theta_\mathrm{j}) - [\mathrm{F}(\mathrm{d};\theta_\mathrm{i}) - \mathrm{F}(\mathrm{c};\theta_\mathrm{i})][\mathrm{F}(\mathrm{d};\theta_\mathrm{j}) - \mathrm{F}(\mathrm{c};\theta_\mathrm{j})].$$

The Eq (2) now becomes,

$$\mathrm{P}(\mathrm{X_i} > \mathrm{X_j}) = \mathrm{F}(\mathrm{d};\theta_\mathrm{i})[\mathrm{F}(\mathrm{d};\theta_\mathrm{j}) - \mathrm{F}(\mathrm{c};\theta_\mathrm{j})] - \mathrm{F}(\mathrm{d};\theta_\mathrm{i})\,\mathrm{F}(\mathrm{d};\theta_\mathrm{j}) + \mathrm{F}(\mathrm{d};\theta_\mathrm{i})\,\mathrm{F}(\mathrm{c};\theta_\mathrm{j}) +$$

$$[\mathrm{F}(\mathrm{d};\theta_\mathrm{i}) - \mathrm{F}(\mathrm{c};\theta_\mathrm{i})][\mathrm{F}(\mathrm{d};\theta_\mathrm{j}) - \mathrm{F}(\mathrm{c};\theta_\mathrm{j})],$$

which on further simplification reduces to,

$$P(X_i > X_j) = F(d;\theta_i)F(d;\theta_j) - F(d;\theta_i)F(c;\theta_j) - F(c;\theta_i)F(d;\theta_j) + F(c;\theta_i)F(c;\theta_j),$$

where, $F(d;\theta_i) = [1 - F(c;\theta_i)]$ and $F(d;\theta_j) = [1 - F(c;\theta_j)]$. Using these specifications, we finally achieve the general expression confirming the preference of object i over object j, as under

$$P(X_i > X_j) = 1 - 2F(c;\theta_i) - 2F(c;\theta_j) + 4\,F(c;\theta_i)F(c;\theta_j). \tag{3}$$

The two features of the devised generalized formation given in Eq (3) remain immediately noticeable. Firstly, it remains verifiable that for any permissible value of lower limit of the support, c, the above given functional reduces to 1, ensuring the ability of the general scheme in establishing the true preferences. Secondly, the preference probabilities remain estimable as a function of worth parameters ensuring the desirable character of decision making that is utility based choices. Both realizations are consistent with classic and eminent luce's choice axiom. One may also notice that the above given functional can also be derived for $P(X_j > X_i)$. Table 2, presents seven PC models based on more prominent exponential family of distributions' member which stay as special cases of aforementioned general scheme. It is to be noted that we are only considering these seven cases for demonstration purposes, in fact every PC model which arises due to the assumption that latent point process follows exponential family of distributions can be easily seen as sub-case of the proposition.

Table 2. Some of the members of proposed generalization.

Model	p.d.f.	Exponential family $f(x;\ \theta) = a(\theta)b(x)e^{g(x)h(\theta)}$	Preference probability (p_{ij})
Beta	$f(x;\ \theta) = \frac{x^{\theta-1}(1-x)}{B(\theta,\ 2)}$, $0 < x < 1$	$a(\theta) = \theta(\theta+1), b(x) = (1-x)$, $g(x) = \ln x, h(\theta) = (\theta - 1)$	$p_{ij} = \frac{\theta_i(1+\theta_i)(2+\theta_i+3\theta_j)}{(\theta_i+\theta_j)(1+\theta_i+\theta_j)(2+\theta_i+\theta_j)}$
Power	$f(x;\ \theta) = \theta x^{\theta-1}$, $0 < x < 1$	$a(\theta) = \theta, b(x) = 1$, $g(x) = \ln x, h(\theta) = (\theta - 1)$	$p_{ij} = \frac{\theta_i}{\theta_i+\theta_j}$
Exponential	$f(x;\ \theta) = \frac{1}{\theta}e^{-\frac{x}{\theta}}$, $0 < x < \infty$	$a(\theta) = \frac{1}{\theta}, b(x) = 1$, $g(x) = x, h(\theta) = \frac{1}{\theta}$	$p_{ij} = \frac{\theta_i}{\theta_i+\theta_j}$
Gamma	$f(x;\ \theta) = \frac{\theta^{\frac{1}{2}}}{\Gamma\left(\frac{1}{2}\right)}x^{\frac{1}{2}-1}e^{-\theta x}$, $0 < x < \infty$	$a(\theta) = \sqrt{\theta}, b(x) = \frac{1}{\Gamma\left(\frac{1}{2}\right)\sqrt{x}}$, $g(x) = -x, h(\theta) = \theta$	$p_{ij} = \frac{2}{\pi}\tan^{-1}\sqrt{\frac{\theta_i}{\theta_j}}$
Maxwell	$f(x;\ \theta) = \sqrt{\frac{2}{\pi}\frac{x^2}{\theta^3}}e^{-\frac{x^2}{2\theta^2}}$, $0 < x < \infty$	$a(\theta) = \frac{1}{\theta^3}, b(x) = \sqrt{\frac{2}{\pi}}x^2$, $g(x) = -\frac{x^2}{2}, h(\theta) = \frac{1}{\theta^2}$	$p_{ij} = 1 + \frac{2}{\pi}\left\{\frac{\theta_i^3\theta_j - \theta_i\theta_j^3}{(\theta_i^2+\theta_j^2)^2} - \tan^{-1}\left(\frac{\theta_j}{\theta_i}\right)\right\}$
Rayleigh	$f(x;\ \theta) = \frac{x}{\theta^2}e^{-\frac{x^2}{2\theta^2}}$, $0 < x < \infty$	$a(\theta) = \frac{1}{\theta^2}, b(x) = x$, $g(x) = -\frac{x^2}{2}, h(\theta) = \frac{1}{\theta^2}$	$p_{ij} = \frac{\theta_i^2}{\theta_i^2+\theta_j^2}$
Weibull	$f(x;\ \theta) = \frac{3x^2}{\theta^3}e^{-\frac{x^3}{\theta^3}}$, $0 < x < \infty$	$a(\theta) = \frac{1}{\theta^3}, b(x) = 3x^2$, $g(x) = -x^3, h(\theta) = \frac{1}{\theta^3}$	$p_{ij} = \frac{\theta_i^3}{\theta_i^3+\theta_j^3}$

The likelihood function, where n judges are deemed to pairwise comparison of m objects, is written by denoting n_{ij} as the total number of times object i and object j are pairwise compared. Also, let us represent, $\underline{r} = (r_{ij}, r_{ji})$ as a vector comprises of the observed preference data in $k'th$ repetition, when $i \neq j$, $i \geq 1$ and $j \leq m$. Based on these specifications, the likelihood function encompassing the preferences of n judges pairwise comparing m objects, is written as under:

$$\mathrm{l}(\underline{\mathrm{r}}, \underline{\theta}) = \prod_{\mathrm{i<j=1}}^{\mathrm{m}} \frac{\mathrm{n_{ij}!}}{\mathrm{r_{ij}!(n_{ij}-r_{ij})!}} \mathrm{p_{ij}^{r_{ij}}}\ \mathrm{p_{ji}^{n_{ij}-r_{ij}}}, \tag{4}$$

where, $p_{ji} = 1 - p_{ij}$ and $\underline{\mathrm{r}}$ represents the preference vector along with $\underline{\theta}$ denoting the vector of worth parameters. As a fact, the number of worth parameters stays equal to the number of objects to be compared, such that $\sum_{i=1}^{m} \theta_i = 1$. The imposed condition resolves the issue of non-identifiability.

2.2. Estimation of worth parameters

The estimation of worth parameters is persuaded under the Bayesian paradigm – well cherished to channelize the historic information in order to enrich the analytical environment and thus assists the estimation procedure. For demonstration purposes, we consider two prior distributions, that is Jeffreys Prior and Uniform Prior.

2.2.1. The Posterior Distribution under the Jeffreys Prior

The kernel of Jeffreys prior for $\underline{\theta}$; $(\theta_1, \theta_2, \theta_3, \dots, \theta_m)$ is written as follows:

$$\mathrm{p_J}(\theta_1, \theta_2, \theta_3, \dots, \theta_m) \propto \sqrt{\det[\mathrm{I}(\theta_1, \theta_2, \theta_3, \dots, \theta_m)]}, \qquad 0 < \underline{\theta} < 1.$$

where, $\det[\mathrm{I}(\underline{\theta})] = (-1)^{\mathrm{m}-1} \begin{vmatrix} \mathrm{E}\left[\frac{\partial^2 \ln \mathrm{L}(.)}{\partial \theta_1^2}\right] & \mathrm{E}\left[\frac{\partial^2 \ln \mathrm{L}(.)}{\partial \theta_1 \partial \theta_2}\right] \dots & \mathrm{E}\left[\frac{\partial^2 \ln \mathrm{L}(.)}{\partial \theta_1 \partial \theta_{m-1}}\right] \\ \mathrm{E}\left[\frac{\partial^2 \ln \mathrm{L}(.)}{\partial \theta_2 \partial \theta_1}\right] & \mathrm{E}\left[\frac{\partial^2 \ln \mathrm{L}(.)}{\partial \theta_2^2}\right] \dots & \mathrm{E}\left[\frac{\partial^2 \ln \mathrm{L}(.)}{\partial \theta_2 \partial \theta_{m-1}}\right] \\ \vdots & \vdots & \vdots \\ \mathrm{E}\left[\frac{\partial^2 \ln \mathrm{L}(.)}{\partial \theta_{m-1} \partial \theta_1}\right] & \mathrm{E}\left[\frac{\partial^2 \ln \mathrm{L}(.)}{\partial \theta_{m-1} \partial \theta_2}\right] \dots & \mathrm{E}\left[\frac{\partial^2 \ln \mathrm{L}(.)}{\partial \theta_{m-1}^2}\right] \end{vmatrix}$. The estimability of the worth parameter associated with $m'th$ object is conferred by ensuring that $\theta_m = 1 - \theta_1 - \theta_2 \dots - \theta_{m-1}$. The joint posterior distribution for $\theta_1, \theta_2, \dots, \theta_m$ is then written as:

$$\mathrm{p_J}(\theta_1, \theta_2, \dots, \theta_m | \mathbf{r}) = \frac{1}{k} \prod_{\mathrm{i<j=1}}^{\mathrm{m}} \mathrm{p_J}(\theta_1, \theta_2, \theta_3, \dots, \theta_m) \mathrm{p_{ij}^{r_{ij}}}\ \mathrm{p_{ji}^{n_{ij}-r_{ij}}}. \tag{5}$$

Here, $k = \int_0^1 \int_0^{1-\theta_1} \dots \int_0^{1-\theta_1 \dots - \theta_{m-1}} \mathrm{p_J}(\theta_1, \theta_2, \theta_3, \dots, \theta_m) \mathrm{p_{ij}^{r_{ij}}}\ \mathrm{p_{ji}^{n_{ij}-r_{ij}}} d\theta_{m-1} \dots d\theta_2 d\theta_1$ and is known as normalizing constant while obliging the above given constraint, such as $\theta_m = 1 - \sum_{i=1}^{m-1} \theta_i$. Also, n_{ij} represents the frequency of pair-wise comparisons by selectors and r_{ij} denotes the frequency of referring object i over object j. The joint posterior distribution of Eq (5) is not of closed form, therefore Bayes estimates are attained by employing Gibbs sampler – a well cherished procedure of MCMC methods [26- 28]. The marginal posterior distributions (MPDs) of parameters determining the comparative worth of each object are achieved by iteratively conditioning on interim value in a continuous cycle. Let $p_J(\underline{\theta}; \underline{r})$ be the joint posterior density, where $\underline{\theta} = (\theta_1, \theta_2, \dots, \theta_m)$, then the conditional densities are given by, $p_J(\theta_1 \mathrm{I} \theta_2, \theta_3 \dots, \theta_m)$, $p_J(\theta_2 \mathrm{I} \theta_1, \theta_3 \dots, \theta_m)$ $\dots p_J(\theta_m \mathrm{I} \theta_1, \theta_2 \dots, \theta_{m-1})$. According to the Gibbs sampler, we assume initial values such as

$\left(\theta_2{}^{(0)}, \theta_3{}^{(0)}, \dots, \theta_m{}^{(0)}\right)$ and pursue the conditional distribution of θ_1 such that $p_J\left(\theta_1{}^{(1)} \mathrm{I} \theta_2{}^{(0)}, \theta_3{}^{(0)}, \dots, \theta_m{}^{(0)}\right)$. The iterative procedure will continue until it converges. Here, for demonstration purposes, we provide the expression of MPD of θ_m, as follows,

$$\mathrm{p}(\theta_\mathrm{m}|\mathrm{r}) = \frac{1}{k}\int_{\theta_1=0}^{1-\theta_\mathrm{m}} \dots \int_{\theta_\mathrm{m}=0}^{1-\sum_{i=1}^{m-2}\theta_\mathrm{i}-\theta_\mathrm{m}} \prod_{i<j=1}^{m-1} \mathrm{p}_\mathrm{J}(\theta_1, \theta_2, \theta_3, \dots, \theta_m)\, \mathrm{d}\theta_{\mathrm{m}-1} \dots \mathrm{d}\theta_1, \tag{6}$$

$$0 < \theta_\mathrm{m} < 1$$

The MPDs of other parameters remain deductible in similar fashion.

2.2.2. The Posterior Distribution under the Uniform Prior

The Uniform prior for $\underline{\theta}$; $(\theta_1, \theta_2, \theta_3, \dots, \theta_m)$, is given as,

$$\mathrm{p_U}(\theta_1, \theta_2, \dots, \theta_\mathrm{m}) \propto 1, \underline{\theta} > 0$$

The joint posterior distribution given the preference data is now determined as,

$$\mathrm{p_U}(\theta_1, \theta_2, \dots, \theta_\mathrm{m}|\mathrm{r}) = \frac{1}{k}\prod_{i<j=1}^{m} \mathrm{p_{ij}^{r_{ij}}}\, \mathrm{p_{ji}^{n_{ij}-r_{ij}}}. \tag{7}$$

Here, the normalizing constant under the estimability condition of $\theta_m = 1 - \sum_{i=1}^{m-1}\theta_i$ takes the form such as $k = \int_0^1\int_0^{1-\theta_1} \dots \int_0^{1-\theta_1 \dots -\theta_{m-1}} \prod_{i<j=1}^{m} p_{ij}^{r_{ij}}\, p_{ji}^{n_{ij}-r_{ij}}\, d\theta_{m-1} \dots d\theta_2 d\theta_1$. Next phase provides the expression of MPD for θ_m using the above mentioned method of Gibbs sampler. The MPD is given as,

$$\mathrm{p_U}(\theta_\mathrm{m}|\mathrm{r}) = \frac{1}{\mathrm{K}}\int_{\theta_1=0}^{1-\theta_\mathrm{m}} \dots \int_{\theta_\mathrm{m}=0}^{1-\sum_{i=1}^{m-2}\theta_\mathrm{i}-\theta_\mathrm{m}} \prod_{i<j=1}^{m-2} \mathrm{p_{ij}^{r_{ij}}}\, \mathrm{p_{ji}^{n_{ij}-r_{ij}}}\, \mathrm{d}\theta_{\mathrm{m}-1} \dots \mathrm{d}\theta_1, 0 < \theta_\mathrm{m} < 1. \tag{8}$$

3. Simulation-based evaluation

We now explore the authenticity of the proposed generalization with respect to above documented seven sub-cases. The objective is persuaded through rigorous simulation investigation mimicking wide range of experimental states. Artificial comparative data sets of two sizes $n = 15$ and 50 are generated comparing three objects, that is $i = 1{,}2$ and 3. The worth parameters are pre-set as $\theta_1 = 0.5$, $\theta_2 = 0.3$ and $\theta_3 = 0.2$. This setting is considered for demonstration purposes only, one can use other settings also. Table 3, presents the data under afore-mentioned settings. The Bayes estimates of worth parameters, estimated preference probabilities and Bayes factor are provided under both priors and for all considered sub-cases of the devised generalization. A detail account of the findings is documented in upcoming sections.

Table 3. Artificial data sets generated under above documented specifications.

	$n_{ij} = 15$		$n_{ij} = 50$	
(i, j)	r_{ij}	r_{ji}	r_{ij}	r_{ji}
(1, 2)	10	5	32	18
(1, 3)	9	6	38	12
(2, 3)	11	4	28	22

3.1. Discussion of MPDs

Figure 1 (a–n) presents the graphical display of the MPDs of worth parameters through side-by-side box plots. The behavior is depicted for both priors, that is Jefferys prior and Uniform priors, while covering sample of sizes $n = 15$ and $n = 50$. The delicacies of displayed outcomes are read with respect to different resultant sub-cases of the proposed family and both sample sizes. Firstly, through side-by-side box plots, it is observed that as the sample size increases more compact behavior of MPDs is observed. This is seen regardless of the considered prior distribution and sub-cases of the proposed family. Furthermore, Uniform prior is found to stand out in terms of the generation of the number of outliers. In most cases, the Uniform prior is noticed to produce a lesser extent of outliers as compared to contemporary prior model of Jefferys. It is thought that the tendency of Uniform prior to outperform Jefferys prior on this front lies in its capability of deducing the same amount of information from the data but through a more parsimonious layout.

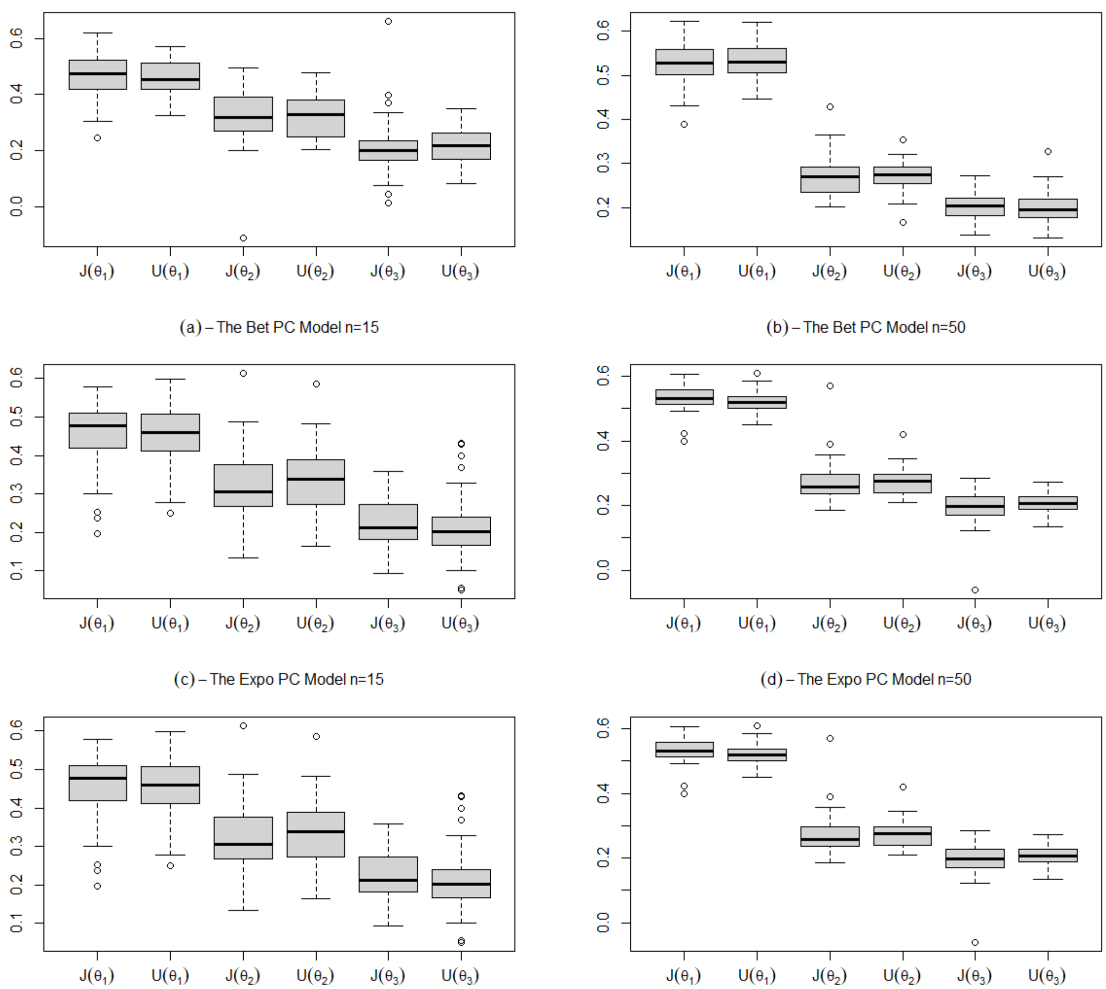

(a) – The Bet PC Model n=15

(b) – The Bet PC Model n=50

(c) – The Expo PC Model n=15

(d) – The Expo PC Model n=50

(e) – The Power PC Model n=15

(f) – The Power PC Model n=50

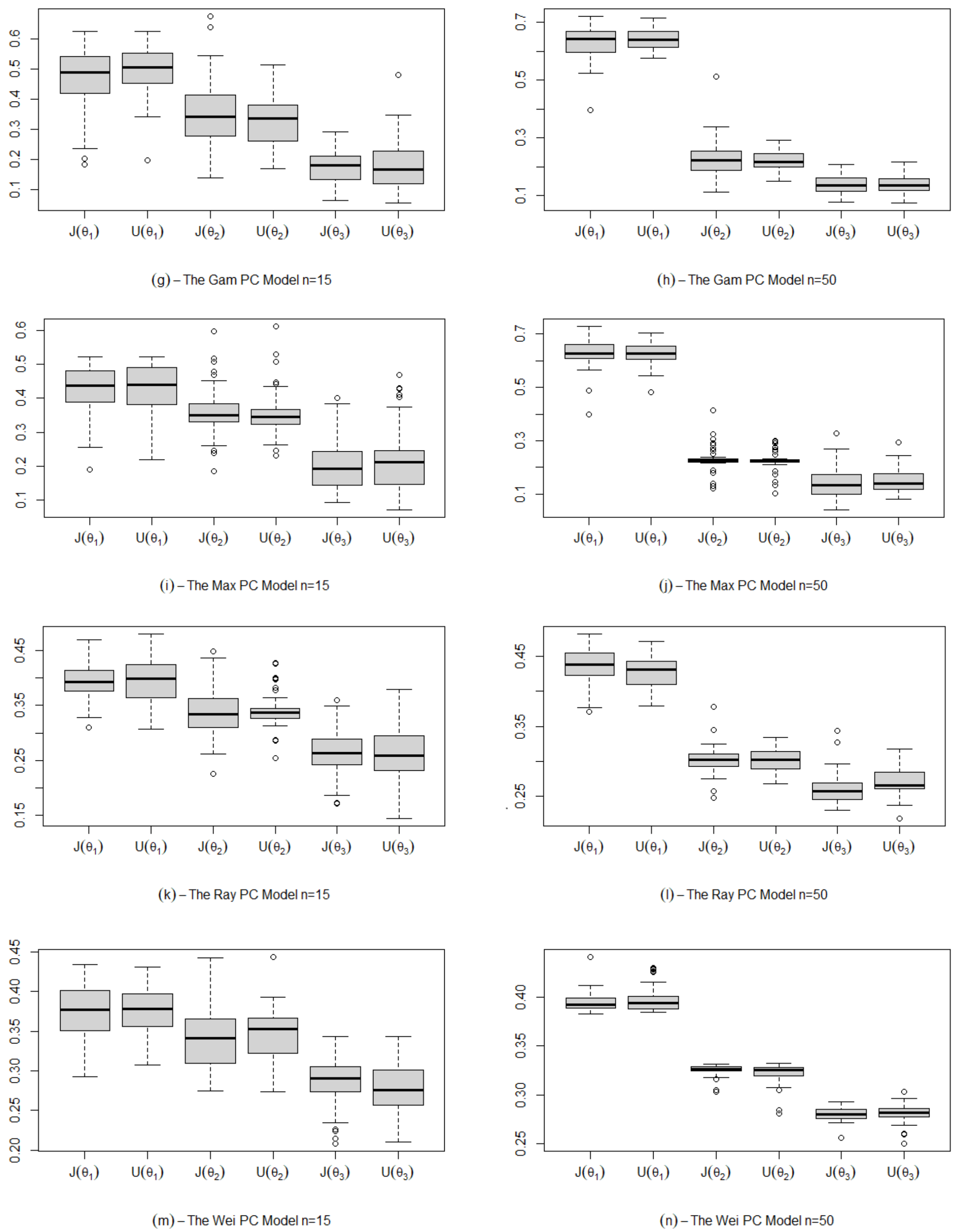

Figure 1. Display of MPDs of worth parameters under both priors and for both sample sizes. Here $J(\theta_i)$ and $U(\theta_i)$ represent MPDs under Jeffery's prior and MPDs under Uniform prior, respectively.

3.2. Estimation of worth parameters

The estimation of worth parameters defining the utility of competing objects is facilitated by providing the posterior means of the MPDs. Table 4 comprehends the outcomes of the estimation efforts along with associated absolute differences. One may notice some interesting patterns revealed in the table. Firstly, regardless of the prior distribution, increased sample size produces more close estimates of the utility. It is important to note that the estimation performance, however, remains subject to the sub-cases of the proposed family. Moreover, the estimated worth parameters for each member remain robust towards the change in the prior distribution. This outcome remains arguable as both considered priors are non-informative and thus provide equally enriched estimation environment. As long as, model-wise estimation performance is concerned, the PC model produces the most prolific estimates and therefore is argued to be most capable in using the comparative information more rigorously. From Table 2, one may notice that the Gamma model is attributed with a more vibrant and rich utility function estimating the preference behaviors by not only involving contemporary worth parameters but also employing geometric functions. The next in line remains Exponential and Power models with equal elegancy. This outcome in fact verify the simplifications provided in the Table 2. The characterization is thought to be a result of tendency of these models to entertain the comparative behaviors by exploiting linear, product and ratio formation of the associated worth parameters through more simple manner. The Beta model is ranked third in this comparative evaluation along with Maxwell model holding the forth level in the hierarchy. Whereas, Rayleigh model and Weibull model are placed at fifth and sixth position as contestant models.

Table 4. Estimates of worth parameters and associated absolute errors.

Models	Estimators	n_{ij} =15		n_{ij} =50	
		Jeffreys	Uniform	Jeffreys	Uniform
Beta	$\widehat{\theta_1}$	0.4424	0.4424	0.5205	0.5205
	$\widehat{\theta_2}$	0.3477	0.3477	0.2783	0.2783
	$\widehat{\theta_3}$	0.2099	0.2099	0.2012	0.2012
	$\lvert\widehat{\theta_1}-\theta_1\rvert$	0.0576	0.0576	0.0205	0.0205
	$\lvert\widehat{\theta_2}-\theta_2\rvert$	0.0477	0.0477	0.0217	0.0217
	$\lvert\widehat{\theta_3}-\theta_3\rvert$	0.0099	0.0099	0.0012	0.0012
Exponential	$\widehat{\theta_1}$	0.4615	0.4465	0.5376	0.5302
	$\widehat{\theta_2}$	0.3434	0.3472	0.2710	0.2738
	$\widehat{\theta_3}$	0.1952	0.2063	0.1914	0.1960
	$\lvert\widehat{\theta_1}-\theta_1\rvert$	0.0385	0.0535	0.0376	0.0302
	$\lvert\widehat{\theta_2}-\theta_2\rvert$	0.0434	0.0472	0.0290	0.0262
	$\lvert\widehat{\theta_3}-\theta_3\rvert$	0.0048	0.0063	0.0086	0.0040
Power	$\widehat{\theta_1}$	0.4615	0.4465	0.5376	0.5302
	$\widehat{\theta_2}$	0.3434	0.3472	0.2710	0.2738
	$\widehat{\theta_3}$	0.1952	0.2063	0.1914	0.1960
	$\lvert\widehat{\theta_1}-\theta_1\rvert$	0.0385	0.0535	0.0376	0.0302
	$\lvert\widehat{\theta_2}-\theta_2\rvert$	0.0434	0.0472	0.0290	0.0262
	$\lvert\widehat{\theta_3}-\theta_3\rvert$	0.0048	0.0063	0.0086	0.0040

Continued on next page

Models	Estimators	n_{ij} =15		n_{ij} =50	
		Jeffreys	Uniform	Jeffreys	Uniform
Gamma	$\widehat{\theta_1}$	0.4872	0.4872	0.6260	0.6260
	$\widehat{\theta_2}$	0.3470	0.3470	0.2340	0.2340
	$\widehat{\theta_3}$	0.1658	0.1658	0.1400	0.1400
	$\lvert\widehat{\theta_1}-\theta_1\rvert$	0.0128	0.0128	0.1260	0.1260
	$\lvert\widehat{\theta_2}-\theta_2\rvert$	0.0470	0.0470	0.0660	0.0660
	$\lvert\widehat{\theta_3}-\theta_3\rvert$	0.0342	0.0342	0.0600	0.0600
Maxwell	$\widehat{\theta_1}$	0.4287	0.4287	0.6294	0.6294
	$\widehat{\theta_2}$	0.3748	0.3748	0.2334	0.2334
	$\widehat{\theta_3}$	0.1966	0.1966	0.1372	0.1372
	$\lvert\widehat{\theta_1}-\theta_1\rvert$	0.0713	0.0713	0.1294	0.1294
	$\lvert\widehat{\theta_2}-\theta_2\rvert$	0.0748	0.0748	0.0666	0.0666
	$\lvert\widehat{\theta_3}-\theta_3\rvert$	0.0034	0.0034	0.0628	0.0628
Rayleigh	$\widehat{\theta_1}$	0.3972	0.3962	0.4336	0.4332
	$\widehat{\theta_2}$	0.3432	0.3442	0.3074	0.3076
	$\widehat{\theta_3}$	0.2597	0.2596	0.2591	0.2592
	$\lvert\widehat{\theta_1}-\theta_1\rvert$	0.1028	0.1038	0.0664	0.0668
	$\lvert\widehat{\theta_2}-\theta_2\rvert$	0.0432	0.0442	0.0074	0.0076
	$\lvert\widehat{\theta_3}-\theta_3\rvert$	0.0597	0.0596	0.0591	0.0592
Weibull	$\widehat{\theta_1}$	0.3756	0.3761	0.3992	0.3996
	$\widehat{\theta_2}$	0.3411	0.3417	0.3174	0.3176
	$\widehat{\theta_3}$	0.2834	0.2822	0.2834	0.2829
	$\lvert\widehat{\theta_1}-\theta_1\rvert$	0.1244	0.1239	0.1008	0.1004
	$\lvert\widehat{\theta_2}-\theta_2\rvert$	0.0411	0.0417	0.0174	0.0176
	$\lvert\widehat{\theta_3}-\theta_3\rvert$	0.0834	0.0822	0.0834	0.0829

3.3. Estimation of preference probabilities

The estimated preference probabilities highlighting the degree of prevailed utility of competing objects are compiled in Table 5. The estimates verify the preference norms established through the observed magnitude of the worth parameters. It is witnessed without exception that object 1 coined with the worth value of $\theta_1 = 0.5$, is overwhelmingly preferred over the objects characterized with $\theta_2 = 0.3$ and $\theta_3 = 0.2$. Similarly, the second item nominated with $\theta_2 = 0.3$ worth of the parameter value is preferred over the third available option. Also, the extent of preferences can be seen consistent with the magnitude of worth parameters. The larger the difference in the associated worth (utility) of the objects, the clearer will be the choices. Moreover, these realizations are seen regardless of the priors and sample sizes. It is to be noted, that all the findings verify that our proposed scheme successfully maintain the common rationale underlying the PC methods along with offering a general device capable of generating various PC models through the exponential family of distributions.

Table 5. The estimates of preference probabilities.

Models	Preferences	n_{ij} =15		n_{ij} =50	
		Jeffreys	Uniform	Jeffreys	Uniform
Beta	$\widehat{p_{12}}$	0.5636	0.5636	0.6603	0.6603
	$\widehat{p_{13}}$	0.6858	0.6858	0.7311	0.7311
	$\widehat{p_{23}}$	0.6281	0.6281	0.5829	0.5829
Exponential	$\widehat{p_{12}}$	0.5734	0.5626	0.6649	0.6595
	$\widehat{p_{13}}$	0.7028	0.6840	0.7374	0.7301
	$\widehat{p_{23}}$	0.6376	0.6273	0.5861	0.5828
Power	$\widehat{p_{12}}$	0.5734	0.5626	0.6649	0.6595
	$\widehat{p_{13}}$	0.7028	0.6840	0.7374	0.7301
	$\widehat{p_{23}}$	0.6376	0.6273	0.5861	0.5828
Gamma	$\widehat{p_{12}}$	0.5535	0.5535	0.6504	0.6504
	$\widehat{p_{13}}$	0.6635	0.6635	0.7185	0.7185
	$\widehat{p_{23}}$	0.6147	0.6147	0.5806	0.5806
Maxwell	$\widehat{p_{12}}$	0.5849	0.5849	0.9313	0.9313
	$\widehat{p_{13}}$	0.8837	0.8837	0.9838	0.9838
	$\widehat{p_{23}}$	0.8414	0.8414	0.7970	0.7970
Rayleigh	$\widehat{p_{12}}$	0.5725	0.5699	0.6655	0.6648
	$\widehat{p_{13}}$	0.7005	0.6996	0.7369	0.7364
	$\widehat{p_{23}}$	0.6359	0.6374	0.5846	0.5848
Weibull	$\widehat{p_{12}}$	0.5718	0.5714	0.6655	0.6657
	$\widehat{p_{13}}$	0.6995	0.7030	0.7365	0.7381
	$\widehat{p_{23}}$	0.6355	0.6397	0.5842	0.5859

3.4. Inferential aspects

This sub-section is dedicated to delineate the attainment of rational decision making through inferentially workable scheme by the launch of sound utility theory. We proceed by drawing conjoint posterior samples of worth parameters, that is $\theta_i's$ and $\theta_j's$, using Eqs (5) and (7). The exercise is conducted under both priors, both samples and with respect to all sub-cases. Table 6 reports the respective hypothesis and their posterior probabilities. Furthermore, the extent of the significance of the dis-agreement between the worth parameters is quantified through the Bayes factor (BF). We decide between the hypothesis, H_{ij}: $\theta_i \geq \theta_j$ *vs* H_{ji}: $\theta_i < \theta_j$ by calculating the posterior probabilities, such as:

$$\mathrm{p_{ij}} = \int_{\zeta=0}^{1} \int_{\eta=\zeta}^{(1+\zeta)/2} \mathrm{p}(\zeta, \eta|\omega)\, \mathrm{d}\eta \mathrm{d}\zeta,$$

where, posterior probability of H_{ji} will be $p_{ji} = 1 - p_{ij}$. Moreover, η represents worth parameter, such as θ_i and ζ denotes the difference of utility associated with comparative strategies, such as, $\zeta = \theta_i - \theta_j$. The BF is then remains quantifiable as a ratio of the above given posterior probabilities that is, $BF = p_{ij}/p_{ji}$ through well known criteria highlighting the degree of dis-agreement between hypotheses as:

$$BF \geq 1, \qquad \text{support } H_{ij}$$

$$10^{-0.5} \leq BF \leq 1, \qquad \text{minimal evidence against } H_{ij}$$

$$10^{-1} \leq BF \leq 10^{-0.5}, \quad \text{substantial evidence against } H_{ij}$$

$$10^{-2} \leq BF \leq 10^{-1}, \quad \text{strong evidence against } H_{ij}$$

$$BF \leq 10^{-2}, \quad \text{decisive evidence against } H_{ij}.$$

Through Table 6, we observe that, the pre-fix preference ordering, that is $\theta_1 > \theta_2 > \theta_3$, remains maintained with overwhelming statistical evidences. This outcome is vividly observable through the table, regardless of priors and for both sample sizes with respect to all sub-cases. Moreover, as the mutual difference of the worth parameters increases, the evidence of choice ordering moves from being substantial to decisive. These findings are consistent with usual PC theory and thus validate the legitimacy of the proposed strategy.

Table 6. Posterior probabilities of hypotheses and associated Bayes factor.

Models	Hypotheses	n_{ij} =15				n_{ij} =50			
		Jeffreys		Uniform		Jeffreys		Uniform	
		P_{ij}	BF	P_{ij}	BF	P_{ij}	BF	P_{ij}	BF
Beta	$H_{12}: \theta_1 \geq \theta_2$	0.7331	2.7467	0.7234	2.6153	0.9975	399.0000	0.9971	343.8276
	$H_{13}: \theta_1 \geq \theta_3$	0.9696	31.8947	0.9671	29.3951	0.9999	9999.0000	0.9999	9999.0000
	$H_{23}: \theta_2 \geq \theta_3$	0.8958	8.5969	0.8882	7.9445	0.9209	11.6422	0.9082	9.8932
Exponential	$H_{12}: \theta_1 \geq \theta_2$	0.7320	2.7313	0.7228	2.6075	0.9975	399.0000	0.9971	343.8276
	$H_{13}: \theta_1 \geq \theta_3$	0.9691	31.3625	0.9666	28.9401	0.9999	9999.0000	0.9999	9999.0000
	$H_{23}: \theta_2 \geq \theta_3$	0.8954	8.5602	0.8879	7.9206	0.9207	11.6103	0.9081	9.8932
Power	$H_{12}: \theta_1 \geq \theta_2$	0.7320	2.7313	0.7228	2.6075	0.9975	399.0000	0.9971	343.8276
	$H_{13}: \theta_1 \geq \theta_3$	0.9691	31.3625	0.9666	28.9401	0.9999	9999.0000	0.9999	9999.0000
	$H_{23}: \theta_2 \geq \theta_3$	0.8954	8.5602	0.8879	7.9206	0.9207	11.6103	0.9081	9.8932
Gamma	$H_{12}: \theta_1 \geq \theta_2$	0.7218	2.5945	0.7156	2.5162	0.9968	311.5000	0.9965	284.7143
	$H_{13}: \theta_1 \geq \theta_3$	0.9626	25.7380	0.9606	24.3807	0.9999	9999.0000	0.9999	9999.0000
	$H_{23}: \theta_2 \geq \theta_3$	0.8876	7.8968	0.8816	7.4459	0.9175	11.1212	0.9066	9.7066
Maxwell	$H_{12}: \theta_1 \geq \theta_2$	0.7379	2.8153	0.7135	2.4904	0.9977	433.7826	0.9967	302.0303
	$H_{13}: \theta_1 \geq \theta_3$	0.9730	36.0370	0.9676	29.8642	0.9999	9999.0000	0.9999	9999.0000
	$H_{23}: \theta_2 \geq \theta_3$	0.9008	9.0806	0.8852	7.7108	0.9217	11.7714	0.8961	8.6246
Rayleigh	$H_{12}: \theta_1 \geq \theta_2$	0.7398	2.8432	0.7212	2.5868	0.9977	433.7826	0.9969	321.5806
	$H_{13}: \theta_1 \geq \theta_3$	0.9730	36.0370	0.9688	31.0513	0.9999	9999.0000	0.9999	9999.0000
	$H_{23}: \theta_2 \geq \theta_3$	0.9014	9.1420	0.8890	8.0090	0.9216	11.7551	0.9020	9.2041
Weibull	$H_{12}: \theta_1 \geq \theta_2$	0.7405	2.8536	0.7118	2.4698	0.9977	433.7826	0.9964	276.7778
	$H_{13}: \theta_1 \geq \theta_3$	0.9736	36.8788	0.9674	29.6748	0.9999	9999.0000	0.9999	9999.0000
	$H_{23}: \theta_2 \geq \theta_3$	0.9023	9.2354	0.8843	7.6430	0.9211	11.6743	0.8912	8.1912

4. Empirical Evaluation: An application to water brand preference data

The applicability of the proposed generalization is demonstrated by using the water brand preference data gathered through a balance paired comparison (PC) experiment. Thirty-five households of Islamabad were requested to report their preferences for drinking water while the pairwise comparing three of leading brands of Pakistan that is, Aquafina (AQ), Nestle (NT) and Kinley (KL). Table 7 comprehends the reported choice data of the respondents. An initial analysis reveals that, when comparing AQ and NT, 40% of the respondents reported AQ as their preferred brand, whereas 60% chose NT over AQ. Further, around 63% of the participants preferred AQ brand over KL brand, where remaining 37% were of the favor of KL. Lastly, in comparison of NT and KL, almost 57% contestants favored NT, while 43% participants stayed with KL. Figure 2 depicts the choice data.

Table 7. Drinking water brand preference data.

Pairs	r_{ij}	r_{ji}	n_{ij}
$(AQ, NT = 1,2)$	14 (40%)	21 (60%)	35
$(AQ, KL = 1,3)$	22 (62.8%)	13 (37.1%)	35
$(NT, KL = 2,3)$	20 (57.1%)	15 (42.8%)	35

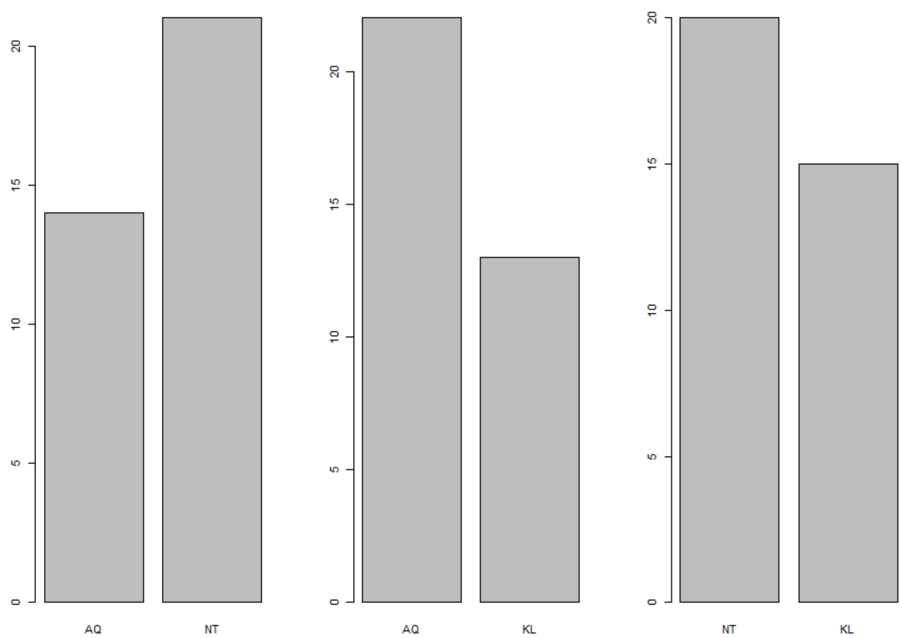

Figure 2. Graphical display of the choices of drinking water brands data.

Next, the estimation of worth parameters deriving the utility of competing brands as latent phenomena is persuaded while considering all sub-cases of the devised generalization and both prior distributions. The results related to estimated worth parameters and resultant preference probabilities are comprehended in the Table 8. Most obviously, the empirical estimation of the proposed procedure stays consistent with the simulation evaluation. Firstly, regardless of the prior distributions, all members of the suggested scheme capably retain the preferences exhibited through the comparative data. The uncovered choice hierarchy is estimated such that, $\hat{\theta}_{NT} > \hat{\theta}_{AQ} > \hat{\theta}_{KL}$ indicating Nestle as the most preferred brand followed by Aquafina which is then stayed preferable in comparison to Kinley. Secondly, all of the members showed an equally tendency of using prior information fetched from the considered prior distributions, however, intra-model variations exist. These delicacies are projected in the resulting estimated preference probabilities compiled in the Table 9. One may notice the vivid functional dependency of the preference ordering over the associated worth parameter. As the utility of the object enhances so is the extent of preference increase. The Bayes factors provided in table 10 also reveal the same trends. As the utility associated with water brands vary, so does the evidence of likely preference. For example, there is substantial evidence in the favor of NT as compared to AQ but this evidence turns to be decisive when NT is compared with KL. These variations are in fact the projection of varying degrees of comparative utility prevalent in the choices of the respondents.

Table 8. Estimated values of worth parameters.

Models	Estimated Parameters	Jeffreys	Uniform
Beta	$\hat{\theta}_{AQ}$	0.3398	0.3398
	$\hat{\theta}_{NT}$	0.4057	0.4057
	$\hat{\theta}_{KL}$	0.2544	0.2544
Exponential	$\hat{\theta}_{AQ}$	0.3414	0.3396
	$\hat{\theta}_{NT}$	0.4108	0.4091
	$\hat{\theta}_{KL}$	0.2478	0.2514
Power	$\hat{\theta}_{AQ}$	0.3414	0.3396
	$\hat{\theta}_{NT}$	0.4108	0.4091
	$\hat{\theta}_{KL}$	0.2478	0.2514
Gamma	$\hat{\theta}_{AQ}$	0.3388	0.3388
	$\hat{\theta}_{NT}$	0.4455	0.4455
	$\hat{\theta}_{KL}$	0.2157	0.2157
Maxwell	$\hat{\theta}_{AQ}$	0.3520	0.3520
	$\hat{\theta}_{NT}$	0.4137	0.4137
	$\hat{\theta}_{KL}$	0.2343	0.2343
Rayleigh	$\hat{\theta}_{AQ}$	0.3384	0.3381
	$\hat{\theta}_{NT}$	0.3723	0.3726
	$\hat{\theta}_{KL}$	0.2892	0.2893
Weibull	$\hat{\theta}_{AQ}$	0.3370	0.3369
	$\hat{\theta}_{NT}$	0.3593	0.3597
	$\hat{\theta}_{KL}$	0.3037	0.3034

Table 9. Estimated preference probabilities.

Models	Preference probabilities	Jeffreys	Uniform
Beta	$\hat{p}_{AQ,NT}$	0.4533	0.4533
	$\hat{p}_{AQ,KL}$	0.5749	0.5749
	$\hat{p}_{NT,KL}$	0.6200	0.6200
Exponential	$\hat{p}_{AQ,NT}$	0.4539	0.4536
	$\hat{p}_{AQ,KL}$	0.5794	0.5746
	$\hat{p}_{NT,KL}$	0.6237	0.6194
Power	$\hat{p}_{AQ,NT}$	0.4539	0.4536
	$\hat{p}_{AQ,KL}$	0.5794	0.5746
	$\hat{p}_{NT,KL}$	0.6237	0.6194

Continued on next page

Models	Preference probabilities	Jeffreys	Uniform
Gamma	$\hat{p}_{AQ,NT}$	0.4564	0.4564
	$\hat{p}_{AQ,KL}$	0.5710	0.5710
	$\hat{p}_{NT,KL}$	0.6127	0.6127
Maxwell	$\hat{p}_{AQ,NT}$	0.3987	0.3987
	$\hat{p}_{AQ,KL}$	0.7395	0.7395
	$\hat{p}_{NT,KL}$	0.8124	0.8124
Rayleigh	$\hat{p}_{AQ,NT}$	0.4524	0.4516
	$\hat{p}_{AQ,KL}$	0.5779	0.5773
	$\hat{p}_{NT,KL}$	0.6237	0.6239
Weibull	$\hat{p}_{AQ,NT}$	0.4521	0.4510
	$\hat{p}_{AQ,KL}$	0.5774	0.5779
	$\hat{p}_{NT,KL}$	0.6235	0.6250

Table 10. Posterior probabilities of hypotheses and associated Bayes factor.

Models	Hypotheses	$n_{ij} = 35$			
		Jeffreys		Uniform	
		P_{ij}	BF	P_{ij}	BF
Beta	H_{12}: $\theta_{AQ} \geq \theta_{NT}$	0.2297	0.2982	0.2297	0.2982
	H_{13}: $\theta_{AQ} \geq \theta_{KL}$	0.8505	5.6890	0.8505	5.6890
	H_{23}: $\theta_{NT} \geq \theta_{KL}$	0.9580	22.8095	0.9580	22.8095
Exponential	H_{12}: $\theta_{AQ} \geq \theta_{NT}$	0.2311	0.3006	0.2236	0.2880
	H_{13}: $\theta_{AQ} \geq \theta_{KL}$	0.8506	5.6934	0.8434	5.3857
	H_{23}: $\theta_{NT} \geq \theta_{KL}$	0.9579	22.7530	0.9554	21.4215
Power	H_{12}: $\theta_{AQ} \geq \theta_{NT}$	0.2311	0.3006	0.2236	0.2880
	H_{13}: $\theta_{AQ} \geq \theta_{KL}$	0.8506	5.6934	0.8434	5.3857
	H_{23}: $\theta_{NT} \geq \theta_{KL}$	0.9579	22.7530	0.9554	21.4215
Gamma	H_{12}: $\theta_{AQ} \geq \theta_{NT}$	0.2417	0.3187	0.2417	0.3187
	H_{13}: $\theta_{AQ} \geq \theta_{KL}$	0.8508	5.7024	0.8508	5.7024
	H_{23}: $\theta_{NT} \geq \theta_{KL}$	0.9561	21.7790	0.9561	21.7790
Maxwell	H_{12}: $\theta_{AQ} \geq \theta_{NT}$	0.2035	0.2555	0.2035	0.2555
	H_{13}: $\theta_{AQ} \geq \theta_{KL}$	0.8349	5.0569	0.8349	5.0569
	H_{23}: $\theta_{NT} \geq \theta_{KL}$	0.9530	20.2766	0.9530	20.2766
Rayleigh	H_{12}: $\theta_{AQ} \geq \theta_{NT}$	0.2088	0.2639	0.2118	0.2687
	H_{13}: $\theta_{AQ} \geq \theta_{KL}$	0.8393	5.2228	0.8420	5.3291
	H_{23}: $\theta_{NT} \geq \theta_{KL}$	0.9546	21.0264	0.9556	21.5225
Weibull	H_{12}: $\theta_{AQ} \geq \theta_{NT}$	0.1912	0.2364	0.1956	0.2432
	H_{13}: $\theta_{AQ} \geq \theta_{KL}$	0.8260	4.7471	0.8301	4.8858
	H_{23}: $\theta_{NT} \geq \theta_{KL}$	0.9497	18.8807	0.9512	14.9.4918

5. Conclusions

This research elucidates the proposition of a generalized framework to assist rational decision-making while dealing with binary choices. The objectives are achieved by devising a general paired comparison modeling scheme by employing an exponential family of distributions. The methodological environment is enriched by illuminating various parametric settings such as sample size and prior distributions. Through tiresome evaluation operations, it is delineated that the suggested model is not capable of retaining the preference hierarchy exhibited through the observed data but also treats seven mainstream paired comparison models as sub-cases. It is estimated that the members of the proposed family robustly use the prior information when offered non-informative priors such as Jeffery's prior and Uniform prior. However, the deducted sub-cases reveal a varying degree of estimating accuracy. Also, the suggested generalized scheme capably elaborates the choice hierarchy among the competing objects as a function of associated utility. This realization is in fact consistent with the theoretical understanding of rational decision-making. Moreover, the inferential aspects of the model are explored in depth through the launch of the Bayesian approach. The outcomes of the investigation demonstrate with clarity that as the utility of rival objects distinguishes the statistical evidence establishing the choice ranking varies accordingly. These mentioned realizations are in support of the fondness for professional and commercial research circles exploring capable mechanisms assisting optimal decision-making by defining sound interlinks between utility theory and its inferential dynamics. Thus, it remains deducible that the study encapsulating various choice behaviors and associated utility functional in accordance with choice axioms, is worth pursuing. The estimating hierarchy of the contemporary sub-cases of the newly devised family is observed such that, $Gamma > Exponntial = Power > Beta > Maxwell > Rayleigh > Weibull.$

At this stage, it is appropriate to mention that this article demonstrates the utility of non-informative priors for the estimation of the worth parameters and directed preferences. In the future, it will be interesting to compare the dynamic behaviors of the devised family while using informative priors as well. Also, it is well known that the self-reported choice data remains vulnerable to the contaminations such as desirability bias, order effects and time-varying subtleties. A more comprehensive framework capable of handling these complexities is an attractive research pursuit.

Conflict of interest

The authors declare no conflict of interest.

Reference

1. S. Esposito, C. Pelullo, E. Agozzino, F. Attena, A paired-comparison intervention to improve quality of medical records, *J. Hosp. Adm.*, **2** (2013), 91–96. https://doi.org/10.5430/jha.v2n3p91
2. B. M. Ringham, T. A. Alonzo, J. T. Brinton, S. M. Kreidler, A. Munjal, K. E. Muller, et al., Reducing decision errors in the paired comparison of the diagnostic accuracy of screening tests with Gaussian outcomes, *BMC Med. Res. Methodol.*, **14** (2014), 37. https://doi.org/10.1186/1471-2288-14-37
3. M. E. Oakes, C. S. Slotterback, The good, the bad, and the ugly: Characteristics used by young, middle-aged, and older men and women, dieters and non-dieters to judge healthfulness of foods, *Appetite*, **38** (2002), 91–97. https://doi.org/10.1006/appe.2001.0444
4. E. Calderón, A. Rivera-Quintero, A., Xia, Y. O. Angulo, M. O'Mahony, The triadic preference test, *Food Qual. Prefer.*, **39** (2015), 8–15. https://doi.org/10.1016/j.foodqual.2014.05.016
5. R. Dittrich, R. Hatzinger, W. Katzenbeisser, Modelling dependencies in paired comparison data: A log-linear approach, *Comput. Stat. Data An.*, **40** (2002), 39–57. https://doi.org/10.1016/S0167-9473(01)00106-2
6. J. Green-Armytage, Cardinal-weighted pairwise comparison. Voting matters, **19** (2004), 6–13.

7. G. Masarotto, C. Varin, The ranking lasso and its application to sport tournaments, *Ann. Appl. Stat.*, **6** (2012), 1949–1970. https://doi.org/10.1214/12-AOAS581
8. M. Cattelan, C. Varin, D. Firth, Dynamic Bradley-Terry modelling of sports tournaments, *J. R. Stat. Soc. C-Appl.*, **62** (2013), 135–150. https://doi.org/10.1111/j.1467-9876.2012.01046.x
9. M. R. Johnson, M. Middleton, M. Brown, T. Burke, T. Barnett, Utilization of a paired comparison analysis framework to inform decision-making and the prioritization of projects and initiatives in a highly matrixed clinical research program, *J. Res. Admin.*, **1** (2019), 46–65.
10. M. Arshad, T. Kifayat, J. L. G. Guirao, J. M. Sánchez, A. Valverde, Using Maxwell Distribution to handle Selector's indecisiveness in choice data: A new latent Bayesian choice model, *Appl. Sci.*, **12** (2022), 6337. https:// doi.org/10.3390/app12136337
11. B. A. Younger, S. D. Furrer, A comparison of visual familiarization and object-examining measures of categorization in 9-month-old infants, *Infancy*, **4** (2003), 327–348. https://doi.org/10.1207/S15327078IN0403_02
12. S. Choisel, F. Wickelmaier, Evaluation of multichannel reproduced sound: Scaling auditory attributes underlying listener preference, *J. Acoust. Soc. Am.*, **121** (2007), 388–400. https://doi.org/10.1121/1.2385043
13. T. A. Mazzuchi, W. G. Linzey, A. Bruning, A paired comparison experiment for gathering expert judgment for an aircraft wiring risk assessment, *Reliab. Eng. Syst. Safe.*, **93** (2008), 722–731.
14. A. M. Amlani, E. C. Schafer, Application of paired-comparison methods to hearing aids, *Trends Amplif.*, **13** (2009), 241–259.
15. D. Beaudoin, T. Swartz, A computationally intensive ranking system for paired comparison data, *Oper. Res. Perspect.*, **5** (2018). 105–112. https://doi.org/10.1016/j.orp.2018.03.002
16. Y. T. Sung, J. S. Wu, The visual analogue scale for rating, ranking and paired-comparison (VAS-RRP): A new technique for psychological measurement, *Behavior Res. Methods*, **50** (2018), 1694–1715. https://doi.org/10.3758/s13428-018-1041-8
17. S. A. Cheema, I. L. Hudson, T. Kifayat, M. Shafqat, Kalim-ullah, A. Hussain, *A New Maxwell Paired Comparison Model: Application to a Study of the Effect of Nicotine Levels on Cigarette Brand Choices*, MODSIM 2019, Australia.
18. S. Liu, C. V. Spiridonidis, M. Abdulrazzqa, Cognitive computational model using machine learning algorithm in artificial intelligence environment., *Appl. Math. Nonlinear Sci.*, **7** (2022), 803–814. https://doi.org/10.2478/amns.2021.2.00065
19. Y. S. Liu, Z. Z. Qiu, X. C. Zhan, H. N. Liu, H. N. Gong, Study of statistical damage constitutive model of layered composite rock under triaxial compression, *Appl. Math. Nonlinear Sci.*, **6** (2021), 299–308. https://doi.org/10.2478/amns.2021.2.00048
20. X. Qi, H. Li, B. Chen, G. Altenbek, A prediction model of urban counterterrorism based on stochastic strategy, *Appl. Math. Nonlinear Sci.*, **6** (2021), 263–268. https://doi.org/10.2478/amns.2021.2.00007
21. W. Q. Duan, Z. Khan, M. Gulistan, A. Khurshid, Neutrosophic exponential distribution: Modeling and applications for complex data analysis, *Complexity*, (2021). https://doi.org/10.1155/2021/5970613
22. R. Yan, W. Tong, C. Jiaona, H. A. Alteraz, H. M. Mohamed, Evaluation of factors influencing energy consumption in water injection system based on entropy Weight-Grey correlation method, *Appl. Math. Nonlinear Sci.*, **6** (2021), 269–280. https://doi.org/10.2478/amns.2021.2.00044

23. W. Jedidi, Local asymptotic normality complexity arising in a parametric statistical levy model, *Complexity*, (2021). https://doi.org/10.1155/2021/3143324
24. Y. Lin, S. Li, K. Jia, K. L. Kingsley, The research of power allocation algorithm with lower computational complexity for non-orthogonal multiple access, *Appl. Math. Nonlinear Sci.*, **6** (2021), 79–88. https://doi.org/10.2478/amns.2021.1.00027
25. Y. Zhong, G. Ruan, E. Abozinadah, J. Jiang, Least-squares method and deep learning in the identification and analysis of Name-plates of power equipment, *Appl. Math. Nonlinear Sci.*, **7** (2022), 103–111. https://doi.org/10.2478/amns.2021.1.00055
26. X. Qiu, L. Yuan, X. Zhou, MCMC sampling estimation of Poisson-Dirichlet process mixture models, *Math. Probl. Eng.*, (2021). https://doi.org/10.1155/2021/6618548
27. L. Liu, M. Niu, D. Zhang, L. Liu, D. Frank, Optimal allocation of microgrid using a differential multi-agent multi-objective evolution algorithm, *Appl. Math. Nonlinear Sci.*, **6** (2021), 111–121.
28. C. Liu, Precision algorithms in second-order fractional differential equations, *Appl. Math. Nonlinear Sci.*, **7** (2021), 155–164. https://doi.org/10.2478/amns.2021.2.00157

3.3 PAPER 3

Article 3.-: Z. Sabir, T. Saeed, J.L.G. Guirao, J.M. Sánchez, A. Valverde, 2023. *A Swarming Meyer Wavelet Computing Approach to Solve the Transport System of Goods*. **Axioms**, **12(5)**, 456, DOI: https://doi.org/10.3390/axioms12050456

EXTENDED ABSTRACT

Methodology: The central aim of this research endeavor revolves around the intricate and highly relevant task of addressing and solving the Reactive Transport Nonlinear Model (RTNM), a complex mathematical model that plays a pivotal role in the realm of goods transportation via road. In this multifaceted exploration, the research places a particular emphasis on the analysis of two critical factors: the level of traffic flow and the behavior of the drivers involved in the transportation process. **Results**: To tackle this formidable challenge, a pioneering approach is introduced, which capitalizes on the Morlet wavelet function transformed into an Artificial Neural Network, herein referred to as the MWNN. This novel methodology takes the form of the MWNN-GA-ASAS hybrid system, where the Global/Local Search Genetic Algorithm (GA) synergistically collaborates with an Active-Set Algorithm Scheme (ASAS). The objective function that drives this hybrid system's optimization is rooted in the differential system of the RTNM and its boundary conditions. This dynamic combination of GA-ASAS within the MWNN framework contributes to the precision, reliability, and feasibility of the solutions generated for this class of nonlinear and stiff differential systems.

EXTENDED ABSTRACT

The credibility and accuracy of the MWNN-GA-ASAS system are meticulously validated by benchmarking its results against reference data, confirming its ability to provide reliable solutions to the RTNM. The research extends its scope to tackle different scenarios and variations of the RTNM, thoroughly investigating the MWNN's performance under varying conditions. A comprehensive analysis is conducted, including examinations of scenarios with both fewer and more neurons in the MWNN, to assess the scheme's adaptability and efficiency for addressing the transportation model. In addition, the research offers a rigorous statistical interpretation, which encompasses various parameters and actions, to ascertain the consistency and effectiveness of the MWNN-GA-ASAS framework. **Conclusions**: The study's conclusions carry profound implications, shedding light on the economic aspects of efficient driving in the transportation of goods via road. It becomes evident that for a given level of traffic, the efficiency of driver behavior significantly influences cost efficiency. The impact of efficient driving practices becomes even more pronounced in scenarios characterized by high traffic flow, underscoring the financial rationale for investing in driver training and education that emphasizes optimal driving practices. In summary, this research highlights the potential economic benefits that can be derived from enhancing driver behavior and promoting efficient driving practices, especially in scenarios characterized by heavy traffic flow. The reduction in transportation costs, as evidenced in this study, reinforces the economic incentive for prioritizing and investing in efficient driving methods.

axioms

MDPI

Article

A Swarming Meyer Wavelet Computing Approach to Solve the Transport System of Goods

Zulqurnain Sabir [1,2], Tareq Saeed [3], Juan L. G. Guirao [4,*], Juan M. Sánchez [4] and Adrián Valverde [4]

[1] Department of Mathematics and Statistics, Hazara University, Mansehra 21120, Pakistan
[2] Department of Computer Science and Mathematics, Lebanese American University, Beirut 11022801, Lebanon
[3] Financial Mathematics and Actuarial Science (FMAS)-Research Group, Department of Mathematics, Faculty of Science, King Abdulaziz University, P.O. Box 80203, Jeddah 21589, Saudi Arabia; tsalmalki@kau.edu.sa
[4] Department of Applied Mathematics and Statistics, Technical University of Cartagena, Hospital de Marina, 30203 Cartagena, Spain; adrian_valverde12@hotmail.com (A.V.)
* Correspondence: juan.garcia@upct.es

Abstract: The motive of this work is to provide the numerical performances of the reactive transport model that carries trucks with goods on roads by exploiting the stochastic procedures based on the Meyer wavelet (MW) neural network. An objective function is constructed by using the differential model and its boundary conditions. The optimization of the objective function is performed through the hybridization of the global and local search procedures, i.e., swarming and interior point algorithms. Three different cases of the model have been obtained, and the exactness of the stochastic procedure is observed by using the comparison of the obtained and Adams solutions. The negligible absolute error enhances the exactness of the proposed MW neural networks along with the hybridization of the global and local search schemes. Moreover, statistical interpretations based on different operators, histograms, and boxplots are provided to validate the constancy of the designed stochastic structure.

Keywords: reactive transport system; transportation; Meyer wavelet; swarming procedure; interior-point

MSC: 35Q55

check for updates

Citation: Sabir, Z.; Saeed, T.; Guirao, J.L.G.; Sánchez, J.M.; Valverde, A. A Swarming Meyer Wavelet Computing Approach to Solve the Transport System of Goods. *Axioms* **2023**, *12*, 456. https://doi.org/10.3390/axioms12050456

Academic Editor: Solomon Manukure

Received: 18 March 2023
Revised: 16 April 2023
Accepted: 23 April 2023
Published: 8 May 2023

1. Introduction

The multiscale framework in the environment represents the steady state predicated by the one-dimensional reactive transport system (RTS). The nonlinear form of the RTS is typically presented to address the problems with the soft tissue, as well as the microvascular solute transport system of fluid [1]. By performing various actions based on earth-related studies, the dynamical RTS is useful to examine biological and physical phenomena [2]. A novel hypothesis related to biology, geochemical processes, and transport, along with quantitative mass transmission, is accessible to incorporate into the field of RTS [3]. The characteristics of diffusion or convection, the transfer of heat or mass based on the phenomenon of RTS, present a dynamic form in the life of a human to examine the shifting impacts on pollutants and transport and water or air temperature [4,5]. The literature RTS form is given as [6]:

$$\begin{cases} D\frac{d^2x}{d\theta^2} - V\frac{dx}{d\theta} - r(\theta) = 0, & 0 \le \theta \le k, \\ x(k) = x_s, \quad \frac{dx(0)}{d\theta} = 0, \end{cases} \tag{1}$$

where $r(\theta)$, V, and D are the reaction process, advective velocity, and parameter of diffusivity, respectively. The system (1) shows the quantities of non-dimensional $x(y) = \frac{x(\theta)}{x_s}$, where $y = \frac{\theta}{k}$ and the Peclet number $p = \frac{Vk}{D}$ is written as:

$$\frac{d^2x}{d\theta^2} - p\frac{dx}{d\theta} - r(\theta) = 0, \quad 0 \le \theta \le 1. \tag{2}$$

The above system (2) is obtained by taking $k = 1$ and $p = 0$, i.e., without applying the advective transport form of the catalyst pellets in diffusion or reaction. Furthermore, the Michaelis–Menten reaction $r(\theta)$ is also assumed, then the system (2) takes the form of:

$$\begin{cases} \frac{d^2x}{d\theta^2} - \frac{cx(\theta)}{d+x(\theta)} = 0, & 0 \le \theta \le 1, \\ \frac{dx}{d\theta}(0) = 0, & x(1) = 1, \end{cases} \tag{3}$$

where $d > 0$ shows the half-saturated concentration and c is the distinctive reaction; the reactive rate by taking $c < 0$ is applied as an alternative reaction product. The RTS shown in Equation (2) without relating the transport values is considered, while the RTS presented in the system (3) is implemented in the modeling of the transport of fluid, which arises in the soft tissues and microvessels [7]. Equation (3) based on the RTS is solvable with different half-saturation concentration values and reaction rates.

The scientific community has offered comprehensive explanations depending on the RTS based on a variety of techniques. In 1995, Toride et al. [8,9] presented the analytical form of the solutions for the steady-state RTS. In 1982, RTS solutions were described by Van Genuchtenet et al. [10]. The nonlinear form of the RTS is presented by applying the Adomian decomposition and homotopy analysis approaches [11–14].

The current study performs the solutions of nonlinear RTS presented in Equation (3) based on the trucks of goods on roads by taking different c and d values. All of the aforementioned research has been presented using RTS and predictable analytical and numerical methodologies, each of which has a different degree of application, benefits, and shortcomings. The solutions of the RTS based on roads have been presented by exploiting the Meyer wavelet (MW) neural network. The RTS model, which carries trucks with goods on roads, has not been applied before by exploiting the MW neural network through the hybridization form of the global and local search procedures, i.e., swarming and interior-point algorithms. Recently, stochastic applications have been applied in biological systems [15], higher forms of singular systems [16,17], fractional models [18,19], prediction systems [20], thermal explosion models [21], and the food chain system [22]. These applications motivated the authors to present the solutions of the RTS using the MW neural network along with swarming and interior-point schemes. Some novel features of this study are highlighted as follows:

- The solutions of the RTS, which carry trucks with goods on roads, are presented successfully by using different values of c and d.
- The design of the MW neural network is presented along with the swarming and interior-point methods for solving the RTS.
- The exactness of the stochastic MW neural network procedure is observed through the comparison of the results.
- The reducible absolute error (AE) performance validates the exactness of the stochastic procedure.
- The reliability of the MW neural network, along with the swarming and interior-point methods, is validated by using different statistical performances.

The other parts of the paper are presented as follows: Section 2 shows the MW neural network enhanced by swarming and interior-point methods along with the statistical performances. Section 3 provides the discussion of the results. Conclusions are reported in the last section.

2. Methodology

In this section, the design of the MW neural network enhanced by the swarming and interior-point schemes is provided to solve the RTS.

2.1. Modeling: MW Neural Networks

$\hat{x}(\theta)$ and $\frac{d^{(n)}x}{d\theta^{(n)}}$ represent the proposed results and nth-order derivative, mathematically given as:

$$\begin{aligned} \hat{x}(\theta) &= \sum_{f=1}^{q} r_f L(w_f\theta + t_f), \\ \tfrac{d^{(n)}\hat{x}}{d\theta^{(n)}} &= \sum_{f=1}^{q} r_f L^{(n)}(w_f\theta + t_f). \end{aligned} \tag{4}$$

In the above framework, the neurons are signified as q, while $\boldsymbol{W} = [\boldsymbol{r}, \boldsymbol{w}, \boldsymbol{t}]$ are the unknown weights, i.e., $\boldsymbol{r} = [r_1, r_2, ..., r_q]$, $\boldsymbol{w} = [w_1, w_2, ..., w_q]$ and $\boldsymbol{t} = [t_1, t_2, ..., t_q]$. The process of the MW neural network has not been presented before for the nonlinear RTS, which carries trucks with goods on roads. The mathematical MW function form is provided as:

$$L(\theta) = 35\theta^4 - 84\theta^5 + 70\theta^6 - 20\theta^7. \tag{5}$$

An efficient form of Equation (4) based on the MW function is shown as:

$$\begin{aligned} \hat{x}(\theta) &= \sum_{f=1}^{q} r_f \Big(35(w_f\theta + t_f)^4 - 84(w_f\theta + t_f)^5 + 70(w_f\theta + t_f)^6 - 20(w_f\theta + t_f)^7\Big), \\ \tfrac{d}{d\theta}\hat{x}(\theta) &= \tfrac{d}{d\theta}\sum_{f=1}^{q} r_f \Big(35(w_f\theta + t_f)^4 - 84(w_f\theta + t_f)^5 + 70(w_f\theta + t_f)^6 - 20(w_f\theta + t_f)^7\Big), \end{aligned} \tag{6}$$

An objective function O_F using the mean square error is presented as:

$$O_F = O_{F.1} + O_{F.2}, \tag{7}$$

where $O_{F.1}$ is known as the unsupervised error, while $O_{F.2}$ presents the boundary conditions, given as:

$$O_{F.1} = \frac{1}{N}\sum_{i=1}^{N}\left(\frac{d^2\hat{x}_i}{d\theta^2} - \frac{c\hat{x}_i}{d + \hat{x}_i}\right)^2, \tag{8}$$

where $Nh = 1, \theta_i = ih, \hat{x}_i = x(\theta_i)$ and h shows the step size.

$$O_{F.2} = \frac{1}{2}\quad \left(\frac{d\hat{x}_0}{d\theta}\right)^2 + (\hat{x}_N - 1)^2\Big). \tag{9}$$

The nonlinear form of the RTS shows the unidentified weights, such as as $O_F \to 0$, and the proposed results overlap with the Adams results. The procedural steps of the scheme are presented in Figure 1. In the 1st step, the RTS is presented, which is based on the nonlinear form of the differential equations. In the 2nd step, the modeling based on the MW neural network including the unsupervised neural network and the error-based fitness function is presented. In the 3rd step, the optimization performances are presented, which are based on the global search swarming scheme, and the local search interior point is provided. In the 4th step, the data are stored based on the trained weights based on the MW neural networks, fitness valuations, time, function count, and iterations. In the last step, a comparison of the results and the statistical performances are provided.

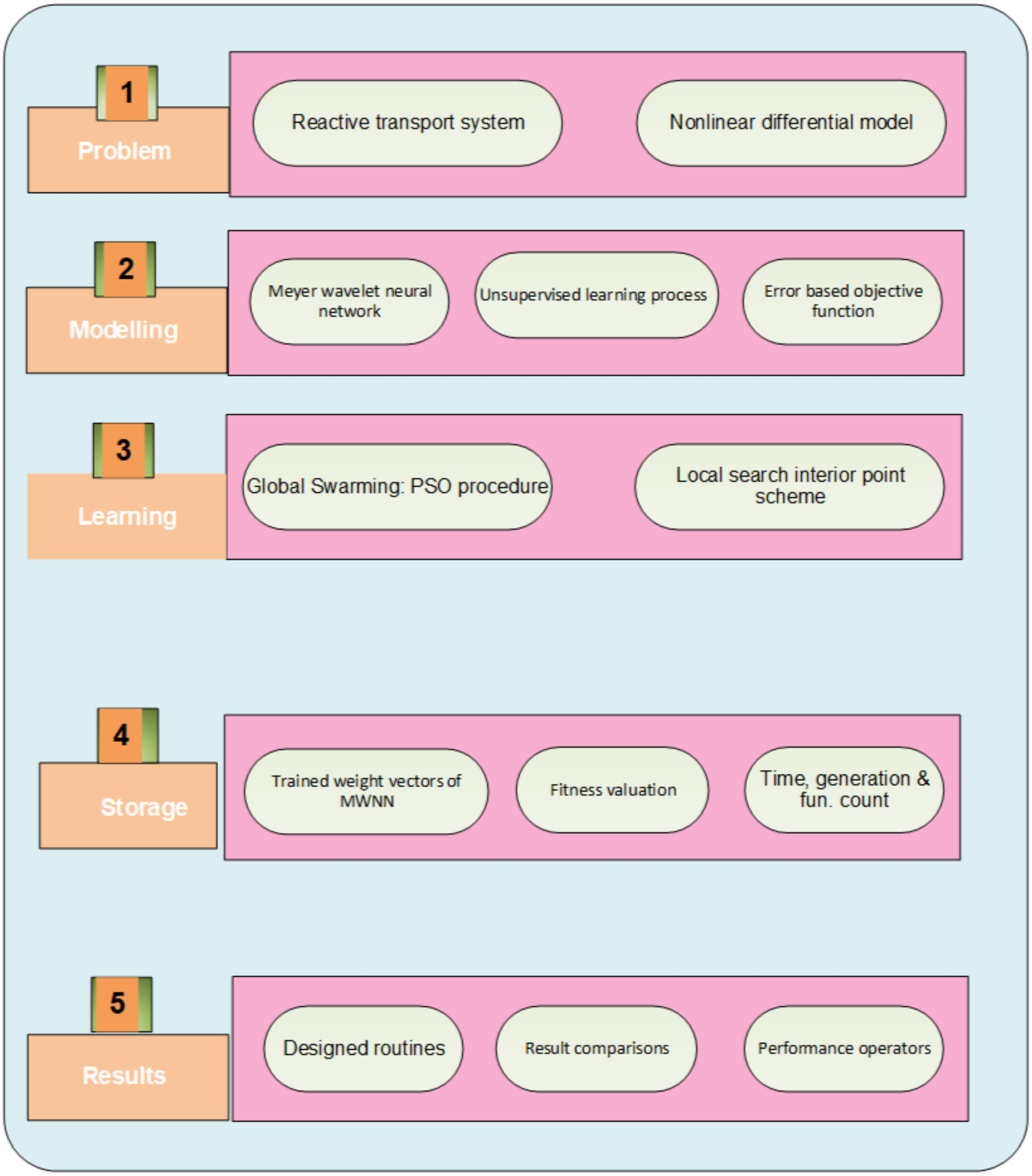

Figure 1. Procedural steps for solving the mathematical nonlinear RTS.

2.2. Optimization: Swarming and Interior Point Schemes

The current section presents the optimization performances based on the hybridization of the swarming (PSO) and interior point schemes for the RTS.

The global search genetic algorithm is modified using the swarming technique PSO. It was documented in the seventh decade of the nineteenth century. For both stiff- and non-stiff-natured situations, PSO presents the optimum solution efficiency. PSO has already been used in diverse fields, such as solar energy systems [23], the cost optimization of microgrids [24], diseased plant diagnoses [25], diode photovoltaic system organization [26], feature selection in cataloging [27], big data digging of hot topics about recycled water use on micro-blog [28], reservoir operation management [29], singular functional models [30], and as a mutation operator for particle filter noise reduction in mechanical fault diagnosis [31].

Quick and efficient performances have been achieved through the combination of optimization-based swarming and local search approaches. Therefore, the interior point is applied as a local search by using the initial inputs of the PSO. It is utilized in order to produce speedy results by applying the original data of PSO. Recently, the interior-point approach has been functional in quantum key distribution rate computation [32], facility layout problems with relative-positioning constraints [33], nonsymmetric exponential-cone optimization [34], nonlinear forms of the third kind of multi-singular differential system [35], and alternating current optimal power flow [36].

2.3. Performance Procedures

The statistical procedures based on mean square error (MSE), Theil's inequality coefficient (TIC), and semi-interquartile range (SIR) are provided to solve the mathematical RTS. The statistical performances are applied to authenticate the reliability of the proposed stochastic solver in the form of large data. The MSE, TIC and SIR performances are mathematically shown as:

$$MSE = \sum_{j=1}^{n} \left(x_j - \hat{x}_j\right)^2, \tag{10}$$

$$\mathrm{TIC} = \frac{\sqrt{\frac{1}{n}\sum\limits_{j=1}^{n}\left(x_j - \hat{x}_j\right)^2}}{\left(\sqrt{\frac{1}{n}\sum\limits_{j=1}^{n} x_j^2} + \sqrt{\frac{1}{n}\sum\limits_{i=1}^{n} \hat{x}_j^2}\right)} \tag{11}$$

$$\mathrm{SIR} = -\,0.5(\text{1st Quartile} - \text{3rd Quartile}), \tag{12}$$

where $x(\theta)$ and $\hat{x}(\theta)$ are the reference and proposed solutions.

3. Results Performance

In this section, numerical performances have been provided for three variations of the nonlinear RTS using the MW neural networks enhanced by the swarming and interior-point schemes. The obtained performances for RTS through the graphical and numerical forms are also presented.

Case 1: Consider the nonlinear RTS is provided for c = 0.1 and d = 1.2 in Equation (3) as:

$$\begin{cases} \frac{d^2x}{d\theta^2} - \frac{0.1x(\theta)}{1.2+x(\theta)} = 0, \quad 0 \le \theta \le 1, \\ \frac{dx}{d\theta}(0) = 0, \quad x(1) = 1. \end{cases} \tag{13}$$

where $0 \le \theta \le 1$, and the fitness O_F is provided as:

$$O_F = \frac{1}{N}\sum_{i=1}^{N}\left(\frac{d^2\hat{x}_i}{d\theta^2} - \frac{0.1\hat{x}_i}{1.2+\hat{x}_i}\right)^2 + \frac{1}{2}\left(\left(\frac{d\hat{x}_0}{d\theta}\right)^2 + (\hat{x}_N - 1)^2\right). \tag{14}$$

where $Nh = 1, \theta_i = ih, \hat{x}_i = x(\theta_i)$ and h shows the step size

Case 2: Consider the nonlinear RTS is provided for c = 0.4 and d = 1.2 in Equation (3) is:

$$\begin{cases} \frac{d^2x}{d\theta^2} - \frac{0.4x(\theta)}{1.2+x(\theta)} = 0, \quad 0 \le \theta \le 1, \\ \frac{dx}{d\theta}(0) = 0, \quad x(1) = 1. \end{cases} \tag{15}$$

The fitness O_F is provided as:

$$O_F = \frac{1}{N}\sum_{i=1}^{N}\left(\frac{d^2\hat{x}_i}{d\theta^2} - \frac{0.4\hat{x}_i}{1.2+\hat{x}_i}\right)^2 + \frac{1}{2}\left(\left(\frac{d\hat{x}_0}{d\theta}\right)^2 + (\hat{x}_N - 1)^2\right). \tag{16}$$

Case 3: Consider the nonlinear RTS is provided for c = 0.7 and d = 1.2 in Equation (3) is:

$$\begin{cases} \frac{d^2x}{d\theta^2} - \frac{0.7x(\theta)}{1.2+x(\theta)} = 0, \quad 0 \le \theta \le 1, \\ \frac{dx}{d\theta}(0) = 0, \quad x(1) = 1. \end{cases} \tag{17}$$

The fitness O_F is provided as:

$$O_F = \frac{1}{N}\sum_{i=1}^{N}\left(\frac{d^2\hat{x}_i}{d\theta^2} - \frac{0.7\hat{x}_i}{1.2+\hat{x}_i}\right)^2 + \frac{1}{2}\left(\left(\frac{d\hat{x}_0}{d\theta}\right)^2 + (\hat{x}_N - 1)^2\right). \tag{18}$$

To check the numerical observations based on the nonlinear form of the RTS for the first to third cases, the computational actions via global and local combinations are provided. The optimization performances used to find the unidentified weight vectors for 30 independent executions are presented in Equations (19)–(21), given as:

$$\begin{aligned} \hat{x}_1(\theta) \quad &= 0.02\Big(35(1.92\theta-0.72)^4 - 84(1.92\theta-0.72)^5 + 70(1.92\theta-0.72)^6 - 20(1.92\theta-0.72)^7\Big) \\ &+1.23\Big(35(-0.5\theta+0.69)^4 - 84(-0.5\theta+0.69)^5 + 70(-0.5\theta+0.69)^6 - 20(-0.5\theta+0.69)^7\Big) \\ &+0.34\Big(35(-0.06\theta+0.4)^4 - 84(-0.06\theta+0.4)^5 + 70(-0.06\theta+0.4)^6 - 20(-0.06\theta+0.4)^7\Big) \\ &+... + 0.26\Big(35(0.02\theta+1.2)^4 - 84(0.02\theta+1.20)^5 + 70(0.02\theta+1.2)^6 - 20(0.02\theta+1.20)^7\Big), \end{aligned} \tag{19}$$

$$\begin{aligned} \hat{x}_2(\theta) \quad &= -0.87\Big(35(1.11\theta-0.2)^4 - 84(1.11\theta-0.2)^5 + 70(1.11\theta-0.2)^6 - 20(1.110\theta-0.20)^7\Big) \\ &-1.08\Big(35(-1.35\theta+1.1)^4 - 84(-1.35\theta+1.1)^5 + 70(-1.35\theta+1.1)^6 - 20(-1.35\theta+1.1)^7\Big) \\ &+4.28\Big(35(0.69\theta+0.6)^4 - 84(0.69\theta+0.67)^5 + 70(0.69\theta+0.67)^6 - 20(0.69\theta+0.67)^7\Big) \\ +... \quad &+0.38\Big(35(-0.42\theta+1.8)^4 - 84(-0.4\theta+1.8)^5 + 70(-0.42\theta+1.8)^6 - 20(-0.42\theta+1.8)^7\Big), \end{aligned} \tag{20}$$

$$\begin{aligned} \hat{x}_3(\theta) \quad &= -0.10\Big(35(2.5\theta-2.76)^4 - 84(2.5\theta-2.76)^5 + 70(2.5\theta-2.76)^6 - 20(2.5\theta-2.76)^7\Big) \\ &+1.10\Big(35(-1.1\theta+0.03)^4 - 84(-1.1\theta+0.03)^5 + 70(-1.1\theta+0.03)^6 - 20(-1.1\theta+0.03)^7\Big) \\ &-1.64\Big(35(1.46\theta-3.94)^4 - 84(1.46\theta-3.94)^5 + 70(1.46\theta-3.94)^6 - 20(1.46\theta-3.94)^7\Big) \\ +... \quad &+2.11\Big(35(0.80\theta-0.31)^4 - 84(0.80\theta-0.31)^5 + 70(0.80\theta-0.31)^6 - 20(0.80\theta-0.31)^7\Big), \end{aligned} \tag{21}$$

The graphical illustrations are described in Figures 2–5 for the mathematics RTS by taking ten as the number of neurons, an input interval of [0, 1], and a step size of 0.05. The numerical outputs are performed using the optimal weights shown in Figure 2i–iii based on Equations (19)–(21). The comparison performances are provided by taking different solutions, which are presented in Figure 2iv–vi. The plots based on the optimal and mean result performances are illustrated together with the comparison of the results. The overlapping of the optimal and mean results gives confidence to the author that the proposed scheme is correct. The illustrations based on the best AE are presented in Figure 2vii–ix, which shows that the AE is calculated at approximately 10^{-7}–10^{-10}, 10^{-7}–10^{-9}, and 10^{-6}–10^{-9} for the first to third cases. The mean values of AE are reported as 10^{-2}–10^{-4}, 10^{-4}–10^{-6}, and 10^{-5}–10^{-6} for the first to third cases, and even the worst form of the AE is calculated as 10^{-1}–10^{-2}, 10^{-3}–10^{-4}, and 10^{-4}–10^{-5} for cases 1–3. The statistical performances based on the best, worse, and mean forms of the mathematical model of RTS are presented in Figure 2x–xii. For the first case, one can authenticate that the best Fitness (Fit), MSE, and TIC are performed at approximately 10^{-11}–10^{-12}, the mean Fit, MSE, and TIC sit at 10^{-4}–10^{-6}, 10^{-1}–10^{-2}, and 10^{-6}–10^{-8}, whereas the worst values of these operators are found in good measures. For the second case, the optimal Fit, MSE, and TIC are reported as 10^{-10}–10^{-12}, 10^{-12}–10^{-14}, and 10^{-11}–10^{-12}, the mean Fit, MSE, and TIC values sit at 10^{-6}–10^{-8}, whereas the worst measures of these operators are found also to be satisfactory. For the third case, it is observed that the best Fit, MSE, and TIC values are calculated as 10^{-10}–10^{-12}, the mean Fit, MSE, and TIC are 10^{-7}–10^{-8}, 10^{-6}–10^{-7}, and 10^{-8}–10^{-9}, and the worst values even show good performances. These accurate values based on the comparison of the outcomes, AE standards, and statistical operators authenticate the precision of the MW neural network along with the swarming and interior-point methods.

The statistical operator values based on the Fit, MSE, and TIC, along with the boxplots (BPs) and histograms (HTs), are presented in Figures 3–5. Figure 3 presents the optimal Fit values, which are found to be 10^{-7}–10^{-11}, 10^{-8}–10^{-12}, and 10^{-9}–10^{-12} for each case. The optimal MSE performances are presented in Figure 4, which are 10^{-7}–10^{-10} for the first to third cases. Likewise, Figure 5 indicates the values of TIC, which are calculated as 10^{-9}–10^{-12}. On behalf of these calculated values, one can observe that the designed scheme is accurate. These statistical performances authenticate the reliability of the proposed scheme for solving the nonlinear mathematical RTS.

For the precision and accuracy of the MW neural network along with the optimization of swarming and interior-point schemes, the statistical presentations are tabulated in Tables 1–4 based on the minimum (best), Mean, median, Maximum (worst), standard deviation (SD), and S.I.R for 30 executions. These operators all produce negligibly small measures for each variation of the RTS, which presents the stability of the proposed scheme.

The complexity measures to solve the mathematical form of the RTS using the MW neural network along with the optimization of swarming and interior-point schemes are provided. The deviation of parameters using the function counts, time complexity, and iterations during the decision variables of the network are also provided. Table 4 presents the computational cost investigations for the RTS in terms of numerical procedures. The iterations, used time, and function count are found to be 15.589116, 401.68888, and 1165.241312 for the respective cases of the model.

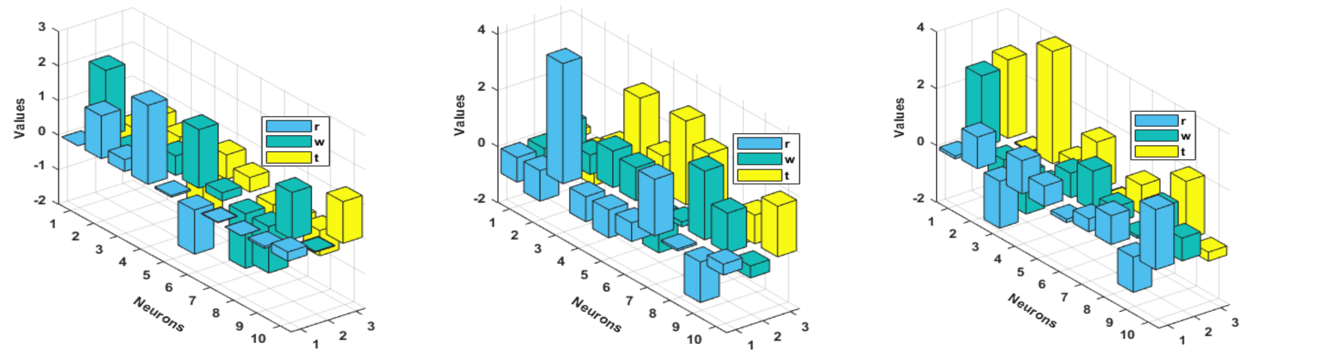

(**i**): Best weight values for case 1

(**ii**): Best weight weight values for case 2

(**iii**): Best weight weight values for case 3

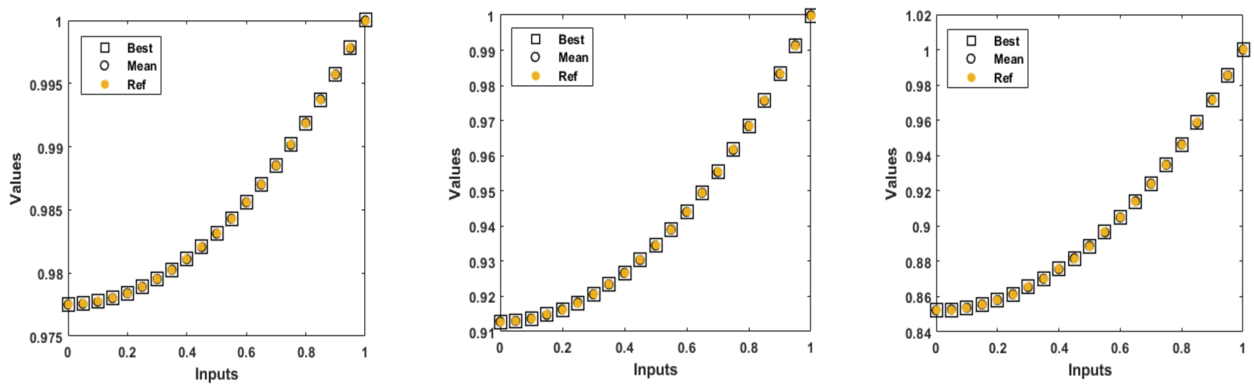

(**iv**): Result's comparison for case 1

(**v**): Result's comparison for case 2

(**vi**): Result's comparison for case 3

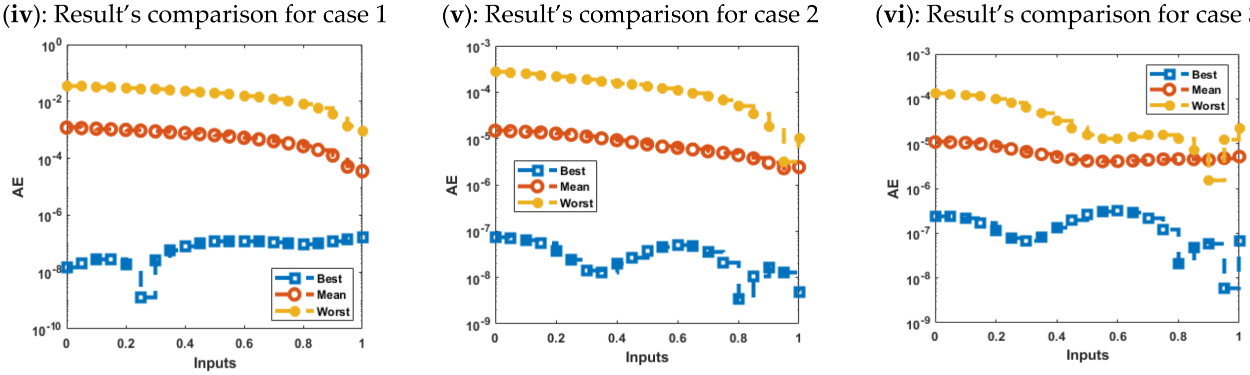

(**vii**): AE performances for case 1

(**viii**): AE performances for case 2

(**ix**): AE performances for case 3

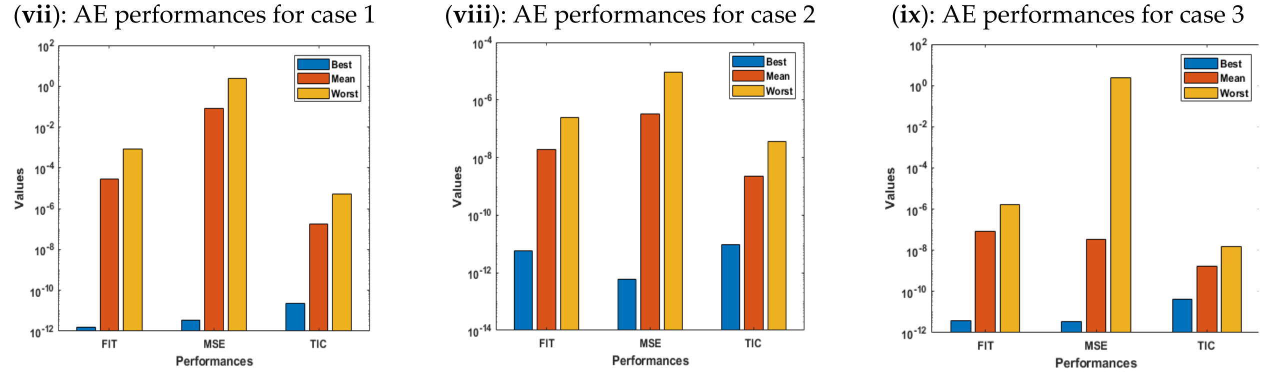

(**x**): Statistical performances (1)

(**xi**): Statistical performances (2)

(**xii**): Statistical performances (3)

Figure 2. Optimal weight vectors, AE, comparison, and statistical values for each case of RTS.

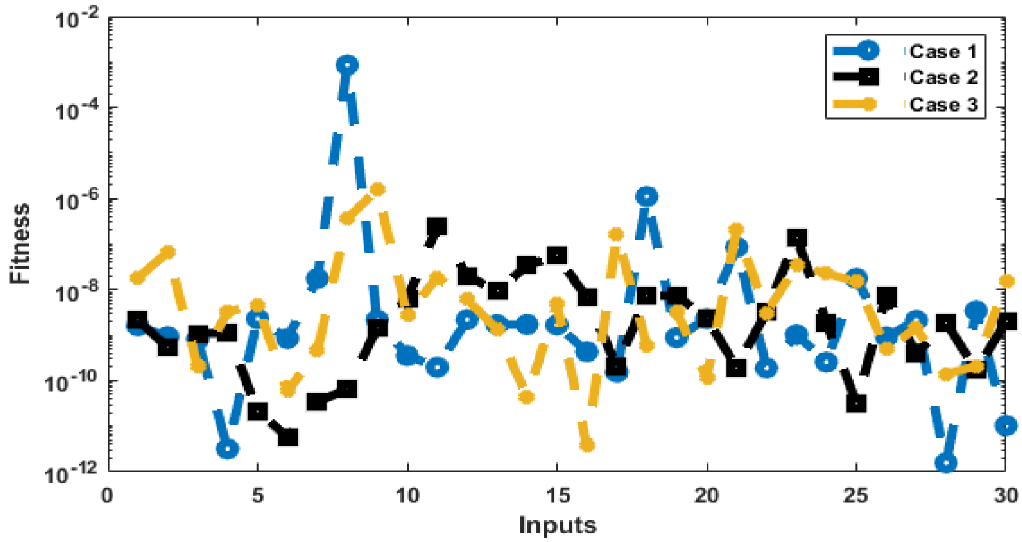

FIT measures for solving the nonlinear RTS

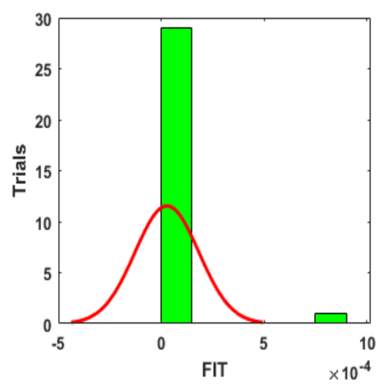

(**i**):HTs for case 1

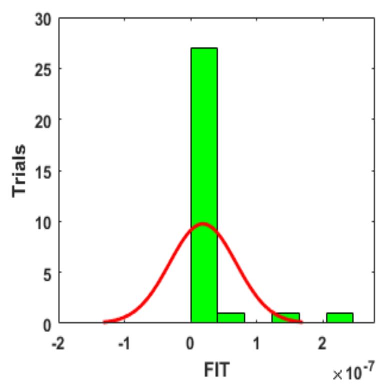

(**ii**): HTs for case 2

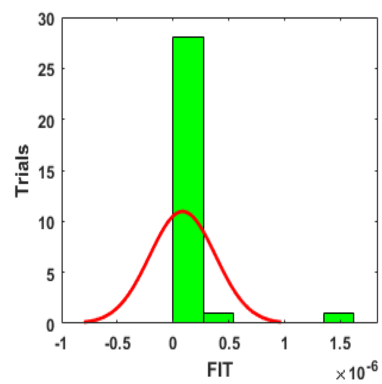

(**iii**): HTs for case 3

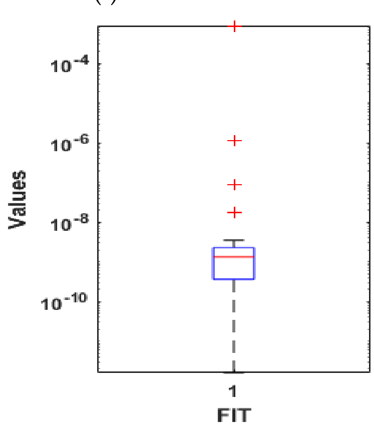

(**iv**): BPs for 1st case

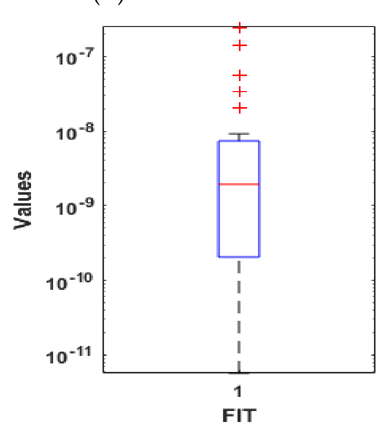

(**v**): BPs for 2nd case

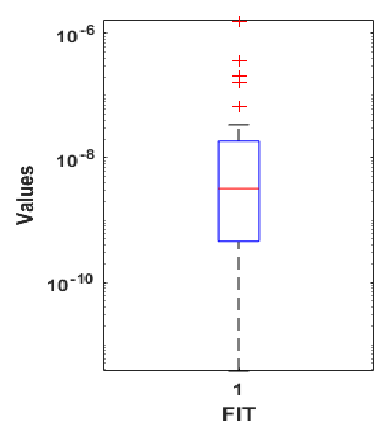

(**vi**): BPs for 3rd case

Figure 3. Convergence performances for the RTS based on the FIT performances.

Figure 3. Convergence performances for the RTS based on the FIT performances.

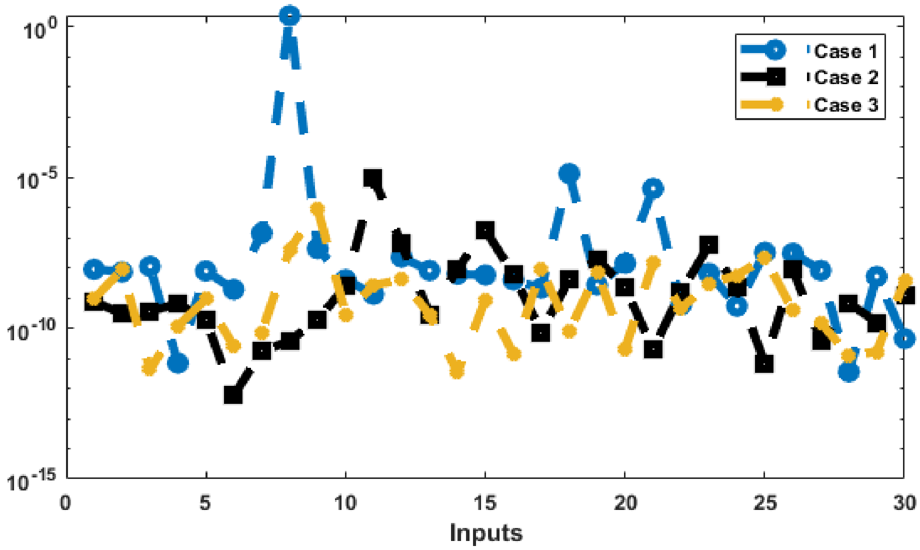

MSE performances for solving the nonlinear RTS

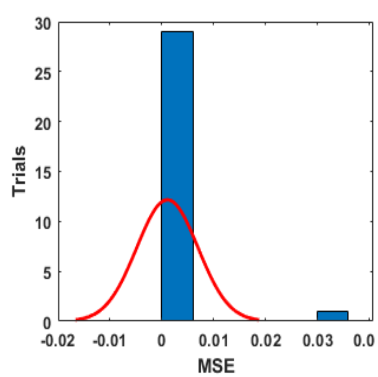

(**i**): HTs for case 1

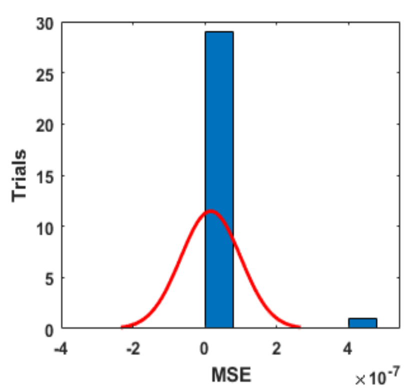

(**ii**): HTs for case 2

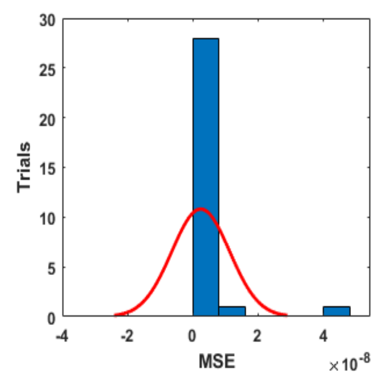

(**iii**): HTs for case 3

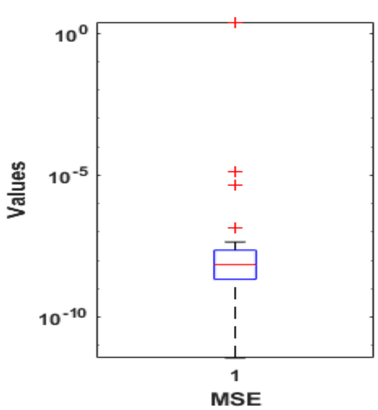

(**iv**): BPs for 1st case

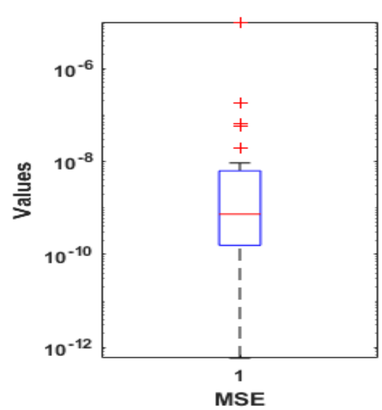

(**v**): BPs for 2nd case

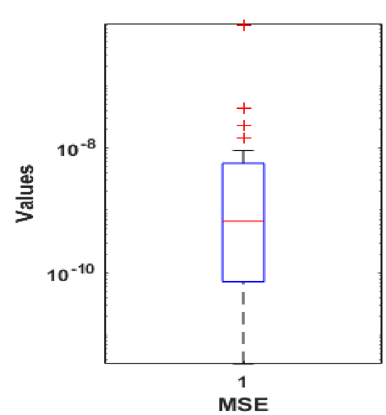

(**vi**): BPs for 3rd case

Figure 4. Convergence measures for the RTS through the MSE operators.

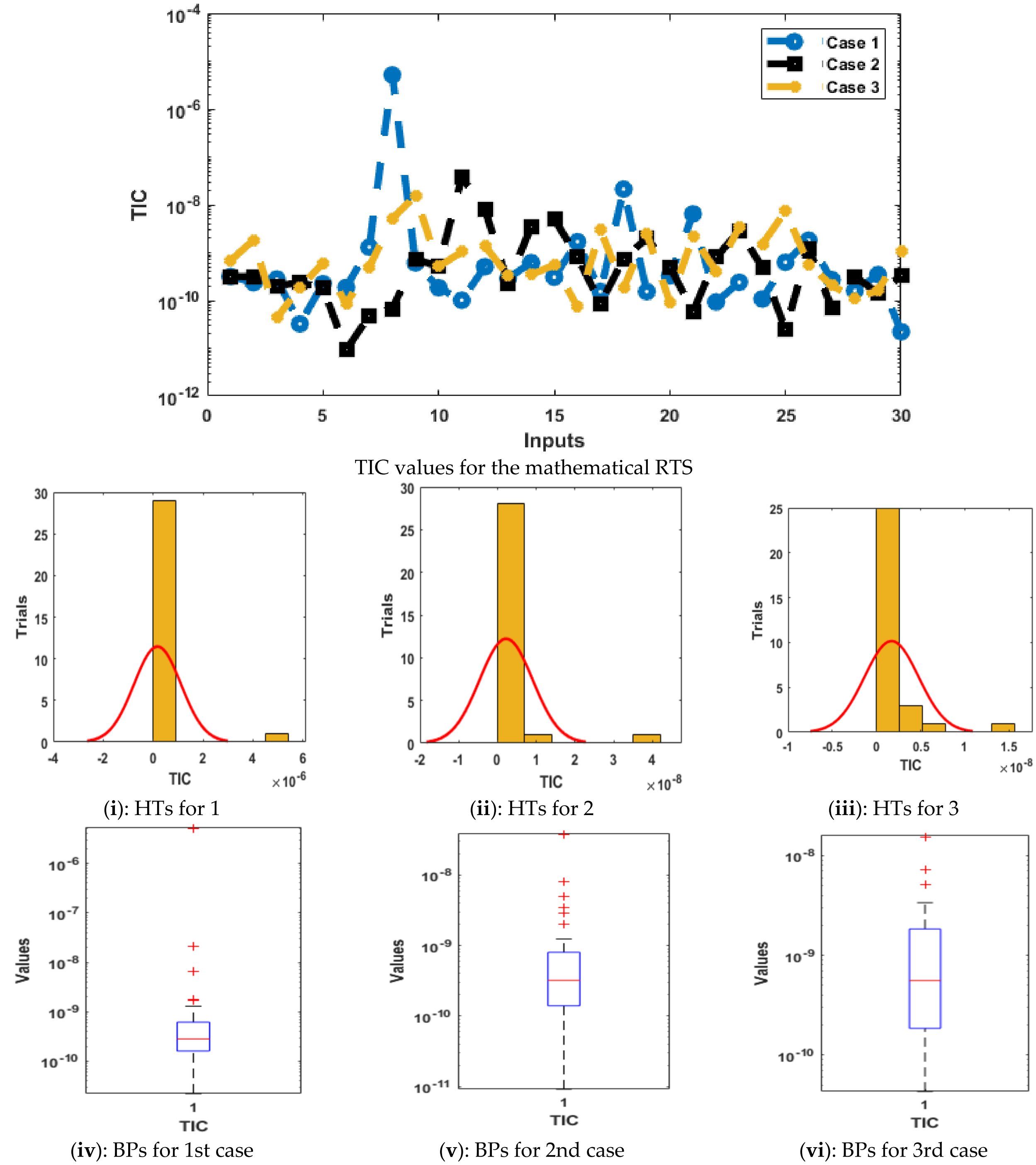

TIC values for the mathematical RTS

(**i**): HTs for 1 (**ii**): HTs for 2 (**iii**): HTs for 3

(**iv**): BPs for 1st case (**v**): BPs for 2nd case (**vi**): BPs for 3rd case

Figure 5. TIC performances for the mathematical RTS.

Figure 5. TIC performances for the mathematical RTS.

For the precision and accuracy of the MW neural network along with the optimization of swarming and interior-point schemes, the statistical presentations are tabulated in Tables 1–4 based on the minimum (best), Mean, median, Maximum (worst), standard deviation (SD), and S.I.R for 30 executions. These operators all produce negligibly small measures for each variation of the RTS, which presents the stability of the proposed scheme.

Table 1. Statistical observations based on stochastic procedure for the first case of the RTS.

θ	Minimum	M × 10 an	M × 10 Dian	Maximum	SD	S.I.R
0	1.4527×10^{-8}	1.1993×10^{-3}	1.9190×10^{-6}	3.5750×10^{-2}	6.5257×10^{-3}	1.2439×10^{-6}
0.05	2.0419×10^{-8}	1.1502×10^{-3}	1.9322×10^{-6}	3.4274×10^{-2}	6.2561×10^{-3}	1.2728×10^{-6}
0.1	3.8890×10^{-9}	1.1002×10^{-3}	1.9125×10^{-6}	3.2774×10^{-2}	5.9823×10^{-3}	1.3728×10^{-6}
0.15	2.8178×10^{-8}	1.0487×10^{-3}	1.8718×10^{-6}	3.1235×10^{-2}	5.7013×10^{-3}	1.4261×10^{-6}
0.2	1.9187×10^{-8}	9.9533×10^{-4}	1.6947×10^{-6}	2.9648×10^{-2}	5.4116×10^{-3}	1.5783×10^{-6}
0.25	1.2690×10^{-9}	9.4028×10^{-4}	1.4543×10^{-6}	2.8014×10^{-2}	5.1134×10^{-3}	1.6929×10^{-6}
0.3	2.6290×10^{-8}	8.8380×10^{-4}	1.2071×10^{-6}	2.6340×10^{-2}	4.8079×10^{-3}	1.4238×10^{-6}
0.35	5.6202×10^{-8}	8.2619×10^{-4}	9.0459×10^{-7}	2.4632×10^{-2}	4.4963×10^{-3}	1.2307×10^{-6}
0.4	3.9326×10^{-8}	7.6774×10^{-4}	6.3965×10^{-7}	2.2898×10^{-2}	4.1798×10^{-3}	1.0408×10^{-6}
0.45	6.7536×10^{-8}	7.0861×10^{-4}	5.3210×10^{-7}	2.1140×10^{-2}	3.8588×10^{-3}	8.1470×10^{-7}
0.5	8.6172×10^{-8}	6.4879×10^{-4}	4.1044×10^{-7}	1.9358×10^{-2}	3.5335×10^{-3}	8.0040×10^{-7}
0.55	1.2342×10^{-7}	5.8831×10^{-4}	5.0963×10^{-7}	1.7549×10^{-2}	3.2034×10^{-3}	5.3053×10^{-7}
0.6	7.3231×10^{-8}	5.2692×10^{-4}	5.6119×10^{-7}	1.5710×10^{-2}	2.8676×10^{-3}	5.8202×10^{-7}
0.65	1.1715×10^{-7}	4.6448×10^{-4}	7.2612×10^{-7}	1.3833×10^{-2}	2.5250×10^{-3}	6.6468×10^{-7}
0.7	1.0742×10^{-7}	4.0064×10^{-4}	8.3261×10^{-7}	1.1913×10^{-2}	2.1744×10^{-3}	8.7671×10^{-7}
0.75	9.8509×10^{-8}	3.3513×10^{-4}	8.2785×10^{-7}	9.9417×10^{-3}	1.8144×10^{-3}	8.2716×10^{-7}
0.8	8.0672×10^{-8}	2.6764×10^{-4}	8.6879×10^{-7}	7.9116×10^{-3}	1.4438×10^{-3}	8.2038×10^{-7}
0.85	3.7794×10^{-8}	1.9791×10^{-4}	7.6176×10^{-7}	5.8157×10^{-3}	1.0611×10^{-3}	8.2012×10^{-7}
0.9	4.8047×10^{-8}	1.2575×10^{-4}	5.1176×10^{-7}	3.6475×10^{-3}	6.6533×10^{-4}	6.6801×10^{-7}
0.95	1.1990×10^{-8}	5.0879×10^{-5}	2.2844×10^{-7}	1.4007×10^{-3}	2.5545×10^{-4}	9.9951×10^{-7}
1	8.1075×10^{-8}	3.5194×10^{-5}	1.7002×10^{-7}	9.3014×10^{-4}	1.6981×10^{-4}	1.0300×10^{-6}

Table 2. Statistical observations based on stochastic procedure for the second case of the RTS.

θ	Minimum	M × 10 an	M × 10 Dian	Maximum	SD	S.I.R
0	1.9638×10^{-8}	1.4758×10^{-5}	2.2665×10^{-6}	2.7830×10^{-4}	5.0733×10^{-5}	2.2574×10^{-6}
0.05	2.3255×10^{-8}	1.4359×10^{-5}	2.3012×10^{-6}	2.6391×10^{-4}	4.8142×10^{-5}	2.2600×10^{-6}
0.1	3.3426×10^{-8}	1.3988×10^{-5}	2.4301×10^{-6}	2.4823×10^{-4}	4.5328×10^{-5}	2.3297×10^{-6}
0.15	3.1179×10^{-8}	1.3481×10^{-5}	2.3980×10^{-6}	2.3151×10^{-4}	4.2342×10^{-5}	2.3230×10^{-6}
0.2	5.6182×10^{-9}	1.2801×10^{-5}	2.2211×10^{-6}	2.1455×10^{-4}	3.9319×10^{-5}	2.3689×10^{-6}
0.25	2.3805×10^{-8}	1.1973×10^{-5}	1.9095×10^{-6}	1.9810×10^{-4}	3.6381×10^{-5}	2.0592×10^{-6}
0.3	1.4197×10^{-8}	1.1043×10^{-5}	1.5541×10^{-6}	1.8266×10^{-4}	3.3609×10^{-5}	2.1100×10^{-6}
0.35	2.3342×10^{-9}	1.0096×10^{-5}	1.3575×10^{-6}	1.6841×10^{-4}	3.1025×10^{-5}	2.0331×10^{-6}
0.4	1.9974×10^{-8}	9.1717×10^{-6}	1.0868×10^{-6}	1.5526×10^{-4}	2.8626×10^{-5}	1.8203×10^{-6}
0.45	8.9137×10^{-9}	8.2857×10^{-6}	1.1243×10^{-6}	1.4296×10^{-4}	2.6388×10^{-5}	1.5645×10^{-6}
0.5	5.4568×10^{-9}	7.4630×10^{-6}	8.7409×10^{-7}	1.3112×10^{-4}	2.4253×10^{-5}	1.3701×10^{-6}
0.55	1.8057×10^{-8}	6.7222×10^{-6}	6.9428×10^{-7}	1.1931×10^{-4}	2.2156×10^{-5}	1.2701×10^{-6}
0.6	4.9173×10^{-8}	6.2622×10^{-6}	6.2897×10^{-7}	1.0713×10^{-4}	1.9971×10^{-5}	1.3442×10^{-6}
0.65	4.0434×10^{-8}	5.7940×10^{-6}	6.0506×10^{-7}	9.4260×10^{-5}	1.7726×10^{-5}	1.4266×10^{-6}

Table 2. *Cont.*

θ	Minimum	M × 10 an	M × 10 Dian	Maximum	SD	S.I.R
0.7	2.3268×10^{-8}	5.2882×10^{-6}	5.0749×10^{-7}	8.0491×10^{-5}	1.5387×10^{-5}	7.6547×10^{-7}
0.75	3.1087×10^{-9}	4.9108×10^{-6}	7.8657×10^{-7}	6.5769×10^{-5}	1.2875×10^{-5}	1.2075×10^{-6}
0.8	3.5008×10^{-9}	4.3955×10^{-6}	7.2060×10^{-7}	5.0222×10^{-5}	1.0321×10^{-5}	1.5987×10^{-6}
0.85	1.0835×10^{-8}	3.7330×10^{-6}	6.4426×10^{-7}	3.4182×10^{-5}	7.8691×10^{-6}	1.4233×10^{-6}
0.9	1.6673×10^{-8}	2.9877×10^{-6}	5.0698×10^{-7}	2.4524×10^{-5}	5.8277×10^{-6}	1.0828×10^{-6}
0.95	1.2772×10^{-8}	2.2740×10^{-6}	4.2338×10^{-7}	2.2550×10^{-5}	4.7879×10^{-6}	1.0993×10^{-6}
1	1.8408×10^{-9}	2.4009×10^{-6}	4.5024×10^{-7}	2.0584×10^{-5}	4.8422×10^{-6}	8.9874×10^{-7}

Table 3. Statistical observations based on stochastic procedure for the third case of the RTS.

θ	Minimum	M × 10 an	M × 10 Dian	Maximum	SD	S.I.R
0	1.2692×10^{-7}	1.0850×10^{-5}	3.5253×10^{-6}	1.3120×10^{-4}	2.4262×10^{-5}	4.5906×10^{-6}
0.05	8.0136×10^{-9}	1.0724×10^{-5}	3.6738×10^{-6}	1.2795×10^{-4}	2.3635×10^{-5}	4.6424×10^{-6}
0.1	8.3734×10^{-8}	1.0465×10^{-5}	3.7088×10^{-6}	1.2305×10^{-4}	2.2713×10^{-5}	4.7483×10^{-6}
0.15	5.5947×10^{-8}	9.7839×10^{-6}	3.3621×10^{-6}	1.1363×10^{-4}	2.1035×10^{-5}	4.1961×10^{-6}
0.2	1.7855×10^{-8}	8.6888×10^{-6}	2.8874×10^{-6}	9.9654×10^{-5}	1.8657×10^{-5}	3.0460×10^{-6}
0.25	2.7752×10^{-8}	7.6144×10^{-6}	2.7272×10^{-6}	8.2601×10^{-5}	1.5766×10^{-5}	2.6415×10^{-6}
0.3	6.6981×10^{-8}	6.5909×10^{-6}	2.1657×10^{-6}	6.4539×10^{-5}	1.2858×10^{-5}	3.1148×10^{-6}
0.35	8.3396×10^{-8}	5.7635×10^{-6}	2.1566×10^{-6}	4.7516×10^{-5}	1.0340×10^{-5}	2.7891×10^{-6}
0.4	1.2963×10^{-7}	5.0440×10^{-6}	1.6800×10^{-6}	3.3704×10^{-5}	8.5866×10^{-6}	2.0396×10^{-6}
0.45	5.2079×10^{-8}	4.4612×10^{-6}	1.4913×10^{-6}	3.3523×10^{-5}	7.6228×10^{-6}	1.4828×10^{-6}
0.5	9.3220×10^{-8}	4.1111×10^{-6}	1.5086×10^{-6}	3.3048×10^{-5}	7.1512×10^{-6}	1.0982×10^{-6}
0.55	1.7663×10^{-7}	4.0022×10^{-6}	1.4248×10^{-6}	3.2201×10^{-5}	6.8970×10^{-6}	9.8590×10^{-7}
0.6	9.3265×10^{-8}	4.0334×10^{-6}	1.4263×10^{-6}	3.0951×10^{-5}	6.7883×10^{-6}	9.4095×10^{-7}
0.65	2.9198×10^{-8}	4.1475×10^{-6}	1.5320×10^{-6}	2.9326×10^{-5}	6.8164×10^{-6}	1.0183×10^{-6}
0.7	1.2750×10^{-8}	4.3450×10^{-6}	1.2376×10^{-6}	2.7398×10^{-5}	6.8970×10^{-6}	1.2565×10^{-6}
0.75	2.6347×10^{-8}	4.5013×10^{-6}	1.4200×10^{-6}	2.5276×10^{-5}	6.9542×10^{-6}	1.6041×10^{-6}
0.8	2.0621×10^{-8}	4.5455×10^{-6}	1.3296×10^{-6}	2.5618×10^{-5}	6.9195×10^{-6}	2.0174×10^{-6}
0.85	1.7131×10^{-8}	4.4486×10^{-6}	1.3861×10^{-6}	2.8828×10^{-5}	6.9066×10^{-6}	2.4376×10^{-6}
0.9	6.6650×10^{-10}	4.3191×10^{-6}	1.3299×10^{-6}	3.2659×10^{-5}	7.2203×10^{-6}	1.8780×10^{-6}
0.95	2.8647×10^{-9}	4.7253×10^{-6}	1.2215×10^{-6}	3.7108×10^{-5}	7.8977×10^{-6}	3.7568×10^{-6}
1	7.1753×10^{-10}	5.1313×10^{-6}	7.7154×10^{-7}	4.1628×10^{-5}	9.0769×10^{-6}	3.8721×10^{-6}

Table 4. Complexity measures for the mathematical form of the RTS.

Case	Iterations		Implemented Time		Fun. Counts	
	Minimum	SD	Minimum	SD	Minimum	SD
1	15.45159273	2.390238385	395.0666667	54.40710738	24,763.46667	3326.960576
2	15.77388434	0.944774262	405	0	25,409.63333	94.49593435
3	15.54187202	0.691946317	405	0	25,400.93333	74.26742607

4. Concluding Remarks

In this study, the design of a novel Meyer wavelet neural network is provided for the numerical performances of the reactive transport model that carries trucks with goods on roads. This nonlinear RTS has been used to carry trucks with goods on roads by taking different c and d values. The conclusions of this study are as follows:

1. When the values of d are taken as greater than zero, a half-saturated concentration is performed.
2. When the values of c are taken as less than zero, which shows the distinctive reaction, the reactive rate is applied as an alternate to the reaction product.
3. The solutions of the nonlinear model based on the TRS have been presented successfully by using the proposed stochastic scheme.
4. An objective function has been constructed through the differential form of the RTS and its boundary conditions.
5. The optimization of the merit function has been performed by using the hybridization of global swarming and local search interior-point algorithms.
6. The correctness of the scheme has been observed by performing a comparison of the results and reducible AE for three cases of the RTS.
7. For the stability of the scheme, the statistical performances based on different operators have been provided using 30 trials.

The designed structure can be tested in the future for solving quantum models [37], lonngren-wave systems [38], singular models [39], nonlinear differential models [40], fractional types of systems [41–44], pricing economy networks [45], Gemini virus models [46], and other related systems [47–50].

Author Contributions: Conceptualization and Methodology: Z.S. and T.S., Solution of the model: J.L.G.G., A.V. and J.M.S., writing the manuscript: A.V. and J.M.S. All authors have read and agreed to the published version of the manuscript.

Funding: Cátedra Primafrio-UPCT, 2023.

Data Availability Statement: This paper does not contain any data not stated in the manuscript.

Conflicts of Interest: The authors declare no conflict of interest.

References

1. Shivanian, E. On the multiplicity of solutions of the nonlinear reactive transport model. *Ain Shams Eng. J.* **2014**, *5*, 637–645. [CrossRef]
2. Steefel, C.I.; DePaolo, D.J.; Lichtner, P.C. Reactive transport modeling: An essential tool and a new research approach for the Earth sciences. *Earth Planet Sci. Lett.* **2005**, *240*, 539–558. [CrossRef]
3. Pabst, T.; Molson, J.; Aubertin, M.; Bussière, B. Reactive transport modelling of the hydro-geochemical behaviour of partially oxidized acid-generating mine tailings with a monolayer cover. *Appl. Geochem.* **2017**, *78*, 219–233. [CrossRef]
4. Vilcáez, J.; Li, L.; Wu, D.; Hubbard, S.S. Reactive transport modeling of induced selective plugging by Leuconostocmesenteroides in carbonate formations. *Geomicrobiol. J.* **2013**, *30*, 813–828. [CrossRef]
5. Regnier, P.; Jourabchi, P.; Slomp, C.P. Reactive-transport modeling as a technique for understanding coupled biogeochemical processes in surface and subsurface environments. *Neth. J. Geosci.* **2003**, *82*, 5–18. [CrossRef]
6. Ellery, A.J.; Simpson, M.J. An analytical method to solve a general class of nonlinear reactive transport models. *Chem. Eng. J.* **2011**, *169*, 313–318. [CrossRef]
7. Lu, Y.; Wang, W. Multiscale modeling of fluid and solute transport in soft tissues and microvessels. *J. Multiscale Model.* **2010**, *2*, 127–145. [CrossRef]
8. Donea, J. A Taylor–Galerkin method for convective transport problems. *Int. J. Numer. Methods Eng.* **1984**, *20*, 101–119. [CrossRef]
9. Toride, N.; Leij, F.J.; Van Genuchten, M.T. *The CXTFIT Code for Estimating Transport Parameters from Laboratory or Filed Tracer Experiments (Volume 2)*; US Salinity Laboratory: Riverside, CA, USA, 1995.
10. De Smedt, F. Analytical solutions of the one-dimensional convective-dispersive solute transport equation: M. Th. van Genuchten and WJ Alves. Technical Bulletin no. 1661, US Department of Agriculture Washington, DC, 1982; 151 pp. *Agric. Water Manag.* **1984**, *9*, 79–80. [CrossRef]
11. Wazwaz, A.M.; Rach, R.; Bougoffa, L. Dual solutions for nonlinear boundary value problems by the Adomian decomposition method. *Int. J. Numer. Methods Heat Fluid Flow* **2016**, *26*, 2393–2409. [CrossRef]
12. Kuzmin, D. *A Guide to Numerical Methods for Transport Equations*; University of Erlangen: Nuremberg, Germany, 2010.

13. Rach, R.; Duan, J.S.; Wazwaz, A.M. On the solution of non-isothermal reaction-diffusion model equations in a spherical catalyst by the modified Adomian method. *Chem. Eng. Commun.* **2015**, *202*, 1081–1088. [CrossRef]
14. Miah, M.M.; Ali, H.S.; Akbar, M.A.; Wazwaz, A.M. Some applications of the $(G'/G, 1/G)$-expansion method to find new exact solutions of NLEEs. *Eur. Phys. J. Plus* **2017**, *132*, 252. [CrossRef]
15. Weera, W.; Botmart, T.; La-inchua, T.; Sabir, Z.; Núñez, R.A.S.; Abukhaled, M.; Guirao, J.L.G. A stochastic computational scheme for the computer epidemic virus with delay effects. *AIMS Math.* **2023**, *8*, 148–163. [CrossRef]
16. Sabir, Z.; Raja, M.A.Z.; Khalique, C.M.; Unlu, C. Neuro-evolution computing for nonlinear multi-singular system of third order Emden-Fowler equation. *Math. Comput. Simul.* **2021**, *185*, 799–812. [CrossRef]
17. Sabir, Z.; Raja, M.A.Z.; Guirao, J.L.; Shoaib, M. Integrated intelligent computing with neuro-swarming solver for multi-singular fourth-order nonlinear Emden–Fowler equation. *Comput. Appl. Math.* **2020**, *39*, 307. [CrossRef]
18. Sabir, Z.; Raja, M.A.Z.; Guirao, J.L.; Shoaib, M. A novel design of fractional Meyer wavelet neural networks with application to the nonlinear singular fractional Lane-Emden systems. *Alex. Eng. J.* **2021**, *60*, 2641–2659. [CrossRef]
19. Sabir, Z.; Raja, M.A.Z.; Shoaib, M.; Aguilar, J.G. FMNEICS: Fractional Meyer neuro-evolution-based intelligent computing solver for doubly singular multi-fractional order Lane–Emden system. *Comput. Appl. Math.* **2020**, *39*, 303. [CrossRef]
20. Sabir, Z.; Raja, M.A.Z.; Wahab, H.A.; Shoaib, M.; Aguilar, J.G. Integrated neuro-evolution heuristic with sequential quadratic programming for second-order prediction differential models. In *Numerical Methods for Partial Differential Equations*; John Wiley & Sons: Hoboken, NJ, USA, 2020.
21. Sabir, Z. Neuron analysis through the swarming procedures for the singular two-point boundary value problems arising in the theory of thermal explosion. *Eur. Phys. J. Plus* **2022**, *137*, 638. [CrossRef]
22. Sabir, Z. Stochastic numerical investigations for nonlinear three-species food chain system. *Int. J. Biomath.* **2022**, *15*, 2250005. [CrossRef]
23. Elsheikh, A.H.; Abd Elaziz, M. Review on applications of particle swarm optimization in solar energy systems. *Int. J. Environ. Sci. Technol.* **2019**, *16*, 1159–1170. [CrossRef]
24. Phommixay, S.; Doumbia, M.L.; Lupien St-Pierre, D. Review on the cost optimization of microgrids via particle swarm optimization. *Int. J. Energy Environ. Eng.* **2020**, *11*, 73–89. [CrossRef]
25. Darwish, A.; Ezzat, D.; Hassanien, A.E. An optimized model based on convolutional neural networks and orthogonal learning particle swarm optimization algorithm for plant diseases diagnosis. *Swarm Evol. Comput.* **2020**, *52*, 100616. [CrossRef]
26. Yousri, D.; Thanikanti, S.B.; Allam, D.; Ramachandaramurthy, V.K.; Eteiba, M.B. Fractional chaotic ensemble particle swarm optimizer for identifying the single, double, and three diode photovoltaic models' parameters. *Energy* **2020**, *195*, 116979. [CrossRef]
27. Xue, Y.; Xue, B.; Zhang, M. Self-adaptive particle swarm optimization for large-scale feature selection in classification. *ACM Trans. Knowl. Discov. Data (TKDD)* **2019**, *13*, 50. [CrossRef]
28. Fu, H.; Li, Z.; Liu, Z.; Wang, Z. Research on big data digging of hot topics about recycled water use on micro-blog based on particle swarm optimization. *Sustainability* **2018**, *10*, 2488. [CrossRef]
29. Dahmani, S.; Yebdri, D. Hybrid algorithm of particle swarm optimization and grey wolf optimizer for reservoir operation management. *Water Resour. Manag.* **2020**, *34*, 4545–4560. [CrossRef]
30. Sabir, Z.; Raja, M.A.Z.; Umar, M.; Shoaib, M. Neuro-swarm intelligent computing to solve the second-order singular functional differential model. *Eur. Phys. J. Plus* **2020**, *135*, 474. [CrossRef]
31. Chen, H.; Fan, D.L.; Fang, L.; Huang, W.; Huang, J.; Cao, C.; Yang, L.; He, Y.; Zeng, L. Particle swarm optimization algorithm with mutation operator for particle filter noise reduction in mechanical fault diagnosis. *Int. J. Pattern Recognit. Artif. Intell.* **2020**, *34*, 2058012. [CrossRef]
32. Hu, H.; Im, J.; Lin, J.; Lütkenhaus, N.; Wolkowicz, H. Robust interior point method for quantum key distribution rate computation. *Quantum* **2022**, *6*, 792. [CrossRef]
33. Ohmori, S.; Yoshimoto, K. A primal-dual interior-point method for facility layout problem with relative-positioning constraints. *Algorithms* **2021**, *14*, 60. [CrossRef]
34. Dahl, J.; Andersen, E.D. A primal-dual interior-point algorithm for nonsymmetric exponential-cone optimization. *Math. Program.* **2022**, *194*, 341–370. [CrossRef]
35. Sabir, Z.; Raja, M.A.Z.; Kamal, A.; Guirao, J.L.; Le, D.N.; Saeed, T.; Salama, M. Neuro-Swarm heuristic using interior-point algorithm to solve a third kind of multi-singular nonlinear system. *Math. Biosci. Eng.* **2021**, *18*, 5285–5308. [CrossRef] [PubMed]
36. Sadat, S.A.; Kim, K. September. Numerical performance of different formulations for alternating current optimal power flow. In Proceedings of the 2021 31st Australasian Universities Power Engineering Conference (AUPEC), Online, 26–30 September 2021; IEEE: Piscataway, NJ, USA, 2021; pp. 1–6.
37. Gençoğlu, M.T.; Agarwal, P. Use of quantum differential equations in sonic processes. *Appl. Math. Nonlinear Sci.* **2021**, *6*, 21–28. [CrossRef]
38. Baskonus, H.M.; Bulut, H.; Sulaiman, T.A. New complex hyperbolic structures to the lonngren-wave equation by using sine-gordon expansion method. *Appl. Math. Nonlinear Sci.* **2019**, *4*, 129–138. [CrossRef]
39. Rahaman, H.; Hasan, M.K.; Ali, A.; Alam, M.S. Implicit methods for numerical solution of singular initial value problems. *Appl. Math. Nonlinear Sci.* **2021**, *6*, 1–8. [CrossRef]

40. Xie, T.; Liu, R.; Wei, Z. Improvement of the Fast Clustering Algorithm Improved by-Means in the Big Data. *Appl. Math. Nonlinear Sci.* **2020**, *5*, 1–10. [CrossRef]
41. Aghili, A. Complete solution for the time fractional diffusion problem with mixed boundary conditions by operational method. *Appl. Math. Nonlinear Sci.* **2021**, *6*, 9–20. [CrossRef]
42. Akdemir, A.O.; Deniz, E.; Yüksel, E. On some integral inequalities via conformable fractional integrals. *Appl. Math. Nonlinear Sci.* **2021**, *6*, 489–498. [CrossRef]
43. Durur, H.; Yokuş, A. Exact solutions of (2 + 1)-Ablowitz-Kaup-Newell-Segur equation. *Appl. Math. Nonlinear Sci.* **2021**, *6*, 381–386. [CrossRef]
44. Ren, L.; Huang, W.; Kodakkadan, Y.; Lakys, Y. Recognition of Electrical Control System of Flexible Manipulator Based on Transfer Function Estimation Method. *Appl. Math. Nonlinear Sci.* 2021. *ahead of print*. [CrossRef]
45. Chen, Q.; Baskonus, H.M.; Gao, W. Ilhan Soliton theory and modulation instability analysis: The Ivancevic option pricing model in economy. *Alex. Eng. J.* **2022**, *61*, 7843–7851. [CrossRef]
46. Nisar, K.S.; Logeswari, K.; Vijayaraj, V.; Baskonus, H.M. Ravichandran Fractional order Modeling the Gemini virus in Capsicum annuum with optimal control. *Fractal Fract.* **2022**, *6*, 61. [CrossRef]
47. Pokle, S.; Deshpande, R.; Paraskar, S.; Sinha, S.; Lalwani, Y.; Thakre, P.N. Performance analysis of NOMA in Rayleigh and Nakagami Fading channel. *3c TIC Cuad. De Desarro. Apl. A Las TIC* **2022**, *11*, 183–193.
48. Dharmik, R.C.; Chavhan, S.; Sathe, S.R. Deep Learning based missing object Detection and Person Identification: An application for Smart CCTV. *3c Tecnol. Glosas De Innovación Apl. A La Pyme* **2022**, *11*, 51–57. [CrossRef]
49. Barapatre, P.; Ingolikar, Y.; Desai, P.; Jajoo, P.; Thakre, P. A secured architecture for iot-based healthcare system. *3c Empresa Investig. Y Pensam. Crítico* **2022**, *11*, 222–230. [CrossRef]
50. Roshni, K.S.; Musthafa, M.M.A. Problems of online mathematics teaching and learning during the pandemic: A reverberation in to the perception of prospective teachers. *3c Empresa Investig. Y Pensam. Crítico* **2022**, *11*, 153–162.

3.4 PAPER 4

Article 4.-: J.M. Sánchez, A. Valverde, J.L.G. Guirao, H. Chen, 2023. *Mathematical Modeling for the development of traffic based on the theory of system dynamics.* **AIMS Mathematics**, **8(11)**, 27626–27642, DOI: 10.3934/math.20231413

EXTENDED ABSTRACT

Methodology: The core aim of this paper is to construct an extensive mathematical model designed to capture and elucidate the intricate dynamics of traffic systems on a global scale. However, due to limitations in data availability, the study narrows its focus to the traffic conditions within the Shandong province. This province, situated in China, serves as the primary canvas for testing and validating the proposed mathematical model. **Results**: The study's chief achievement is the establishment of a system dynamics model, which serves as the foundation for comprehending the progression of traffic in the Shandong region. This model, created through a systematic methodology, brings to light several fundamental outcomes that have practical implications.

EXTENDED ABSTRACT

Conclusions: The insights derived from this model are multifaceted. Firstly, it becomes evident that the operation and existence of well-developed highway systems and efficient rail transit networks significantly contribute to the growth and development of traffic within the region. This insight underscores the importance of transportation infrastructure and the role it plays in driving economic and social activity. It also provides a basis for further investment and development planning in these areas. Conversely, the research unearths a less favorable aspect of traffic dynamics. Traffic accidents, as determined by the model, act as significant inhibitors to the development of traffic. This finding highlights the urgent need for safety measures and accident prevention strategies to safeguard commuters and ensure the smooth and efficient flow of traffic. To gauge the model's accuracy, a comparative analysis is undertaken, pitting the model's output data against statistical data provided by the pertinent government bureau. The maximum error, determined through this comparison, is a crucial metric for assessing the model's reliability and predictive capability. Furthermore, the research leverages this model for predictive purposes. It provides forecasts regarding the future development of traffic in the Shandong province, offering valuable insights into potential trends and challenges in traffic management. These forecasts can serve as invaluable inputs for policymakers and stakeholders in the transportation sector. In addition to these findings, the paper goes a step further by suggesting actionable recommendations and optimization schemes for improving traffic development. These recommendations can serve as practical guidelines for decision-makers aiming to enhance traffic infrastructure and management in the region. Finally, the study extends its scope by introducing a neural network model dedicated specifically to the development of traffic within the Shandong province. This neural network model is designed to offer a dynamic and adaptable tool for predicting and understanding traffic patterns, enabling real-time decision-making and long-term planning to ensure efficient and sustainable traffic management.

Mathematics

http://www.aimspress.com/journal/Math

AIMS Mathematics, 8(11): 27626–27642.
DOI: 10.3934/math.20231413
Received: 02 May 2023
Revised: 25 July 2023
Accepted: 15 August 2023
Published: 07 October 2023

Research article

Mathematical modeling for the development of traffic based on the theory of system dynamics

Juan Manuel Sánchez[1], Adrián Valverde[1], Juan L. G. Guirao[1,*] and Huatao Chen[2]

[1] Department of Applied Mathematics and Statistics, Technical University of Cartagena, Hospital de Marina, Cartagena 30203, Spain

[2] Division of Dynamics and Control, School of Mathematics and Statistics, Shandong University of Technology, Zibo 255000, China

* **Correspondence:** Email: juan.garcia@upct.es.

Abstract: This paper is concerned with mathematical modeling for the development of Shandong traffic. The system dynamics model of the development of traffic in Shandong is established. In terms of this model, it is shown that highway operation as well as rail transit promotes the development of traffic, while traffic accidents inhibit traffic development. Moreover, the maximum error between the output data and the statistics bureau, based on which some forecasts for the development of traffic in the future are given, is obtained, some suggestions and optimization schemes for traffic development are given. Finally, a neural network model of the development of Shandong traffic is also derived.

Keywords: traffic development; system dynamics; neural network model
Mathematics Subject Classification: 34A37

1. Introduction

Recently, the traffic situation has been improved, which is reflected by the amount of passenger on a highway of 15 billion people in 2018, and the total length of rail lines in China has reached 5761.4 kilometers, therefore, the study of the traffic system by different theories is crucial. For example, based on mathematical modeling, reference [11] shows that the emergency vehicle management solution can reduce travel times of EVs without causing any performance degradation of normal vehicles. Zhu [30] proposed a bayesian updating approach based on the dirichlet model to describe the traffic system performance. Via machine learning, Saleem [21] proposed a fusion-based intelligent traffic congestion control system to alleviate traffic congestion in smart cities.

The traffic system is a complex dynamic system whose influencing factors are complex and diverse, thus, the mathematical modeling of traffic system is difficult. In order to understand the dynamic behavior of traffic systems comprehensively, the system dynamic (SD) method is one of the most powerful tools [10]. The theory of system dynamics founded by Forrester [7] can be used to simplify the multi-variable system, and it is widely used to deal with social and economic problems. As for the application of the theory of system dynamics, one can refer to [4, 18, 25, 26], to name but a few. The basic concepts of system dynamics are as follows:

(1) Level variable, represented by a rectangle in VENSIM software, are affected by rate variables, which can be expressed by integrating the rate variables.
(2) Rate variables are time functions, and they determine the level variable.
(3) For ease of communication and clarity, it is often to define auxiliary variables, which are neither stock nor flow.
(4) The constant variable is a constant, and it can be characterized by table functions.
(5) Table functions conveniently represent nonlinear relationships.
(6) Flow graph is a characteristic diagram in system dynamics. It simplifies the equations of models. In the sequel, the flow graph can be transformed into VENSIM equations.

The modeling steps for system dynamics in VENSIM software are shown by Figure 1.

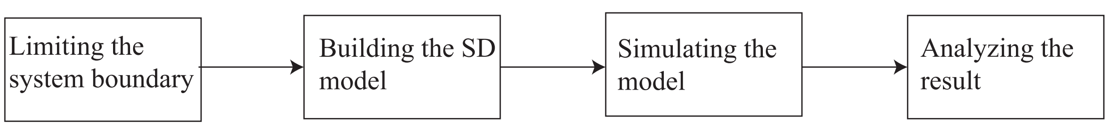

Figure 1. Modeling steps of system dynamics.

Recently, research based on system dynamic theory mainly focuses on urban traffic, low-carbon traffic as well as traffic policies. According to the restriction policy, Wen [27] calculated that the implementation of the tail licensing restriction policy could effectively reduce carbon dioxide emissions by 3.86%. Moreover, they found that the vehicle license limit policy could effectively curb the growth of car ownership, and alleviate traffic congestion. Jia [14] established an SD model of traffic congestion charge and subsidy. Furthermore, it can be found that zero-subsidy and low charge reduce carbon dioxide emissions. He [10] concluded that the railway occupation rate was directly proportional to the railway length. Additionally, in order to assess the relation between numbers of available public traffic and traffic congestion in Jakarta, Sardjono [24] developed an SD model for traffic conditions, which can reduce traffic congestion. Based on road accident statistics, Victor [16] proposed the methodology of evaluated long-term trends in the dynamics of traffic safety improvement. Rajput [20] present a system dynamics simulation model to reduce traffic congestion by implementing an Intelligent Transportation System in metropolitan cities of India. Ye [29] concluded that highway investment had a certain pulling effect on economic growth based on a concrete analysis on the relationship between highway construction and economic growth.

In China, the traffic system mainly includes taxi, road vehicles, private cars and rail transit [8]. The interactive communication between them forms a complex dynamic system of traffic. To the knowledge of the author, there still lacks proper mathematical models to study traffic systems, including the six subsystem by the SD method. Based on the actual situation of the traffic system in Shandong Province, this paper proposes an SD model to describe the relationship among the six subsystem which contains the highway vehicle subsystem, the private car subsystem, the highway mileage subsystem, the rail transit subsystem and the traffic accident subsystem. Based on the SD model of the traffic system, some forecasts for the development of traffic in the future are given and some suggestions and optimization schemes for traffic development are given. This model is helpful for improving the convenience of traffic service and to promote stable traffic.

2. Main results

2.1. SD model

In highway vehicle subsystems, the number of operating vehicles is affected by highway mileage and highway density [6]. Generally speaking, highway has positive effects on the number of vehicles. In addition, the scrap of private cars can force people to take public traffic, which requires the increasing of investment in public traffic [3]. Thus, the above factors are defined as the influencing factors of the number of operating vehicles.

In taxi subsystems, taxi growth and taxi scrap are considered as two main factors which lead to the overall change in the number of taxis. As for the private car subsystems, it is used in traffic frequently, but it brings a lot of exhaust pollution [13]. In highway mileage subsystem, with the increasing of all kinds of vehicles, highway construction has been accelerated. On the contrary, old roads reduce highway mileage [6]. Highway mileage is an important embodiment of traffic development. In order to indicate the situation of highway mileage, we represent it by old roads and the number of vehicles.

In rail transit subsystems, with the increase of damage to the track, the length of rail transit has decreased. Track is influenced by the use of various vehicles and track investment [9, 28]. Then, the number of private cars and track damage are chosen as the influencing factors of rail transit length.

In traffic accident subsystems, the national economy can be affected by traffic accidents, and a suitable traffic condition can reduce the number of occurrences of traffic accidents effectively. Public traffic can affect the number of traffic accidents directly, which changes the choice of travel modes. Hence, we can get the influencing factors for the number of operating vehicles.

In terms of the fact indicated above, the following parameters are selected as Level variables: traffic accidents, number of road vehicles, highway mileage, number of taxis, number of private cars owned and length of rail transit line. For the sake of convenience, in the following context, all the elements are summarized in Table 1. In addition, the scenario diagram of the SD model is displayed in Figure 2.

According to the scenario diagram of traffic shown in Figure 2, each subsystem is associated with one state variable, such as T_1, T_9, T_{15}, T_{20}, T_{26}, T_{33} and so on. All the subsystems and their influence parameters can be found in Table 1.

In order to evaluate the situation of traffic, an SD model of the traffic system in Shandong Province was established by VENSIM software, the feedback process of flow diagram is marked by a blue arrow in Figure 3. Furthermore, it can be obtained that the influence between the parameters is multiplex and the influences between the six subsystems are mutual.

Table 1. All parameters in the SD model.

Subsystem	Parameter	Initial value	Description
Traffic accident	T		Traffic development index
	T_1	14.56 thousand times	Traffic accident
	T_2		Growth of traffic accident
	T_3		Mortality rate of traffic accidents
	T_4		Number of deaths in traffic accident
	T_5		Reduction of traffic accident
	T_6		Input of relevant personnel
	T_7		Relevant policy
	T_8		Education influence coefficient
Highway vehicle	T_9	913.8 thousand units	Number of vehicles in operation
	T_{10}		Road density
	T_{11}		Travel volume of highway operation
	T_{12}		Growth of road vehicles
	T_{13}		Car scrapping in highway operation
	T_{14}		Average car scrap rate
Highway mileage	T_{15}	229.9 thousand km	Highway mileage
	T_{16}		Growth of highway mileage
	T_{17}		Growth rate of highway mileage
	T_{18}		Reduction of highway mileage
	T_{19}		Reduction rate of highway mileage
Taxis	T_{20}	57.7 thousand units	Number of taxi
	T_{21}		Taxi trips
	T_{22}		Growth of taxi
	T_{23}		Growth rate of taxi
	T_{24}		Taxi scrap
	T_{25}		Taxi scrap rate
Private car	T_{26}	5.77 million units	Number of private car
	T_{27}		Private car trip
	T_{28}		Damage of private car
	T_{29}		Growth of private car
	T_{30}		GDP
	T_{31}		Growth rate of private cars
	T_{32}		Private car scrapping
Rail transit	T_{33}	38 million km	Length of rail transit
	T_{34}		Line down
	T_{35}		Travel volume of rail transit
	T_{36}		Growth of rail transit line length
	T_{37}		Reduction of rail transit line
	T_{38}		Track damage
	T_{39}		Growth rate of track
	T_{40}		Investment

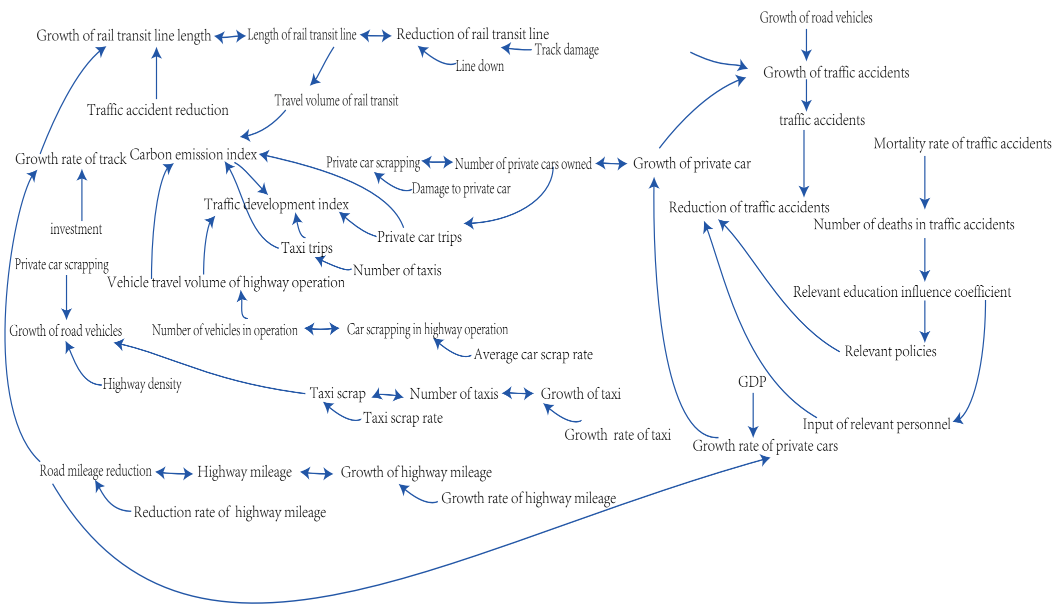

Figure 2. Scenario diagram of SD model.

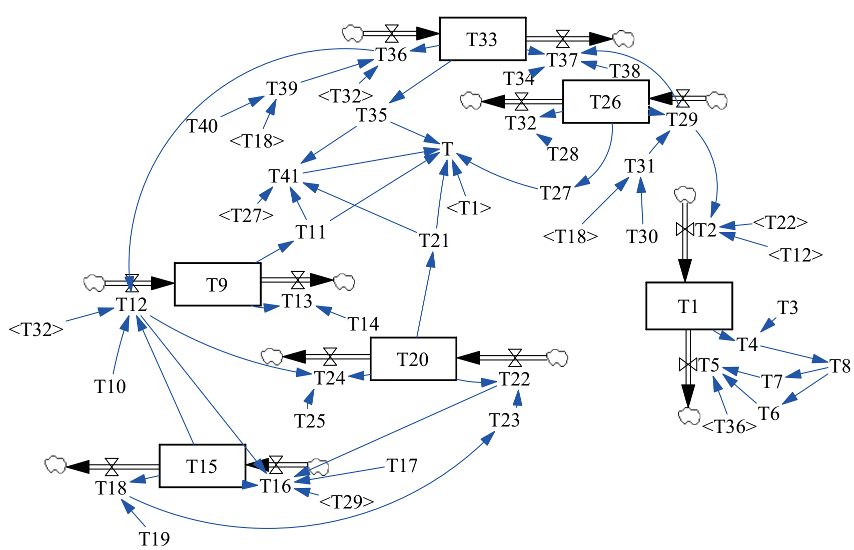

Figure 3. Flow diagram of the SD model.

2.2. *Mathematical model*

In light of the flow diagram (see Figure 3), the SD model can be established by translating the SD flow diagram into VENSIM equations, and thus the level variable can be expressed as the following integral equation [25]

$$Level(t) = \int_{t_0}^{t} Rate_{in}(s) - Rate_{out}(s)ds + Level(t_0), \tag{2.1}$$

in which, $Level(t)$ represents level variables, $Rate_{in}$ and $Rate_{in}$ signify inflow rate variables and outflow rate variables respectively. Thus, we have

$$\begin{cases} T_1(t) = \int_{t_0}^{t} T_2(s) - T_5(s)ds, \\ T_9(t) = \int_{t_0}^{t} T_{12}(s) - T_{13}(s)ds, \\ T_{15}(t) = \int_{t_0}^{t} T_{16}(s) - T_{18}(s)ds + 25.96, \\ T_{20}(t) = \int_{t_0}^{t} T_{22}(s) - T_{24}(s)ds + 60.119, \\ T_{26}(t) = \int_{t_0}^{t} T_{29}(s) - T_{32}(s)ds, \\ T_{33}(t) = \int_{t_0}^{t} T_{36}(s) - T_{37}(s)ds + 0.5, \end{cases} \tag{2.2}$$

where s is time at any time between the initial time t_o to the current time t, the unit of time assumed here is a year. On the other hand, we find

$$\frac{dLevel(t)}{dt} = Rate_{in}(t) - Rate_{out}(t),$$

hence

$$\begin{cases} \frac{dT_1(t)}{dx} = T_2(t) - T_5(t), \\ \frac{dT_9(t)}{dx} = T_{12}(t) - T_{13}(t), \\ \frac{dT_{15}(t)}{dx} = T_{16}(t) - T_{18}(t), \\ \frac{dT_{20}(t)}{dx} = T_{22}(t) - T_{24}(t), \\ \frac{dT_{26}(t)}{dx} = T_{29}(t) - T_{32}(t), \\ \frac{dT_{33}(t)}{dx} = T_{36}(t) - T_{37}(t). \end{cases} \tag{2.3}$$

Following $Increment = Growth\ rate \times Original\ data$, we have

$$\begin{cases} T_4(t) = T_1(t) \times T_3, \\ T_{13}(t) = T_9(t) \times T_{14}, \\ T_{18}(t) = T_{15}(t) \times T_{19}, \\ T_{22}(t) = T_{20}(t) \times T_{23}(t), \\ T_{29}(t) = T_{26}(t) \times T_{31}(t). \end{cases} \tag{2.4}$$

In traffic accident subsystems, the mortality rate is affected by travel modes, highway vehicles and taxis, and these are often selected as the analysis objects [15, 23], rail transit can decrease the accident rate [17]. In light of the data on the traffic accidents, we can find that the increase in the number of car leads to an increase in the number of traffic accidents, and the implementation of rail transit as well as positive policy can reduce the number of accidents. In addition, education on the safety awareness for people can also reduce the number of accidents. With respect to the highway subsystem, the number of cars is proportional to the number of roads and the miles of highway [12]. Investment in traffic can increase the mileage of highway [29]. In taxi subsystems, the expenditure on taking a taxi is higher than use of public traffic, but it is necessary to increase taxis reasonably, and the use of taxis is accompanied by the scrapping of taxis [19]. As for the private car subsystem, private cars are contradictory to public traffic, and they are positively related to highway mileage [3, 6]. In rail transit subsystem, the increase of the length of rail transit results in increasing of the investment of rail [9]. On the other hand, there exists the conflict between rail transit and private car [28]. The state of GDP is an important index of national development and it can reflect the government investment on traffic infrastructure construction. As indicated above, we obtain the following expressions on the rest of variables,

$$
\begin{cases}
T_2(t) = 0.316T_1(t) + 0.126T_{12}(t) + 0.512T_{22}(t),\\
T_5(t) = T_6(t) + 0.223T_7(t) + 0.125T_{36}(t),\\
T_7(t) = 0.656T_8(t),\\
T_8(t) = 5.89T_4(t),\\
T_{12}(t) = 0.316T_{10} + 0.233T_{15}(t) + 0.14T_{36}(t),\\
T_{16}(t) = T_{40} \times T_{15}(t),\\
T_{23}(t) = 0.205T_{25} - 0.065,\\
T_{24}(t) = T_{25} \times T_{20}(t) + 0.19T_{12},\\
T_{31}(t) = 0.344T_{18}(t) + 0.756T_{28},\\
T_{32}(t) = 0.625T_{22}(t) + 0.365T_{28},\\
T_{36}(t) = 0.872T_{39} \times T_{33} + 0.128T_{32},\\
T_{37}(t) = 0.233T_{29}(t) + 0.569T_{38},\\
T_{39}(t) = 0.456T_{18}(t) + 0.544T_{40}.
\end{cases}
\tag{2.5}
$$

2.3. Optimization of SD model

This subsection is devoted to optimize the SD model (see Figures 4 and 5). By comparing the output data with real data, four factors were selected in the model to judge the relative error of an SD model. The data of the National Bureau of Statistics and output date are expressed by R and C respectively, O denotes the output data of optimized model, and the relative error of the optimized model is signified by Oe. The following expressions to calculate the Oe of four curves is defined as

$$
Oe = \frac{|R - O|}{|R|}. \tag{2.6}
$$

$T_3, T_{10}, T_{14}, T_{17}, T_{19}, T_{25}, T_{28}, T_{30}, T_{34}, T_{38}$ and T_{40} are selected as the optimized parameters to examine. There are four optimization models related to the eleven objectives, see Figure 5. It is shown that the optimized curves O 1:4 are close to the real curves R 1:4. It can be seen that the O curves are closer to the R curves.

Table 2 shows that the relative error of the output data is less than the limit of error of 10% in system dynamics, which means that the precision of the model is enough.

Maximum payoff found at:
T3 = 0.0966794
T10 = 80
T14 = 0.291712
T17 = 1.74955
T19 = -0.010023
T25 = -0.135105
T28 = 0.0669325
T30 = 2.49007
T34 = 0.977206
T38 = 0.233964
T4O = 41.878

Figure 4. Optimization results of the SD model.

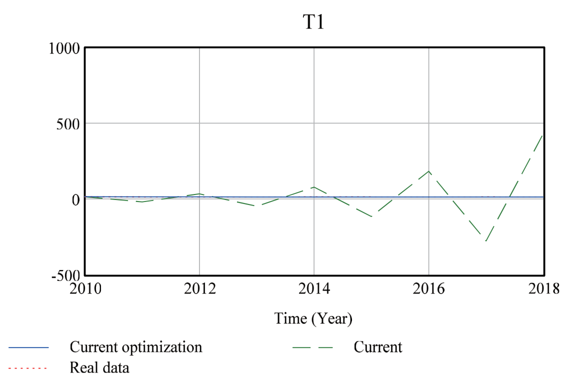

(a) Optimization of T_1.

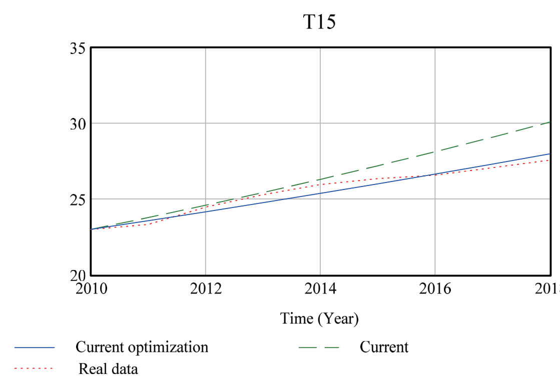

(b) Optimization of T_{15}.

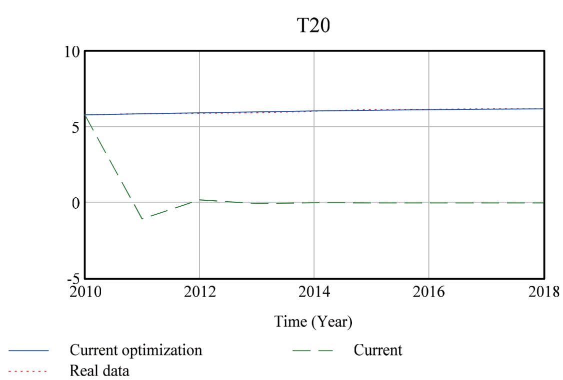

(c) Optimization of T_{20}.

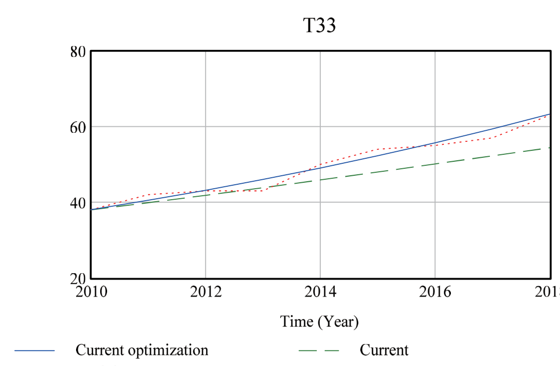

(d) Optimization of T_{33}.

Figure 5. Optimization of SD model.

Table 2. The relative error of SD model.

Year	2013	2014	2015	2016	2017	2018
C T_1	-48.05	77.94	-115.93	182.81	-277.03	431.36
C T_{15}	25.42	26.29	27.18	28.11	29.07	30.06
C T_{20}	-0.08	-0.04	-0.04	-0.04	-0.04	-0.05
C T_{33}	43.82	45.88	47.98	50.10	52.25	54.39
R T_1	12.88	13.57	13.38	13.16	13.40	13.23
R T_{15}	25.28	25.95	26.34	26.57	27.06	27.56
R T_{20}	5.91	6.01	6.12	6.13	6.17	6.17
R T_{33}	43	50	54	55	57	63
O T_1	13.39	13.21	13.12	13.10	13.15	13.27
O T_{15}	24.75	25.36	25.99	26.64	27.30	27.98
O T_{20}	5.96	6.024	6.071	6.11	6.14	6.16
O T_{33}	45.98	48.88	51.98	55.24	58.66	62.23
Oe T_1	3.97%	2.62%	1.89%	0.46%	1.87%	0.36%
Oe T_{15}	2.09%	2.25%	1.3%	0.28%	0.91%	1.55%
Oe T_{20}	1.04%	0.02%	0.84%	0.32%	0.39%	0.07%
Oe T_{33}	6.83%	2.23%	3.73%	0.45%	2.92%	1.22%

Note: The date of this table comes from China's National Bureau of Statistics.

2.4. Parameter analysis

Based on the SD model, ten debugging models are established, in which T is taken as the objective function, and T_3, T_{10}, T_{30} and T_{40} are taken as the design variables. By using these debugging models, the optimal design of traffic can be obtained to provide a better traffic control strategy. Based on the results of debugging, the effects of different debugging models on the traffic are evaluated.

From Figure 6, which shows the current optimization curve of T, we have:

(1) The variation of T associated with the traffic accident subsystem is the maximal one in scheme 1 (see Figure 6a), which means that the government should take measures to reduce the number of traffic accidents.
(2) Although there exist relationships between T and all parameters of the global system, the road density is more important than others, therefore, by adjusting road density, we can control the process of development of traffic effectively. As the length of highway can increase T, the government should improve the quality and length of a high utilization factor of highways must be kept.
(3) Figure 6 shows the comparison between current optimization curves and the schemes proposed. By Figure 6c and Table 3, we assert that T_{30} exerts dominant influence on the increasing of T, and the best way to promote development of traffic is to improve the quality and length of highway and rail transit [5].
(4) Figure 7 indicates that the relationship between debugging two parameters and debugging one parameter is not linear. Furthermore, the effect of two parameters is better than one parameter.

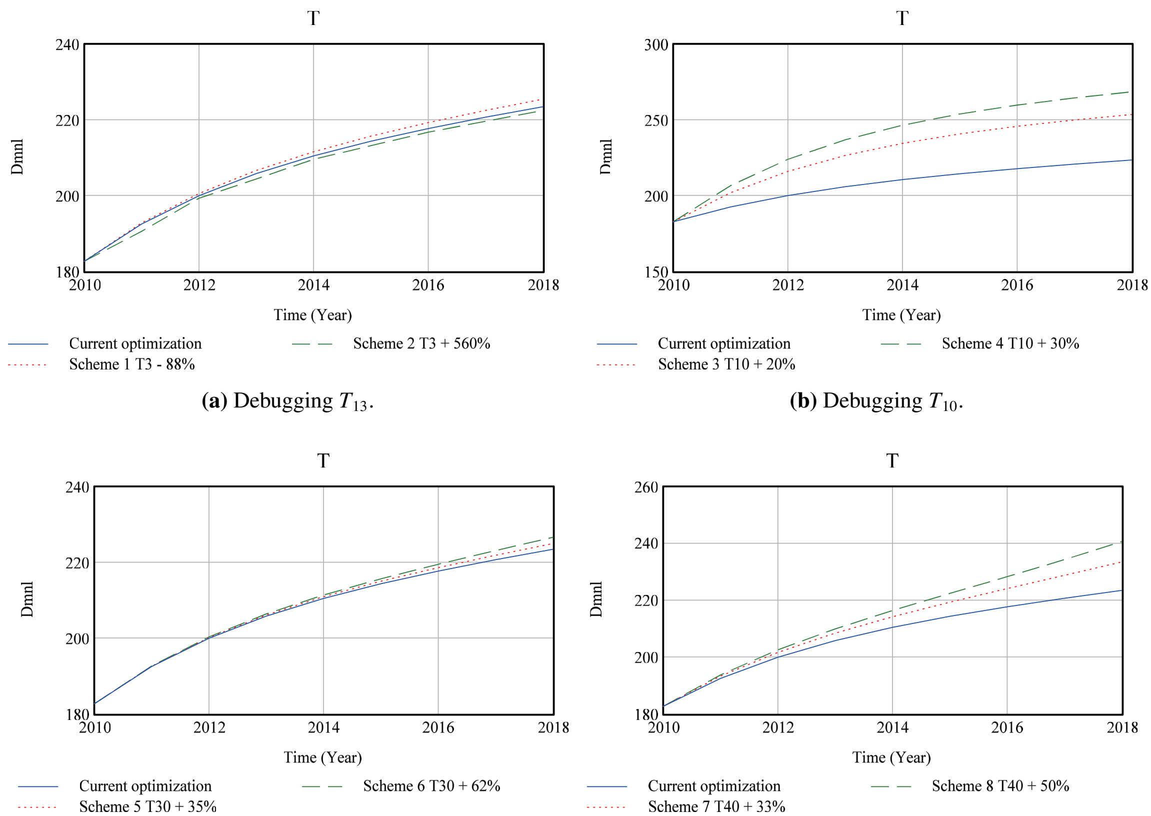

(a) Debugging T_{13}. **(b)** Debugging T_{10}.

(c) Debugging T_{30}. **(d)** Debugging T_{40}.

Figure 6. Debugging results of one parameter.

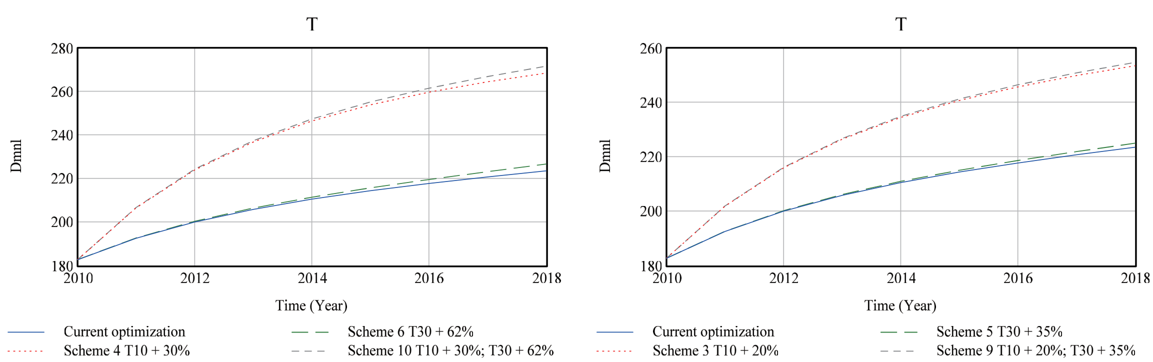

(a) Debugging T_{10} and T_{35}. **(b)** Debugging T_{10} and T_{35}.

Figure 7. Debugging results of two parameters.

2.5. Data estimation

Table 3 shows that the relative error of $T_1,\ T_9,\ T_{15},\ T_{20}$ and T_{33} are under 6.83% and thus the model has high accuracy. In light of this SD model, Table 4 displays the next ten years developments of traffic in Shandong Province, and it is found that the following trends of traffic in the future.

(1) The number of traffic accidents is increasing every year, which may be related to the growth of private cars and taxis. The growth of private cars and taxis is inevitable. Therefore, the government must take active measures to reduce the number of traffic accidents.
(2) Due to the needs of the citizen and environmental protection, the number of operating vehicles will always keep rising. The increase of operating vehicles means that the number of buses on remote roads and the diversification of routes are improved, which is convenient for citizens.
(3) The larger number of all kinds of vehicles leads to the increase in loading of roads, which will bring more traffic accidents. Obviously, the length of highway mileage should be enlarged.
(4) Although the number of taxis will continue to rise in the next ten years, its growth is slower than other means of traffic. Taxis and buses are convenient for people to take, but the taxi results in more serious pollution than buses. Furthermore, unlike the bus, the taxi is not as safe. Therefore, the number of taxis will decrease in the future.
(5) The number of private cars will grow rapidly in the future. The private cars not only bring convenience to people, but also bring great burden to traffic. The citizens should appropriately reduce the use of private cars and take public traffic.
(6) The rail transit's length will maintain rapid growth in the next decades, which means that government will pay more attention to the development of rail transit, and the rail transit can greatly reduce traffic accidents and environmental pollution.

Table 3. Growth rate of Debugged models.

	Index of 2018	Growth rate
Scheme 1 $T_3 - 88\%$	226.36	0.73%
Scheme 2 $T_3 + 560\%$	223.67	-0.46%
Scheme 3 $T_{10} + 20\%$	254.68	13.34%
Scheme 4 $T_{10} + 30\%$	269.67	20.01%
Scheme 5 $T_{30} + 35\%$	243.78	8.49%
Scheme 6 $T_{30} + 62\%$	229.28	2.03%
Scheme 7 $T_{40} + 33\%$	234.68	4.44%
Scheme 8 $T_{40} + 50\%$	241.82	7.61%
Scheme 9 $T_{10} + 20\%, T_{30} + 35\%$	258.25	14.91%
Scheme 10 $T_{10} + 30\%, T_{30} + 62\%$	276.45	23.02%

Table 4. Data estimation based on SD model.

Year	2019	2020	2021	2022	2023	2024	2025	2026	2027	2028
T_1	13.46	13.74	14.11	14.59	15.18	15.92	16.83	17.93	19.25	20.85
T_9	1126	1136	1147	1157	1167	1178	1188	119.9	1210	1221
T_{15}	61.8	61.8	61.8	61.7	61.4	61.1	60.68	60.1	59.4	58.6
T_{20}	28.68	29.39	30.12	30.88	31.65	32.44	33.25	34.09	34.95	35.83
T_{26}	237.9	278.2	325.2	380.1	444.2	518.9	606.1	707.8	826.4	964.5
T_{33}	65.94	69.79	73.76	77.84	81.99	86.19	90.40	94.57	98.64	102.52

2.6. The neural network model

Based on the SD model, the following neural network model of traffic problem considered can be represented as

$$\begin{cases} \frac{d(T_{33}(t))}{dt} = a_1 T_{33}(t) + b_{11} T_{33}(t) + b_{13} T_{15}(t) T_{33}(t) + b_4 T_{26}^2(t) + c_1, \\ \frac{T_{15}(t)}{dt} = -a_2 T_{15}(t) + b_{21} T_{15}(t) + b_{23} T_{26}(t) + b_{24} T_{15}(t) + b_{25} T_{33}(t) T_{15}(t) + \\ \qquad b_{26} T_{26}(t) T_{15}(t) + b_{27} T_{20} T_{15}(t) + c_2, \\ \frac{d(T_{26}(t))}{dt} = -a_3 T_{26}(t) + b_{31} T_{26}(t) + b_{32} T_{15}(t) T_{26}(t), \\ \frac{d(T_{20}(t))}{dt} = -a_4 T_{20}(t) + b_{41} T_{33}(t) + b_{42} T_{33}(t) + b_{43} T_{26}(t) + b_{44} T_{33}(t) T_{15}(t) + \\ \qquad b_{45} T_{20}(t) T_{15}(t)) + c_4, \\ \frac{d(T_9(t))}{dt} = -a_5 T_9(t) + b_{51} T_{33}(t) + b_{52} T_{15}(t) + b_{53} T_{26}(t) + b_{54} T_{33}(t) T_{15}(t) + c_5, \\ \frac{d(T_1(t))}{dt} = -a_6 T1_(t) + b_{62} T_{15}(t) + b_{63} T_{26}(t) + b_{64} T_{20}(t) + b_{65} T_{33}(t) T_{15}(t) + \\ \qquad b_{66} T_{26}(t) T_{15}(t) + b_{67} x_4(t) T_{15}(t) + c_6, \\ T(t) = a_{11} T_{33}(t) + a_{12} T_{15}(t) + a_{13} T_{26}(t) + a_{14} T_{20}(t) + a_{15} T_9(t) + a_{16} T_1(t), \end{cases} \tag{2.7}$$

where the meaning of the coefficients of (2.7) can be found in (A.1). The five neurons are represented by T_3, T_{14}, T_{19}, T_{25} and T_{28}. The capacitance of each neuron is fixed to be 1. $\gamma_i = \frac{1}{T_i}$ $(i = 3, 14, 19, 25, 28)$ are the resistances of per neuron [1, 2, 22]. If T_0 is the initial value, I signifies the expected value, S_i are the years to achieve I of each neuron, and T_s is T_0 after s years, then the neural network model is

$$T_s = T_0 + (I - T_0) \times (1 - \exp \frac{-S_i}{\gamma_i}),$$

further

$$S_i = \gamma_i \times \ln \frac{I - T_0}{I - T_s}, \tag{2.8}$$

which provides an algorithm to calculate I (see Example 2.1).

Example 2.1. If T in 2015 and 2018 are noted as $T_0 = 214.74$ and $T_s = 224.73$ respectively, I is set to be 300, then

$$S_i = \gamma_i \times \ln \frac{I - T_0}{I - T_s} = \gamma_i \times \ln \frac{85.27}{75.29}, \tag{2.9}$$

where

$$\gamma_3 = 10.34,\ \gamma_{14} = 3.43,\ \gamma_{19} = 99.80,\ \gamma_{25} = 7.40,\ \gamma_{28} = 14.94,$$

so we can get

$$S_3 = 1.29,\ S_{14} = 0.43,\ S_{19} = 12.42,\ S_{25} = 0.92,\ S_{28} = 1.86.$$

Model 2.9 shows that the length of time to achieve the expected value of each subsystem are $1.29, 0.43, 12.42, 0.17, 0.92$, and 1.86 years respectively. Obviously, the maximum is 12.42 years, which is the length of time to arrive the expected value. The SD and neural network models are advantageous to improve the speed and efficiency of the development of the traffic system.

3. Conclusions

This paper considers the development of the traffic system of Shandong Province, based on the system dynamics method, and the SD model of traffic system related to the six subsystem which contains the highway vehicle subsystem, the private car subsystem, the highway mileage subsystem, the rail transit subsystem and the traffic accident subsystem, in light of which prediction on the future situation of the traffic system of Shandong Province is derived. Furthermore, the neural network model of the problem considered in paper is also given. In terms of the SD model and neural network model, we can give some policies to force the traffic systems to develop to the situation we want. For example, the government need to develop rail transit and take some measures to reduce the number of traffic accidents. The model is helpful to improve the convenience of traffic services and to promote to development the stable traffic. Furthermore, based on the neural network model, we can investigate the dynamics of the traffic system, and we will pursue this line in the future.

Use of AI tools declaration

The authors declare they have not used Artificial Intelligence (AI) tools in the creation of this article.

Acknowledgments

This work is supported by Natural Science Foundation of Shandong Province (No. ZR2020MA054) and Research Foundation for Talented Scholars of SDUT (No. 4041/419023).

Conflict of interest

The authors declare that there is no conflict of interest.

References

1. S. A. Aamir, P. Müller, A. Hartel, J. Schemmel, K. Meier, A highly tunable 65-nm CMOS LIF neuron for a large scale neuromorphic system, *ESSCIRC Conference 2016: 42nd European Solid-State Circuits Conference*, IEEE, 2016, 71–74. https://doi.org/10.1109/ESSCIRC.2016.7598245
2. D. Bau, J. Y. Zhu, H. Strobelt, A. Lapedriza, B. Zhou, A. Torralba, Understanding the role of individual units in a deep neural network, *Proc. Natl. Acad. Sci. USA*, **117** (2020), 30071–30078. https://doi.org/10.1073/pnas.1907375117
3. R. Cervero, Y. Tsai, City CarShare in San Francisco, California: second-year travel demand and car ownership impacts, *Transp. Res. Rec.*, **1887** (2004), 117–127. https://doi.org/10.3141/1887-14

4. R. G. Coyle, System dynamics modelling: a practical approach, *J. Oper. Res. Soc.*, **48** (1997), 544. https://doi.org/10.1057/palgrave.jors.2600682

5. T. Dyr, P. Misiurski, K. Ziółkowska, Costs and benefits of using buses fuelled by natural gas in public transport, *J. Clean. Prod.*, **225** (2019), 1134–1146. https://doi.org/10.1016/j.jclepro.2019.03.317

6. L. Fan, A. Wang, CO_2 emissions and technical efficiency of logistics sector: an empirical research from China, *Proceedings of 2013 IEEE International Conference on Service Operations and Logistics, and Informatics*, IEEE, 2013, 89–94. https://doi.org/10.1109/SOLI.2013.6611388

7. J. W. Forrester, Industrial dynamics, *J. Oper. Res. Soc.*, **48** (1997), 1037–1041.

8. J. M. García, *Theory and practical exercises of system dynamics*, Modeling and Simulation with Vensim PLE, Preface by John Sterman, 2020.

9. Q. W. Guo, S. Chen, P. Schonfeld, Z. Li, How time-inconsistent preferences affect investment timing for rail transit, *Transport. Res. B: Meth.*, **118** (2018), 172–192. https://doi.org/10.1016/j.trb.2018.10.009

10. S. He, J. Li, A study of urban city traffic congestion governance effectiveness based on system dynamics simulation, *Int. Ref. J. Eng. Sci.*, **8** (2019), 37–47.

11. M. Humayun, M. F. Almufareh, N. Z. Jhanjhi, Autonomous traffic system for emergency vehicles, *Electronics*, **11** (2022), 510. https://doi.org/10.3390/electronics11040510

12. G. K. Ingram, Z. Liu, Determinants of motorization and road provision, *Policy Research Working Paper*, The World Bank, 1999.

13. S. Jia, L. Bi, W. Zhu, T. Fang, System dynamics modeling for improving the policy effect of traffic energy consumption and CO_2 emissions, *Sustain. Cities Soc.*, **90** (2023), 104398. https://doi.org/10.1016/j.scs.2023.104398

14. S. Jia, G. Yan, A. Shen, J. Zheng, A system dynamics model for determining the traffic congestion charges and subsidies, *Arab. J. Sci. Eng.*, **42** (2017), 5291–5304. https://doi.org/10.1007/s13369-017-2637-5

15. A. Jusuf, I. P. Nurprasetio, A. Prihutama, Macro data analysis of traffic accidents in Indonesia, *J. Eng. Technol. Sci.*, **49** (2017), 132–143. https://doi.org/10.5614/j.eng.technol.sci.2017.49.1.8

16. V. Kolesov, A. Petrov, System dynamics of process organization in the sphere of traffic safety assurance, *Transp. Res. Proc.*, **36** (2018), 286–294. https://doi.org/10.1016/j.trpro.2018.12.085

17. W. Li, S. Yin, Analysis on cost of urban rail transit, *J. Transp. Syst. Eng. Inf. Tech.*, **12** (2012), 9–14. https://doi.org/10.1016/S1570-6672(11)60190-6

18. A. Monirabbasi, A. R. Khansari, L. Majidi, Simulation of delay factors in sewage projects with the dynamic system approach, *Ind. Eng. Strategic Manage.*, **1** (2021), 15–30. https://doi.org/10.22115/iesm.2020.232300.1006

19. H. Qu, Z. Zhao, The application of Lagrange relaxation on taxi dispatchments during evening rush hours, *J. Phys.: Conf. Ser.*, **1650** (2020), 032019. https://doi.org/10.1088/1742-6596/1650/3/032019

20. A. Rajput, M. Jain, System dynamics simulation model to reduce the traffic congestion of metropolitan cities of India by implementing intelligent transportation system, *International Conference on Mathematical Sciences and Statistics 2022 (ICMSS 2022)*, Atlantis Press, 2022, 440–455. https://doi.org/10.2991/978-94-6463-014-5_38

21. M. Saleem, S. Abbas, T. M. Ghazal, M. A. Khan, N. Sahawneh, M. Ahmad, Smart cities: Fusion-based intelligent traffic congestion control system for vehicular networks using machine learning techniques, *Egypt. Inform. J.*, **23** (2022), 417–426. https://doi.org/10.1016/j.eij.2022.03.003

22. S. Samanta, S. Suresh, J. Senthilnath, N. Sundararajan, A new neuro-fuzzy inference system with dynamic neurons (NFIS-DN) for system identification and time series forecasting, *Appl. Soft Comput.*, **82** (2019), 105567. https://doi.org/10.1016/j.asoc.2019.105567

23. S. P. Santosa, A. I. Mahyuddin, F. G. Sunoto, Anatomy of injury severity and fatality in Indonesian traffic accidents, *J. Eng. Technol. Sci.*, **49** (2017), 412–422. https://doi.org/10.5614/j.eng.technol.sci.2017.49.3.9

24. W. Sardjono, E. Selviyanti, W. G. Perdana, Modeling the relationship between public transportation and traffic conditions in urban areas: a system dynamics approach, *J. Phys.: Conf. Ser.*, **1465** (2020), 012023. https://doi.org/10.1088/1742-6596/1465/1/012023

25. J. D. Sterman, *System dynamics: systems thinking and modeling for a complex world*, Massachusetts Institute of Technology, Engineering Systems Division, 2002, 1–31.

26. J. Usenik, T. Turnšek, Modeling conflict dynamics with fuzzy logic inference, *J. US-China Public Adm.*, **10** (2013), 457–474.

27. L. Wen, L. Bai, System dynamics modeling and policy simulation for urban traffic: a case study in Beijing, *Environ. Model. Assess.*, **22** (2017), 363–378. https://doi.org/10.1007/s10666-016-9539-x

28. N. Wu, S. Zhao, Q. Zhang, A study on the determinants of private car ownership in China: findings from the panel data, *Transport. Res. A: Pol.*, **85** (2016), 186–195. https://doi.org/10.1016/j.tra.2016.01.012

29. N. J. Ye, W. J. Li, Y. Li, Y. F. Bai, Spatial econometric research on the relationship between highway construction and regional economic growth in China: evidence from the nationwide panel data, *IOP Conf. Ser.: Earth Environ. Sci.*, **100** (2017), 012138. https://doi.org/10.1088/1755-1315/100/1/012138

30. Z. Zhu, S. Zhu, Z. Zheng, H. Yang, A generalized Bayesian traffic model, *Transp. Res. C: Emer.*, **108** (2019), 182–206. https://doi.org/10.1016/j.trc.2019.09.011

Appendix

$$
\begin{aligned}
a_1 &= 0.125T_{34},\\
a_2 &= T_{19},\\
a_3 &= 0.135T_{30},\\
a_4 &= 3.1550e-05T_{30}+T_{25}-0.245,\\
a_5 &= T_{14},\\
a_6 &= 0.223a_2+4.031T_3,\\
b_{11} &= 0.0047T_{40},\\
b_{12} &= 0.0040T_{19},\\
b_{13} &= -0.00801T_{19},\\
b_{14} &= -0.00561T_{30},\\
b_{21} &= 7.0176e-06T_{40},\\
b_{22} &= 0.010.751T_{17}+0.233,\\
b_{23} &= 9.1428e-06T_{19}\times T_{30}+9.3700e-05T_{30},\\
b_{24} &= -9.6500e-05,\\
b_{25} &= 0.000129,\\
b_{26} &= 7.3600e-05T_{19},\\
b_{27} &= 3.0500e-04a_2,\\
b_{31} &= 0.075T_{30}, b_{32} = 0.0344T_{19},\\
b_{41} &= -1.3375e-05T_{40},\\
b_{42} &= -4.4720e-04,\\
b_{43} &= -0.1801,\\
b_{44} &= -1.1172e-05T_{19},\\
b_{45} &= 0.205a_2,\\
b_{51} &= 7.0176e-04T_{40},\\
b_{52} &= 0.233,\ b_{52} = 0.0233,\\
b_{53} &= 0.0166T_{30},\\
b_{54} &= 5.9098e-04T_{19},\\
b_{25} &= 0.205a_2,\\
b_{51} &= 0.0070T_{40},\\
b_{53} &= 0.016644T_{30},\\
b_{54} &= 5.8824e-04T_{19},\\
b_{61} &= -5.2550e-04T_{40},\\
b_{62} &= 0.02935,\ b_{64} = -0.0331,
\end{aligned}
$$

$$
\begin{aligned}
&b_{63} = -0.0259T_{30},\\
&b_{65} = -4.4050e-04T_{19},\\
&b_{66} = 0.0108a_2, b_{67} = 0.104a_2,\\
&a_{11} = 0.0703,\ a_{12} = 0.298,\\
&a_{13} = 1.765,\ a_{14} = 0.226,\\
&a_{15} = 0.096,\ a_{16} = 0.011,\\
&c_1 = 4.6720e-04T_{28} - 0.569T_{38},\\
&c_2 = 0.316T_{10} + 1.3128e-06T_{28}\\
&c_4 = -6.0040e-04T_{10} + 1.3128e-06T_{28}\\
&c_5 = 0.316T_{10} + 6.9146e-05T_{28},\\
&c_6 = -5.8400e-05T_{28} + 0.0398T_{10} + 8.6899e-06T_{28},\\
&a = 0.456T_{19},\ \bar{a} = T_{19},\ b = 0.544T_{40}, d = 0.04672T_{28},\ \bar{d} = T_{30},\\
&f = 0.751T_{17},\ k = 5.8T_3, j = 0.569T_{38},\ h = 0.316T_{10},\ r = T_{25},\ q = T_{14}.
\end{aligned} \tag{A.1}
$$

Chapter 4

Conclusions

As conclusions of the current PhD thesis we can state that mathematical modeling in general and dynamical systems in particular are good tools to deals with problems related with the optimization at logistic processes and reduction of carbon footprint via implementation of efficient driving.

We enumerate the output that we have obtained:

- We have created a handle selector's indecisiveness in choice data model via a Max which will help at logistic processes regarding the indecisiveness in choice. A new latent Bayesian choice model has been stated.

- In terms of binary choices, we have stated a generalization of choice models for the binary scenario. A detailed analysis, covering a wide range of parametric settings, through the launch of Gibbs Sampler, a notable extension of Markov Chain Monte Carlo methods, is conducted under the Bayesian paradigm.

- We have stated and solved, creating a swarming Meyer wavelet, a reactive model of traffic where we can measure the role of the driver. The conclusions were that for the same level of traffic a better efficiency at driving reduce costs. When traffic level is high this save is even more important, therefore make not sense to reduce cost invest in the driving formation on efficient driving.

- We have developed and solved a global model of traffic, where we combine for first time the effect of train in the logistic process of moving goods. The maximum error between the output data and the statistics bureau, based on which some forecasts for the development of traffic in the future are given, is obtained, some suggestions and optimization schemes for traffic development are given. Finally, a neural network model of the development of Shandong traffic is also derived.

References

[1] B. Fischhoff; S.B. Broomell, *Judgment and decision making*, Annu. Rev. Psychol. 2020, **71**, (2020), 331–355

[2] M.K. Dhami; D.R. Mandel; B.A. Mellers; P.E. Tetlock, *Improving Intelligence Analysis with Decision Science*. Perspect. Psychol. Sci., **10**, (2015) 753–757

[3] H.P. Young, *Condorcet's theory of voting*. Am. Pol. Sci. Rev., **82**, (1988), 1231–1244.

[4] M.D. Condorcet, *Essay on the Application of Analysis to the Probability of Majority Decisions*; Imprimerie Royale: Paris, France, 1785.

[5] L.L. Thurstone, *A law of comparative judgment*. Psychol. Rev., **34**, (1927), 273–286.

[6] R.A. Bradley; M.E. Terry, *Rank Analysis of Incomplete Block Designs: I. The Method of Paired Comparisons*. Biometrika, **39**, (1952), 324.

[7] T.A. Mazzuchi; W.G. Linzey; A. Bruning, *A paired comparison experiment for gathering expert judgment for an aircraft wiring risk assessment*. Reliab. Eng. Syst. Saf., **93**, (2008) 722–731.

[8] M. Cattelan; C. Varin; D. Firth, *Dynamic Bradley–Terry modelling of sports tournaments*. J. R. Stat. Soc. Ser. C Appl. Stat., 62, (2013), 135–150.

[9] G. Schauberger; G.Tutz, *Subject–specific modeling of paired comparison data: A lasso-type penalty approach*. Statist. Modell., **17**, (2017) 223–243. [CrossRef]

[10] Y.T. Sung; J.S. Wu, *The Visual Analogue Scale for Rating, Ranking and Paired-Comparison (VAS-RRP): A new technique for psychological measurement.* Behav. Res. Methods 2018, **50**, (2018), 1694–1715.

[11] C.G. Chorus, *Capturing alternative decision rules in travel choice models: A critical discussion.* In Handbook of Choice Modelling; S. Hess, A. Daly, Eds.; Edward Elgar: Northampton, MA, USA, 2014; pp. 290–310.

[12] U. Liebe; P. Mariel; H. Beyer; J. Meyerhoff, *Uncovering the nexus between attitudes, preferences and behavior in sociological applications of stated choice experiments.* Soc. Methods Res., **50**, (2021), 310–347.

[13] C. Elsenbroich; N. Payette, *Choosing to cooperate: Modelling public goods games with team reasoning.* J. Choice Model. 2020, **34**, (2020) 100203.

[14] S.Pink; D. Kretschmer; L. Leszczensky. *Choice modelling in social networks using stochastic actor–oriented models.* J. Choice Model., **34**, (2020) 100202.

[15] U. Liebe; J. Meyerhoff, *Mapping potentials and challenges of choice modelling for social science research.* J. Choice Model., **38**, (2021), 100270.

[16] A. Borriello; J.M. Rose, *Global versus localised attitudinal responses in discrete choice.* Transportation, **48**, (2019), 131–165.

[17] M.J. Frith, *Modelling taste heterogeneity regarding offence location choices.* J. Choice Model., **33**, (2019), 100187.

[18] F. Feinberg; E. Bruch; M. Braun; B.H. Falk; N. Fefferman; E.M. Feit; J. Helveston; D. Larremore; B.B. McShane; A. Patania et al. *Choices in networks: A research framework.* Mark. Lett., **31**, (2020), 349–359.

[19] T.J. Leeper; S.B. Hobolt; J. Tilley, *Measuring subgroup preferences in conjoin experiments.* Polit. Anal., **28**, (2020) 207–221.

[20] M. Dras, *Evaluating Human Pairwise Preference Judgments.* Comput. Linguist., **41**, (2015) 337–345.

[21] E. Shivanian, *On the multiplicity of solutions of the nonlinear reactive transport model*, Ain Shams Engineering Journal **5**(**2**), (2014), 637–645.

[22] C.I. Steefel, D.J. De Paolo, P.C. Lichtner, *Reactive transport modeling: an essential tool and a new research approach for the Earth sciences*, Earth Planet Sci. Lett. **240**(**3 – 4**), (2005), 539–558.

[23] T. Pabst, J. Molson, M. Aubertin, B. Bussière, *Reactive transport modelling of the hydro-geochemical behaviour of partially oxidized acid-generating mine tailings with a monolayer cover*, Applied Geochemistry **78**, (2017), 219–233.

[24] P. Regnier, P. Jourabchi, C.P. Slomp, *Reactive-transport modeling as a technique for understanding coupled biogeochemical processes in surface and subsurface environments*, Netherlands Journal of Geosciences **82**(**1**), (2003), 5–18.

[25] J. Vilcáez, L. Li, D. Wu, S.S. Hubbard,*Reactive transport modeling of induced selective plugging by Leuconostoc mesenteroides in carbonate formations*, Geomicrobiology Journal **30**(**9**), (2013), 813–828.

[26] A.J. Ellery, M.J. Simpson, *An analytical method to solve a general class of nonlinear reactive transport models*, Chemical Engineering Journal **169**(**1 – 3**), (2011), 313–318.

Chapter 5

Appendix on Impact Factors

5.1 Applied Sciences-Basel where Paper 1 was published

- 2022 Impact Factor 2.7,
- Q2 Engineering, Multididisciplinary

Journal Impact Factor Trend 2022

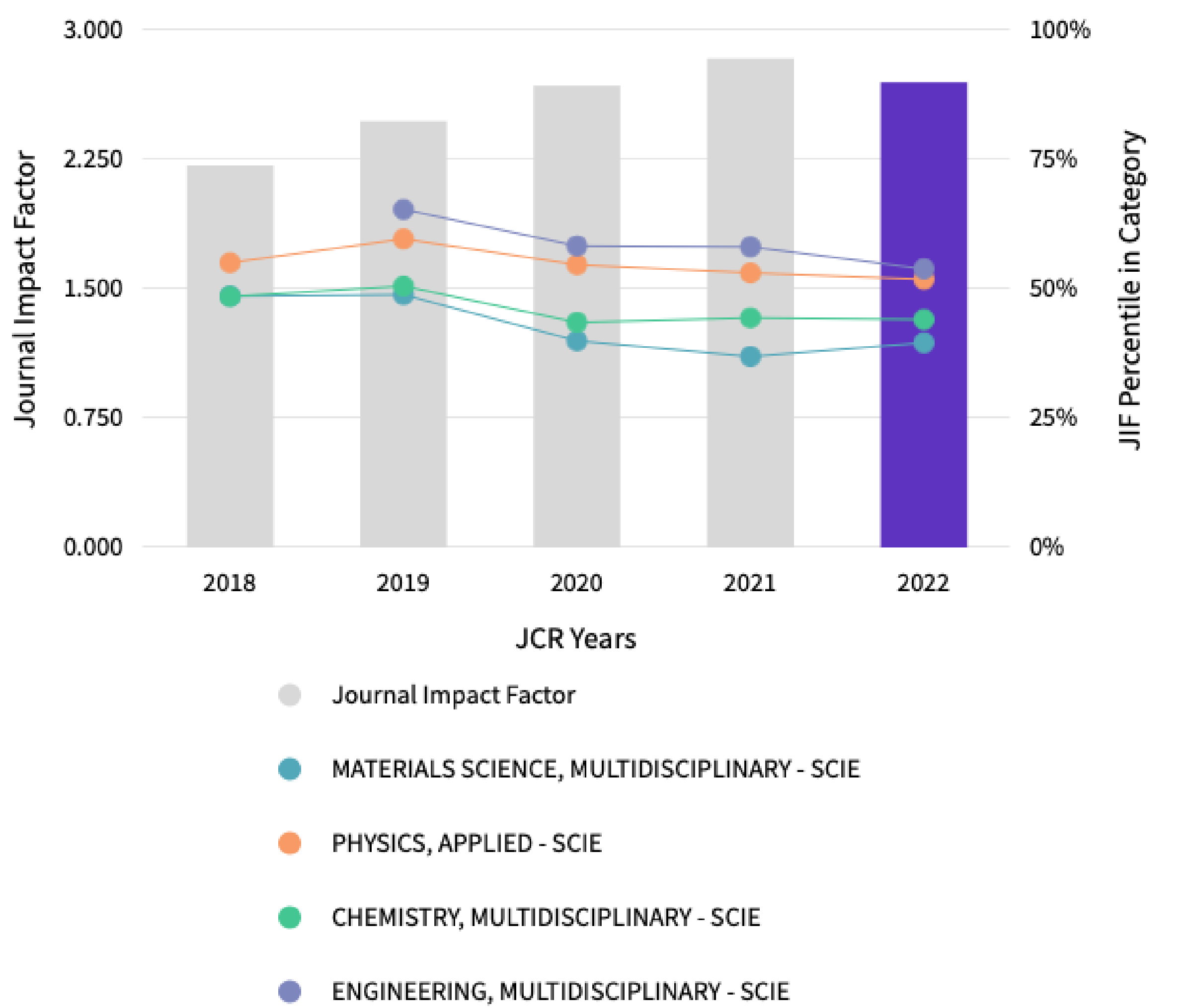

EDITION

Science Citation Index Expanded (SCIE)

CATEGORY

ENGINEERING, MULTIDISCIPLINARY

42/90

JCR YEAR	JIF RANK	JIF QUARTILE	JIF PERCENTILE
2022	42/90	Q2	53.9
2021	39/92	Q2	58.15
2020	38/90	Q2	58.33
2019	32/91	Q2	65.38
2018	N/A	N/A	N/A

5.2 AIMS Mathematics where Papers 2 and 4 were published

- 2022 Impact Factor 2.2,
- Q1 Mathematics, Applied

Journal Impact Factor Trend 2022

Export

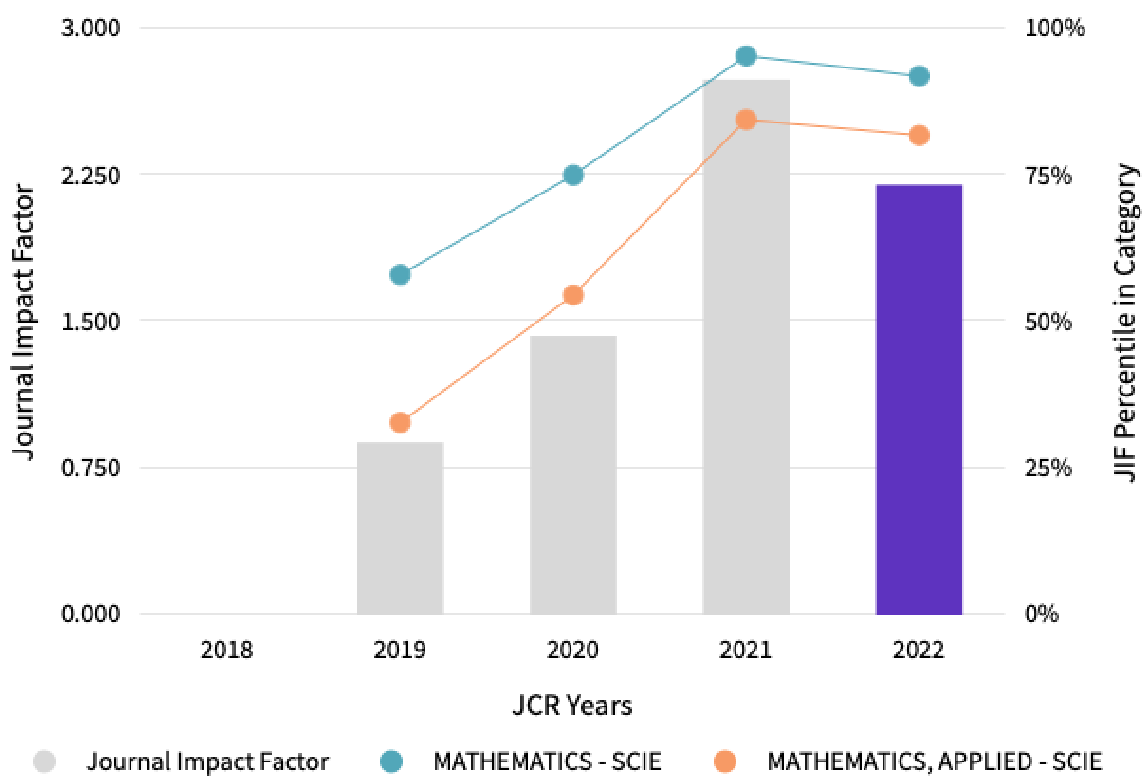

EDITION

Science Citation Index Expanded (SCIE)

CATEGORY

MATHEMATICS, APPLIED

49/267

JCR YEAR	JIF RANK	JIF QUARTILE	JIF PERCENTILE
2022	49/267	Q1	81.8
2021	42/267	Q1	84.46
2020	121/265	Q2	54.53
2019	176/261	Q3	32.76

5.3 Axioms where paper 2 was published

- 2022 Impact Factor 2,
- Q2 Mathematics, Applied

Journal Impact Factor Trend 2022

Export

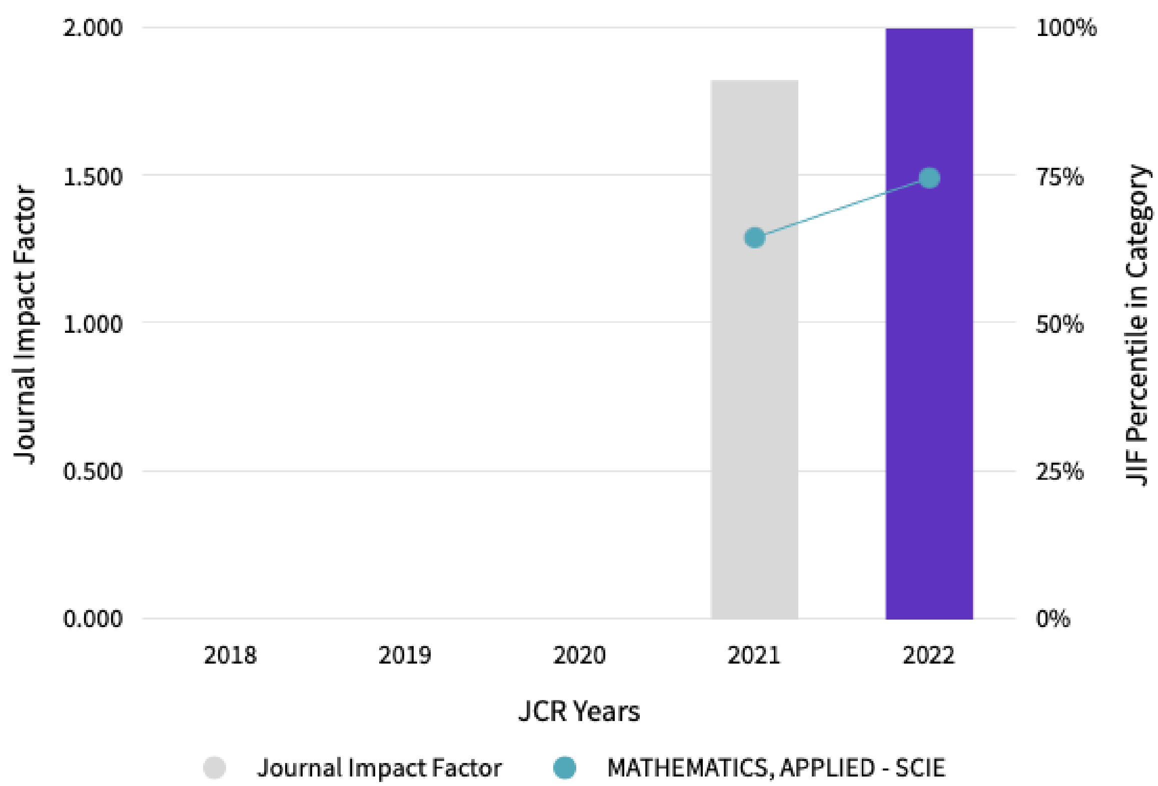

EDITION

Science Citation Index Expanded (SCIE)

CATEGORY

MATHEMATICS, APPLIED

68/267

JCR YEAR	JIF RANK	JIF QUARTILE	JIF PERCENTILE
2022	68/267	Q2	74.7
2021	95/267	Q2	64.61
2020	N/A	N/A	N/A